



UNIVERSITÀ  
DEGLI STUDI  
DI PADOVA

Sede Amministrativa: Università degli Studi di Padova

Dipartimento di Medicina Molecolare

CORSO DI DOTTORATO DI RICERCA IN: MEDICINA MOLECOLARE

CURRICOLO: BIOMEDICINA

CICLO XXXII

**DEVELOPMENT AND VALIDATION OF INNOVATIVE TECHNOLOGIES FOR HIGHLY ACCURATE  
AND COST-EFFECTIVE PREIMPLANTATION GENETIC TESTING: TECHNICAL AND CLINICAL  
PERSPECTIVES**

**Coordinatore:** Ch.mo Prof. Stefano Piccolo

**Supervisore:** Ch.mo Prof. Stefano Piccolo

**Co-Supervisore:** Dott.ssa Cristina Patassini

**Dottorando:** Laura Girardi



## Index

LIST OF ABBREVIATION .....	1
ABSTRACT .....	5
ABSTRACT .....	7
1 INTRODUCTION .....	9
1.1 Evolution of technologies for chromosomal assessment .....	12
2 AIM OF THE PROJECT.....	16
3 PREIMPLANTATION GENETIC TEST FOR CHROMOSOMAL ASSESSMENT ....	17
3.1 VALIDATION OF A NEW QPCR-BASED PROTOCOL WITH 4-PLEX PLATES 17	
3.1.1 Introduction and aim of the study .....	17
3.1.2 Study design and outcome measure .....	17
3.1.3 MATERIALS AND METHODS.....	18
3.1.4 RESULTS .....	22
3.2 VALIDATION OF THE NEW ION REPROSEQ PROTOCOL AND INTERPLATFORM COMPARISON BETWEEN Q-PCR AND NGS-BASED PGT-A...25	
3.2.1 Introduction and aim of the study .....	25
3.2.2 Study design and outcome measure .....	25
3.2.3 MATERIAL AND METHODS .....	27
3.2.4 RESULTS .....	32
3.3 SEGMENTAL ANEUPLOIDIES CHARACTERIZATION AND PREDICTIVE VALUE ANALYSIS.....	39
3.3.1 Introduction and aim of the study .....	39
3.3.2 Study design and outcome measure .....	39
3.3.3 MATERIAL AND METHODS .....	41
3.3.4 RESULTS .....	42
4 PREIMPLANTATION GENETIC TEST FOR MONOGENIC CONDITIONS .....	53
4.1 EVALUATION OF A NOVEL NON-INVASIVE PGT-M PROTOCOL USING BLASTOCOEL FLUID AND SPENT EMBRYO CULTURE MEDIA .....	53
4.1.1 Introduction.....	53
4.1.2 Aim of the study and study design.....	54
4.1.3 Outcome measure.....	55
4.1.4 MATERIALS AND METHODS.....	55
4.1.5 RESULTS .....	56

4.2	VALIDATION OF A NEW TECHNOLOGY TO PERFORM PGT-M USING INFINIUM KARYOMAPPING PROTOCOL AND ILLUMINA NEXTSEQ 550 PLATFORM.....	62
4.2.1	Introduction and aim of the study .....	62
4.2.2	Study design and outcome measure .....	62
4.2.3	MATERIAL AND METHODS .....	63
4.2.4	RESULTS .....	69
5	DISCUSSION AND CONCLUSIONS .....	76
6	REFERENCES .....	87
	Appendix 1 .....	95
	Appendix 2 .....	96

## **LIST OF ABBREVIATION**

ADI	Allele drop-in
ADO	Allele drop-out
AF	Amplification failure
aCGH	Array comparative genomic hybridization
ART	Assisted reproductive technologies
BF	Blastocoel fluid
cfDNA	Cell free DNA
CCS	Chromosome screening technologies
CN	Number of copies
CNV	Copy number variation
FISH	Fluorescent in situ hybridization
ICM	Inner cell mass
IVF	In vitro fertilization
NGS	Next Generation Sequencing
Ni-PGT	Non-invasive PGT
NPV	Negative predictive value
PCR	Polymerase chain reaction
PGT-A	Preimplantation genetic test for aneuploidies
PGT-M	Preimplantation genetic test for monogenic conditions
PND	Prenatal diagnosis
PPV	Positive predictive value
qPCR	Quantitative polymerase chain reaction
SBM	Spent blastocyst media
SD	Standard deviation
SGD	Single gene disorders
SMA	Spinal muscular atrophy
SMN1	Survival motor neuron 1

SNP	Single nucleotide polymorphisms
STR	Short tandem repeat
TE	Trophectoderm
WGA	Whole genome amplification







## **ABSTRACT**

(English)

Testing preimplantation embryos, obtained during in vitro fertilization treatments, using preimplantation genetic tests have been introduced into clinical practice in recent years. First applications involved the possibility of detecting embryos affected by monogenic disorders (PGT-M) inherited from parents. Subsequently, preimplantation genetic testing for aneuploidy (PGT-A) was introduced to improve IVF transfer outcomes. Indeed, identification of aneuploid and transfer of euploid embryos has demonstrated improved rates for implantation, pregnancy and live birth per transfer and reduced implantation failures. Developments in genomic technologies for PGT have revolutionized the ability to detect genetic abnormalities of various kinds, starting from a small number of cells biopsied from the embryo. The increased sensitivity and resolution of these methods has allowed to identify not only the gain or loss of entire chromosome but also partial or segmental aneuploidies and chromosomal mosaicism, introducing novel diagnostic categories with greater difficult management and interpretation. Of note the knowledge of the biology of these alterations and the outcomes is incomplete and still evolving. In recent years the demand for PGT has increased considerably. At the same time, the novel technologies adapted for preimplantation genetic diagnosis have allowed to increase the number of samples simultaneously analyzed, reducing the costs and time associated with analyses this allowed a greater diffusion and accessibility of PGT to a greater number of patients. Moreover, partial automation of procedures, increased analytical flexibility and simplified data analysis, provided by recent technologies, have significantly improved laboratory workflow and clinical management. The central theme of this thesis is the evolution of technologies and analytical methods employed in our laboratory for preimplantation genetic diagnosis. In this project the main application of PGT, chromosomal aneuploidies and monogenic disease, are presented separately. Since the beginning of my PhD training, I've been involved in the development and validation of new molecular genetics methodologies: the new Ion Reproseq protocol on Ion Torrent platform was validated and introduced into clinical practice for aneuploidy screening. Later Karyomapping approach was validated for monogenic disorders but didn't replace the technology already in use. During the last year I focused my activity on the characterization of segmental aneuploidies: a considerable proportion was found to be mosaic in origin, reducing their diagnostic predictive value compared to whole chromosome aneuploidies.



## **ABSTRACT**

(Italiano)

L'analisi degli embrioni preimpianto, ottenuti durante i trattamenti di fecondazione in vitro, mediante test genetici preimpianto è stata recentemente introdotta nella pratica clinica. Le prime applicazioni riguardavano la possibilità di rilevare embrioni affetti da malattie monogeniche (PGT-M) ereditate dai genitori. Successivamente, sono stati introdotti test genetici preimpianto per le aneuploidie (PGT-A) per migliorare i risultati dei trasferimenti embrionari da FIV. Infatti, l'identificazione delle aneuploidie e il trasferimento di embrioni euploidi ha dimostrato un aumento dei tassi di impianto, gravidanze e di nati vivi per trasferimento e riduzione dei fallimenti dell'impianto. Gli sviluppi delle tecnologie genomiche per PGT hanno rivoluzionato la capacità di rilevare anomalie genetiche di vario tipo, partendo da un piccolo numero di cellule biopsiate dall'embrione. La maggiore sensibilità e risoluzione di questi metodi ha permesso di identificare non solo aneuploidie dell'intero cromosoma, ma anche aneuploidie parziali o segmentali e il mosaicismo cromosomico, introducendo nuove categorie diagnostiche di difficile gestione e interpretazione. Da notare che la conoscenza della loro biologia e i risultati clinici sono incompleti e in continua evoluzione. Negli ultimi anni la richiesta di PGT è molto aumentata. Allo stesso tempo, le nuove tecnologie adattate per la diagnosi genetica preimpianto hanno permesso di aumentare il numero di campioni analizzati simultaneamente, riducendo i costi e i tempi associati alle analisi e consentendo una maggiore accessibilità del PGT a un maggior numero di pazienti. Inoltre, l'automazione parziale delle procedure, la maggiore flessibilità analitica e un'analisi dei dati semplificata, fornite dalle recenti tecnologie, hanno notevolmente migliorato il flusso di lavoro del laboratorio e la gestione clinica. Il tema centrale di questa tesi è l'evoluzione delle tecnologie e dei metodi analitici impiegati nel nostro laboratorio per la diagnosi genetica preimpianto. In questo progetto le principali applicazioni del PGT vengono presentate separatamente, aneuploidie cromosomiche e malattie monogeniche. Dall'inizio del mio dottorato di ricerca, sono stata coinvolta nello sviluppo e nella validazione di nuove metodologie: il protocollo Ion Reproseq sulla piattaforma Ion Torrent è stato validato e introdotto nella pratica clinica per lo screening delle aneuploidie. In seguito, l'approccio di Karyomapping è stato validato per le malattie monogeniche ma non ha sostituito la tecnologia già in uso. Durante l'ultimo anno ho focalizzato la mia attività sulla caratterizzazione delle aneuploidie segmentali: una

proporzione considerevole è stata trovata a mosaico, riducendo il loro valore predittivo diagnostico rispetto alle aneuploidie dell'intero cromosoma.

## **1 INTRODUCTION**

### **1.1 Preimplantation genetic test for monogenic defects: indications and evolution of diagnostic methods**

The field of assisted reproductive medicine has dramatically advanced during the last decades. Recent discoveries in genetics and improvements in diagnostic test to reveal monogenic conditions combined with the reduction of costs for the simultaneous screen of multiple diseases, have recently led to the development of comprehensive carrier screening panels. Consequently, healthy individuals are likely to be identified as carriers for several genetic conditions. Both diagnostic test for the most frequent conditions and preconception carrier screening have increased the reproductive autonomy of individuals and couples by providing them with knowledge about their available reproductive options. In this background of increased reproductive awareness, the testing of healthy status for embryos and prioritization of the embryos to transfer using preimplantation genetic test is increasingly considered as a reproductive choice. Indeed, the spread of genetic tests with greater diagnostic ability for the detection of susceptibility to cancer (BRCA1 and BRCA2 genes) and multifactorial diseases, in addition to the monogenic ones with complete penetrance (autosomal dominant, recessive), has increased the number of the indications for preimplantation genetic test for inheritable genetic conditions cases (PGT-M) year by year. PGT-M is an alternative to invasive prenatal diagnosis for those couples with known risk of transmitting a genetic condition to their offspring and can be used to screen embryos for almost any kind of genetic disorder in which the genetic cause is characterized. Preimplantation embryos obtained by in vitro fertilization (IVF) are analysed and only those embryos free of the disorder under study are transferred to the uterus to achieve pregnancy. The first successful application of PGT in humans was performed in 1990 by Handyside and colleagues (Handyside *et al.*, 1990), who carried out sexing of embryos by polymerase chain reaction (PCR) to avoid males affected with an X-linked disorder. Gender was determined in single blastomeres by PCR using primers for amplifying Y-chromosome-specific DNA sequences. Embryos identified as female were selectively transferred to the uterus. Later, successful PGT was reported for cystic fibrosis, based on the amplification of a DNA fragment containing the causative mutation and its detection by fragment analysis (Handyside *et al.*, 1992). The main diagnostic strategies employed have been changed from the first case. Since PGT indications have been expanded and the development and optimization of increasingly sensitive technologies and molecular protocols, able to produce reliable

diagnostic results, became necessary in the PGT laboratory. Multiplex PCR and fragment analysis using targeted primers designed specifically for point mutation or deletions of interest combined with primers for closely linked short tandem repeats (STR) markers represents the gold standard to perform PGT-M. Point mutation analysis is most frequently performed using minisequencing. Other strategies such as real time-PCR, (Treff *et al.*, 2012) have been successfully employed to detect both point mutation and co-segregating flanking SNPs. More recently, Karyomapping technology was developed and commercialized, providing a comprehensive and robust linkage-based diagnosis (Handyside *et al.*, 2010). By genotyping the parents at several hundred thousand SNP sites throughout the genome, a dense set of informative SNP markers are identified for each of the four parental chromosomes. The phase of the alleles for each informative SNP locus and linkage of the risk alleles with the parental chromosomes can then be established by reference to the genotype of a relative of known disease status. The parental origin of each chromosome in the embryo is then ascertained by comparison with the genotype of the reference. The main advantages for PGT-M cases comes from the possibility of genotyping 300000 SNPs across the genome, to perform indirect linkage analysis for virtually every region of interest without performing patient-specific custom set-up. More recently NGS-based platforms have been employed for PGT-M (Treff *et al.*, 2013), however many concerns regarding technological limitation (false positive, artefacts and allele drop-out, ADO) and the high costs associated are still preventing their spread and applicability in clinical context.

## **1.2 Preimplantation genetic test for aneuploidies**

During the last few decades, in parallel with the increase in the application of PGT-M tests, *in vitro* fertilization (IVF) has emerged as the main treatment option for patients affected by infertility, especially for those of advanced maternal age. However, success rates remained relatively low. For this reason, novel techniques aimed at improving overall success rates of IVF treatments, both increasing pregnancy rates and reducing implantation failure and risk of miscarriage were developed. With this aim, preimplantation evaluation procedures, to identify the most competent embryo to be prioritized or selected for transfer, have been developed. Traditionally, embryos were evaluated and selected based on morphological parameters assessed on day 2, day 3, and day 5/6 post fertilization, however, this strategies failed to reliably predict reproductive ability (Capalbo *et al.*, 2014). This is commonly demonstrated by the fact that an appreciable fraction of embryos with suboptimal appearance

leads to healthy pregnancies (Capalbo *et al.*, 2014). Later, the cytogenetic analysis of products of conceptions revealed that a high percentage of spontaneous abortions were chromosomally abnormal, mainly due to aneuploidy. This shifted the focus of reproductive research to the development of methodologies that evaluate the embryo's genetic composition. The introduction of assisted reproductive technologies (ART) to ensure that the embryo transferred to the patient has a correct number of chromosomes (preimplantation genetic test for aneuploidies, PGT-A), has allowed to understand that chromosomal abnormalities identified in abortion material of *in vivo* conceptions are also frequently identified in preimplantation embryos generated by IVF (Fragouli *et al.*, 2013; Franasiak *et al.*, 2014). Moreover, population-based studies revealed important features related to human aneuploidies: firstly the majority of them derived from the mother and their incidence increased with maternal age (Nagaoka 2012), secondly chromosomes displayed different susceptibilities to aneuploidy, especially the two smallest chromosomes 21 and 22 but also 15 and 16. In addition, population studies of new-borns and product of conception, suggested that all monosomies, except X0, are incompatible with late embryonic development and early foetal life and although some autosomal trisomies and sex chromosome abnormalities are permissive of implantation, most of them result in developmental arrest within the first 12 weeks of gestation. The age/related processes that lead to exponential increase in aneuploid conceptions are now increasingly understood and novel insights into the molecular mechanism of chromosome segregation during meiosis are being explored (Ottolini *et al.*, 2015). Regarding their origin, direct assessment of human oocytes and polar bodies showed that most of uniform aneuploidies derive from meiotic errors (Hassold and Hunt, 2001; Ottolini *et al.*, 2015; Capalbo *et al.*, 2017a) arising during oogenesis and revealed segregation patterns that predispose to aneuploidy: meiosis I non-disjunction, precocious sister chromosome segregation or pre-division, meiosis II non-disjunction and reverse segregation (Ottolini *et al.*, 2015). An additional source of chromosomal abnormalities derives from mitotic segregation errors occurring in post-zygotic developmental stages. These errors give rise to the phenomenon of mosaicism, that involves the presence of cell lines with different karyotypes within the same embryo. Because there are no therapies available to counteract the age-related increase of aneuploidies, diagnostic programmes worldwide, either on preimplantation embryos during IVF treatments or in the prenatal period (prenatal diagnosis, PND), were established to detect aneuploid conceptions. Indeed PGT-A is increasingly being

offered to all patients who undergo in vitro fertilization IVF especially to advanced maternal age patients, to whom the likelihood of producing abnormal embryos is significantly higher than in the younger population. In the last years social and cultural changes have greatly influenced the reproductive choices leading to an increase in the overall reproductive maternal age. In this clinical setting becomes evident the need of optimization of genetic laboratory procedures, both in terms of workflow and costs associated to the analysis in order to be able to offer PGT to a greater number of patients. Technological progress had clearly favoured the reduction of costs allowing to simultaneously analyze more samples offering more analytical flexibility and reliable diagnostic solutions.

### 1.3 Evolution of technologies for chromosomal assessment

Over the years the molecular strategies employed for preimplantation aneuploidy screening (PGT-A) have changed and improved, taking advantage of the technological progressions introduced in molecular genetics (Figure 1) (Poli *et al.*, 2019).

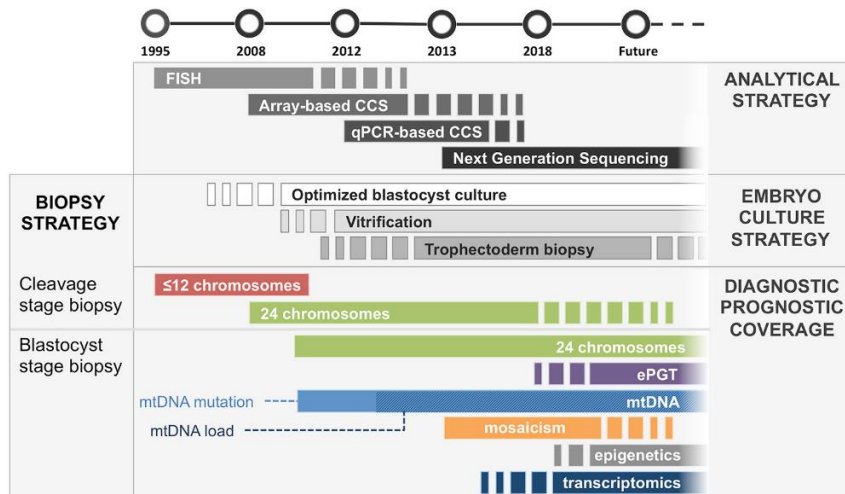


**Figure 1:** Timeline of introduction to clinical practice of embryological and analytical achievements. *Analytical strategy, dark gray bars section:* FISH was first employed for assessment of a limited amount of chromosomes in mid ‘90s, followed by microarray-based comprehensive chromosomal screening techniques (e.g., aSNP, aCGH) in mid 2000’s. Comprehensive quantitative PCR methods were introduced in ‘10s, shortly followed by NGS-based methods, which is now employed for most of chromosomal screening analyses, progressively replacing other less sensitive, more expensive and labour intensive techniques (Poli *et al.*, 2019, Front. Endocrinol. 10:154).

Initially, PGT-A was performed by fluorescent in situ hybridization (FISH), involving the spreading of a single cell biopsied from a cleavage stage embryo on a glass slide and the hybridization of its DNA with chromosome-specific fluorescent probes. FISH was employed to detect aneuploidies related to spontaneous miscarriage or compatible with life birth, such as chromosome 15, 16, 17, 18, 21, 22, X e Y. Several limitations of this approach have been described in the literature, including not only the limited number of chromosomes that could



be simultaneously assessed but also the high incidence of false positive results (Treff *et al.*, 2010; Capalbo *et al.*, 2013). Most importantly, the removal of one cell from cleavage stage embryo was shown to have an impact on its developmental and reproductive potential due to the risk of removing cells already committed to inner cell mass lineage differentiation (Scott *et al.*, 2013). In the mid 2000's, it became clear that these shortcomings and diagnostic unreliability, coupled with the negative consequences of cleavage stage biopsy, were compromising clinical outcomes of patients undergoing PGT, highlighting the necessity of a safer, more robust and precise strategy (Cohen *et al.*, 2007). Subsequently, the development of comprehensive chromosome screening technologies (CCS), including comparative genomic hybridization arrays (aCGH) and single nucleotide polymorphisms arrays (SNP arrays) and quantitative polymerase chain reaction (qPCR), provided significant improvement to PGT clinical application. These technologies not only are able to accurately evaluate all 24 chromosomes in a single analysis, but also are applicable to small number of cells with sufficient accuracy. When tested on single cells from fibroblast cell lines with known karyotype, all platforms provided accuracy rates above 98% for whole chromosome aneuploidies (Gutiérrez-Mateo *et al.*, 2011; Treff *et al.*, 2012; Kung *et al.*, 2015). The largest comparative study between two methodologies (aCGH and qPCR) conducted on embryo biopsies reported high concordance across the two platforms (Capalbo *et al.*, 2015). In this study, qPCR and aCGH showed similar sensitivity (98.2 vs. 98.8%, respectively, not significant), whereas qPCR displayed a significantly higher specificity compared with aCGH (99.9 vs. 99.6%, respectively,  $P = 0.01$ ). Despite the need for larger comparative studies, technological performance appears to be similar across all platforms when standard criteria for diagnosis of whole chromosome aneuploidies are used. All CCS strategies allow parallel sample analysis and produce higher throughput compared to FISH. Also, some of the CCS strategies now available avoid time consuming and high labor-intensive steps required for FISH analysis, allowing more reproducible and streamlined processing conditions (i.e., qPCR, aCGH). In recent years, Next Generation Sequencing (NGS) platforms have been adapted for embryo aneuploidy testing using low-depth genome sequencing and copy number variation analysis (Fiorentino *et al.*, 2014; Huang *et al.*, 2016). Different protocols and platforms have been recently validated and due to its sensitivity, coupled with further extended chromosome coverage, NGS provides higher accuracy in the assessment of sub-chromosomal abnormalities (i.e., segmental aneuploidies) compared to previous CCS

methods (Vera-Rodríguez *et al.*, 2016). Additionally, NGS is currently employed for the detection of chromosomal mosaicism, where two karyotypically different cell populations coexist in the same embryo. Despite lacking significant level of diagnostic validation, NGS was suggested to be able to detect low-level mosaicism (i.e., 20%) and accurately discriminate the proportion of cells showing abnormal karyotype (Munné and Wells, 2017). Nonetheless, mosaicism detection at low and high levels (e.g., 20 and 80%, respectively) is yet to be confirmed as a true biological finding, rather than a technical variation, hence its clinical impact still requires evidence support (Capalbo *et al.*, 2017c). Today, the main advantage provided by NGS in PGT is the possibility to analyse multiple samples in parallel, indeed through barcoding procedure different samples are labelled with unique sequences so that they later can be mixed, sequenced, and matched to their original patient and/or embryo. This lead to a significant reduction of both costs and sample running time and allows a wider accessibility to PGT for patients worldwide. Similarly to other platforms, NGS is compatible with combined assessment of both aneuploidy and single gene mutation, where the initial round of whole genome amplification (WGA) is integrated with targeted amplification of loci of interest (Treff *et al.*, 2013; Zimmerman *et al.*, 2016).

Prior to all PGT analyses, preimplantation embryos are subjected to in vitro fertilization procedures involving fertilization via intracytoplasmic sperm injection, embryo culture, biopsy procedure and subsequent vitrification and cryopreservation. PGT can be applied to different preimplantation developmental stages, including polar bodies, day 3 blastomeres and blastocyst stage at day 5/6 or 7. All PGT procedures require an initial amount of embryonic DNA and embryo biopsy represents a crucial step in embryo genetic assessment both from biological and technical standpoints. There are three major types of embryo biopsy: polar body, blastomere, and trophoctoderm (TE) biopsy. Polar body-based screening has been suggested as a less invasive strategy that avoids the potential problems associated with mosaicism, but it is also more expensive (requiring testing of two samples for each oocyte) and has a poor predictive value for the ploidy of the resulting blastocyst and its reproductive potential, specifically in that it analyses only the maternal contribution to aneuploidy. More emphasis has been placed on embryo biopsy which was originally performed on cleavage stage embryos by removing one single blastomere from an 8-cell embryo. This approach was shown to have an impact on its developmental and reproductive

potential due to the risk of removing cells already committed to inner cell mass lineage differentiation (Scott *et al.*, 2013). The development of extended culture systems has allowed the postponement of embryo biopsy to the blastocyst stage (Figure 2).

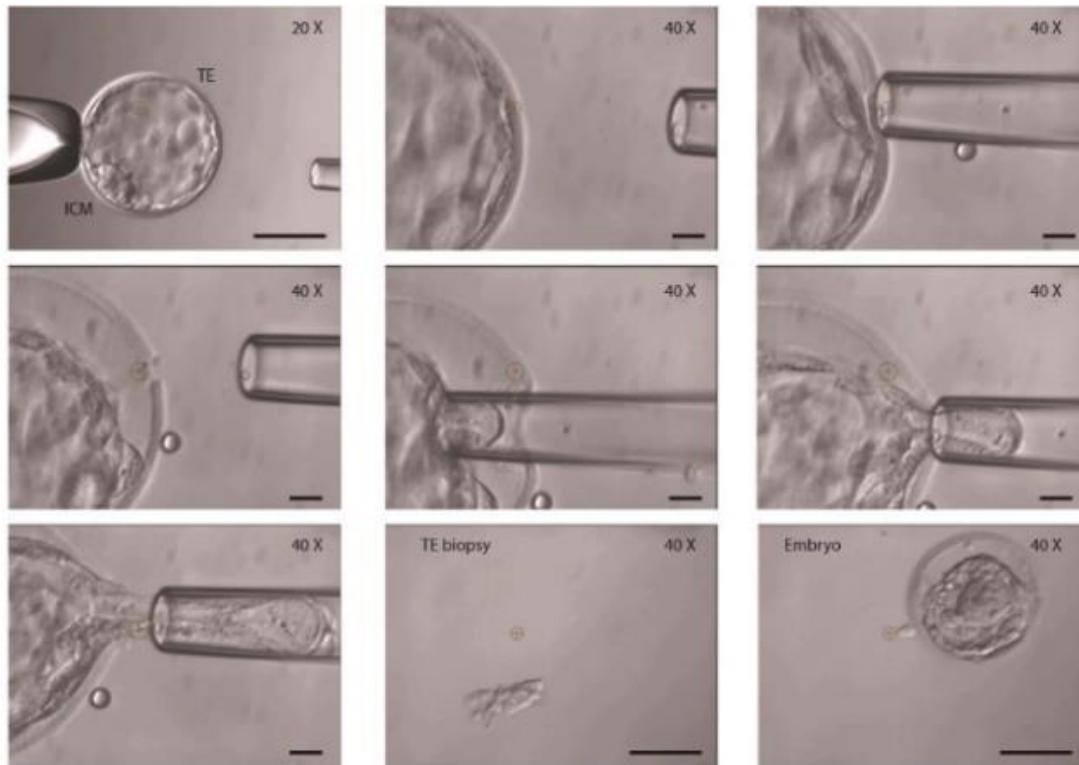


**Figure 2:** Trophectoderm biopsy strategy

At this stage, embryo genome activation is completed, and cellular differentiation resulted in two morphologically detectable cell lineages: the inner cell mass (ICM) and trophoctoderm cells (TE). By collecting 5–8 cells from the TE wall, the proportion of the embryonic biomass removed is selectively obtained from the extra-embryonic lineage and does not affect embryo development (Scott *et al.*, 2013). Moreover, previous studies have demonstrated identical genetic constitution of both ICM and TE from the same embryo (Fragouli *et al.*, 2008). Other advantages of TE biopsy are related to the higher number of cells collected, which provides a larger amount of DNA template for downstream amplification and analysis and generates more robust results compared to single cell analysis. All these factors have contributed to the development of a global strategy for the investigation of embryos genetic features based on multicellular samples supplying reliable source of template DNA for robust downstream analysis.

## **2 AIM OF THE PROJECT**

The aim of this project was the development and optimization of new molecular protocols using novel analytical platforms to perform preimplantation genetic test on IVF embryos. The first part of the project was focused on validating two novel approaches for embryo chromosomal assessment: a qPCR-based protocol with 4-plex plates and a NGS-based approach. Particular attention was put on increasing the number of samples simultaneously analysed, and to increase in resolution capabilities of aneuploidy screening, in order to provide a more complete view of the genetic constitution of the embryo. The qPCR protocol base on 4-plex plates is an evolution of the previous strategy routinely applied in our laboratory, performed using the same real time qPCR approach. The new approach allows to simultaneously analyse the double of the samples in the same plate. The use of the new NGS-based aneuploidy screening is characterized by advanced analytical sensitivity and higher processivity, allowing the simultaneous analysis of up to 96 samples per sequencing run. The first part of the thesis was concluded with the introduction of the new NGS platform into clinical practice and the realization of a study able to clarify new molecular aspects of segmental aneuploidies and to provide information about their impact on the PGT laboratory workflow and clinical management. The second part of the project focused on assessing the applicability of two approaches for PGT-M. In details, the reliability of a new non-invasive approach using embryo spent culture media was evaluated, taking advantage of the in house technology available for PGT-M. Lastly, karyomapping technology based on SNP array was verified and introduced in our laboratory, in order to potentially avoid the preliminary phase of SET-UP, necessary in the current PGT-M approach.

### **3 PREIMPLANTATION GENETIC TEST FOR CHROMOSOMAL ASSESSMENT**

#### **3.1 VALIDATION OF A NEW QPCR-BASED PROTOCOL WITH 4-PLEX PLATES**

##### **3.1.1 Introduction and aim of the study**

The first technology introduced at Igenomix Italy laboratory to perform preimplantation genetic test for aneuploidies based on TaqMan PCR chemistry. The protocol employed was firstly validated in 2012 (Treff *et al.*, 2012) and then extensively applied for routine analysis in our PGT-A programme until December 2017. This 4-hour method for comprehensive chromosome screening in human blastocysts, is based on locus-specific multiplex PCR which interrogates 4 assays located for each chromosome, in quadruplicate reactions with the use of TaqMan Copy Number Assays and TaqMan Preamplification Master Mix (Applied Biosystems). Next, the preamplified sample is aliquoted into a 384-well plate where each of the individual 96 loci is interrogated by qPCR using Quant Studio DX instrument (Applied Biosystems). Each well contains two different assays allowing the simultaneous analysis of 2 embryos per run. To determine the 24-chromosome copy number in each sample a unique method of the standard delta delta threshold cycle ( $\Delta\Delta Ct$ ) is applied, based on the comparison with delta cycle threshold values of normal male embryos. To further reduce time and costs of PGT-A with qPCR protocol we decided to design a new plate layout including two more fluorophores in the same well (4 in total, VIC, FAM, ABY, and JUN). The introduction of two more fluorophores allowed to interrogate four different assays per well, testing a total of four embryos in the same plate (4-plex). Prior to the introduction of the new protocol into clinical practice we have subjected the new plate layout to extensive validation.

##### **3.1.2 Study design and outcome measure**

The validation of this new protocol was divided into two phases: in the first phase 9 different human fibroblast cell lines with known karyotype (Coriell Institute) have been used to prepare 20 samples clinically equivalent to TE biopsy, of 5 cells each. Blinded analysis of all samples was performed using 4-plex plates following the same qPCR-based protocol for duplex-plate. In the second phase of the validation three more biopsies (C, D, E) were obtained from 41 aneuploid blastocysts (123 biopsies total) previously analyzed with duplex plates by an external laboratory (RMA NJ) . Blinded reanalysis of the biopsy samples was performed on 4-plex plates and confirmed with duplex plates in our laboratory. With this approach we have been able to validate the new protocol using a more relevant tissue type with respect to cell lines. Consistency of the cell line samples qPCR-based 24-chromosome

copy number predictions with the cell lines' karyotype (previously established by the Coriell Cell Repository by conventional karyotyping) was evaluated at the level of individual chromosome copy numbers and for the entire 24 chromosomes of each sample tested. Consistency of embryo 24-chromosome copy number assignments with previously established duplex-plate diagnoses was also evaluated at the level of individual chromosome copy numbers for the entire 24 chromosomes of each sample tested and for the overall diagnosis of aneuploidy or euploidy.

### 3.1.3 MATERIALS AND METHODS

#### 3.1.3.1 Samples included in the validation

The validation of the new 4-plex protocol was performed on 20 samples obtained from 9 different cell lines and on 123 trophoctoderm biopsies obtained from 41 different aneuploid blastocyst. Cell samples from Coriell Institute and from RMA NJ laboratory with the corresponding karyotypes are indicated in table1 and table 2.

Sample ID	Karyotype	Sample type
GM04435	48,XY,+16,+21	5 cells
GM02948	47,XY,+13	5 cells
GM01359	47,XY,+18	5 cells
GM00323	46,XY	5 cells
GM02067_38	47,XY,+21	5 cells
GM11873_15	46,XY	5 cells
GM11872_13	46,XY	5 cells
GM03184_2	47,XY,+15	5 cells
GM03184_1	47,XY,+15	5 cells
GM01359_479	47,XY,+18	5 cells
GM01359_478	47,XY,+18	5 cells
GM00323_404	46,XY	5 cells
GM00323_403	46,XY	5 cells
GM00323_402	46,XY	5 cells
GM00323_401	46,XY	5 cells
GM00980_9	46,XX	5 cells
GM00980_8	46,XX	5 cells
GM04626_30	47,XXX	5 cells
GM01201_47	45,XX,-21	5 cells
GM11875_7	46,XX	5 cells

**Table 1:** karyotype and sample type for each sample employed in the first phase of 4-plex validation procedure.

Sample ID	Karyotype	Sample type
48967_3	45,XX,-13	TE biopsy
48822_1	45,XX,-15	TE biopsy
49252_4	45,XX,-17	TE biopsy
49262_15	45,XX,-19	TE biopsy
49199_1	45,XX,-2	TE biopsy
49200_2	45,XX,-22	TE biopsy
48921_1	45,XX,-4	TE biopsy
48973_1	47,XX,+10	TE biopsy
49174_7	47,XX,+18	TE biopsy
49193_8	47,XX,+2	TE biopsy
48820_8	47,XX,+21	TE biopsy
49253_1	47,XX,+7	TE biopsy
49174_2	47,XX,+9	TE biopsy
49012_11	47,XXX	TE biopsy
48863_2	45,XY,-10	TE biopsy
48831_11	45,XY,-14	TE biopsy
49255_2	45,XY,-15	TE biopsy
48995_1	45,XY,-16	TE biopsy
48858_6	45,XY,-17	TE biopsy
48849_3	45,XY,-21	TE biopsy
48863_17	45,XY,-5	TE biopsy

Sample ID	Karyotype	Sample type
49177_30	45,XY,-9	TE biopsy
48834_2	47,XY,+1	TE biopsy
48973_3	47,XY,+13	TE biopsy
48917_2	47,XY,+16	TE biopsy
48917_11	47,XY,+16	TE biopsy
49048_11	47,XY,+17	TE biopsy
48837_6	47,XY,+21	TE biopsy
48837_12	47,XY,+5	TE biopsy
48837_27	47,XY,+9	TE biopsy
49170_17	46,XX,+9,-21	TE biopsy
48858_7	46,XX,-15,+19	TE biopsy
48864_21	46,X0,+3	TE biopsy
49193_10	46,XX,-17,+22	TE biopsy
49200_9	46,XX,-18,+22	TE biopsy
49200_28	46,XY,+16,-22	TE biopsy
48828_1	46,XY,-18,+22	TE biopsy
48849_1	48,XY,+16,+19	TE biopsy
49029_3	49,XX,+3,+10,+11	TE biopsy
49262_13	49,XX,+6,+8,+10	TE biopsy
48752_9	47,XY,+11,-18,+21	TE biopsy

**Table 2:** karyotype and sample type for each sample employed in the second phase of 4-plex validation procedure.

### 3.1.3.2 Lysis and preamplification

Cell line samples and embryo biopsies were processed by alkaline lysis adding 6 µl of molecular grade water and 1 µl of KOH. Samples are then incubated at 60°C for 10 min and finally treated with 1 µl of neutralisation solution. Multiplex amplification of 96 loci (four for each chromosome, as previously described (Treff *et al.*, 2012) was performed with the use of TaqMan Copy Number Assays and TaqMan Preamplification Master Mix (Thermofisher Scientific) according to the proportions specified in Table 3. 40 µl of freshly prepared master mix were added to each sample and the negative control (total volume 50 µl).

TaqMan PreAmp Master mix	PreAmp Primer Pool	MBG Water
25 µl	12.5 µl	2.5 µl

**Table 3:** preamplification master mix components and quantities

The samples were incubated in a PCR 2720 AB thermo-cycler using the following program settings:

Stage	Number of cycles	Temperature of cycle	Incubation time
1. Enzyme activation (hold)	1	75 °C	10 min
2. PCR (cycle)	18	95 °C	15 sec
		60 °C	4 min
3. Hold	1	22 °C	Hold

**Table 4:** thermic profile of preamplification reaction

### 3.1.3.3 Amplification

A master mix was prepared for each sample adding 500 µl of TaqMan™ Gene Expression Master Mix (Thermofisher Scientific) and 483 µl of Sterile nuclease free water (VWR). Then 17 µl of each preamplification product were added to the correspondent master mix tube. 5ul of the reaction mix was added into each well of the dried assay plate containing 4 different TaqMan probes for chromosomal analysis linked with 4 different fluorescent dyes: VIC, FAM, ABY and JUN. Real-time PCR was performed in quadruplicate for each of the individual 96 loci filling the plate as follow: first sample aliquot down the odd column (blue arrows) from A to H, the second sample aliquot down the odd columns (orange arrows) from I to P, the third sample down the even column (blue arrows) from A to H, and then the fourth sample aliquot down the even columns (green arrows) from I to P (Figure 3).

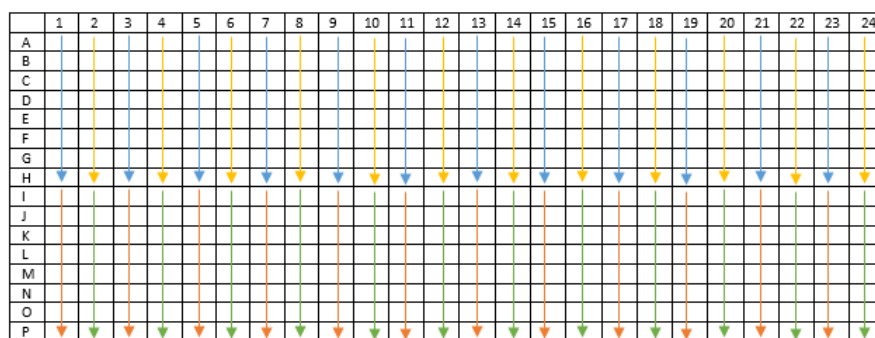


**Figure 3:** sample loading scheme on 4-plex plate

The plate was then loaded in the QuantStudio™ Dx Real-Time PCR Instrument using program setting in table below:



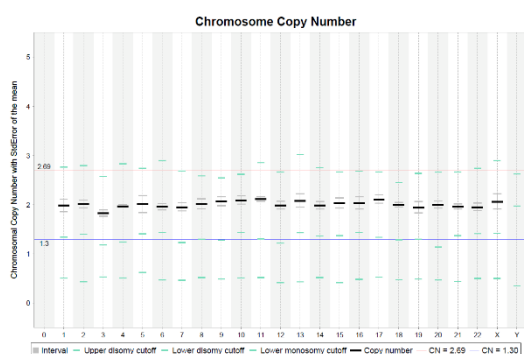
Stage	Number of cycles	Temperature of cycle	Incubation time
1. Hold	1	50 °C	2 min
2. Enzyme activation	1	95 °C	10 min
3. PCR cycle	40	95 °C	15 sec
3. Hold	1	60 °C	1 min

**Table 5:** thermic profile of amplification reaction

A unique method of the standard delta delta threshold cycle ( $\Delta\Delta C_t$ ) of relative quantitation was applied (Treff *et al.*, 2012). First, a chromosome-specific  $\Delta C_t$  was calculated from the average  $C_t$  of the 16 reactions targeting a specific chromosome (four replicates of four loci) minus the average  $C_t$  of all of the 336 reactions targeting all of the remaining autosomes (four replicates of four loci of 21 remaining autosomes). The same process was used to individually determine the  $\Delta C_t$  for each of the 24 chromosomes in the test sample. Each chromosome-specific  $\Delta C_t$  was then normalized to the average chromosome specific  $\Delta C_t$  values derived from the same evaluation of a pool of normal male samples (reference set). The resulting chromosome-specific  $\Delta\Delta C_t$  values were used to calculate fold change by considering the  $\Delta\Delta C_t$  values as the negative exponent of 2, as previously described (Schmittgen and Livak, 2008). All autosome fold changes were then multiplied by 2, whereas the sex chromosome fold changes were used as is, to determine the 24-chromosome copy number in each sample. This methodology was designed to specifically identify whole chromosome but not segmental aneuploidies.

### 3.1.3.4 Bioinformatic analysis

Export files are loaded on the qPCR software version 1.1.13 for the copy number variation analysis (CNV) analysis of the chromosomes. Once the excel files have been uploaded, the group of reference samples (all with known karyotype 46, XY) is selected. The result is displayed as a graph showing all the chromosomes in the abscissa and the number of copies in the ordinate. Moreover, in the graph there are 2 specific reference limits (cut-offs) for each chromosome: the upper cutoff and the lower one of the disomy. In this way, the software automatically identifies any chromosomal aneuploidies.



21

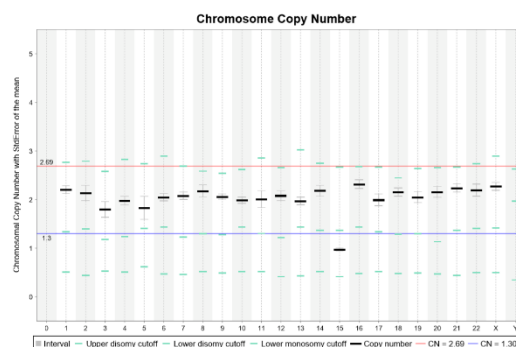


**Figure 4:** examples of resulting profiles from a normal female embryo (A) and an aneuploid male embryo carrying a monosomy of chromosome 15 (B). In the first plot, chromosome copy number is inside the upper and lower cutoff for disomy. In the second plot, copy number for chromosome 15 is below the cutoff of monosomy.

In order to define sensitivity and specificity of cell line or TE result with respect to their reference karyotype, we firstly classified each aneuploidy as true positive (TP, abnormal reference karyotype and abnormal PGT-A result), true negative (TN, normal reference karyotype and normal PGT-A result), false positive (FP, normal reference karyotype and abnormal PGT-A result), false negative (FN, abnormal reference karyotype and normal PGT-A result). Sensitivity was calculated as the percentage of abnormal chromosome correctly predicted as aneuploid, while specificity was defined as the percentage of euploid chromosomes detected for all chromosomes expected to be normal. Positive (PPV) and negative predictive values (NPV) were calculated as the proportion of positive and negative results that were true positive and true negative [PPV=TP/(TP+FP); NPV=TN/(TN+FN)].

### 3.1.3.5 Quality control measure

There are several quality criteria that must be satisfied to make a diagnosis with this method. The main quality parameters in qPCR are based on the number of copies (CN) of each single technical replicate of the 4 assays amplified in each chromosome. Chromosomal CN and chromosomal concordance are calculated, which are the mean and standard deviation (SD) of the CN of each replicate on that chromosome, respectively. Finally, an overall inter-chromosomal SD is also calculated, thus the CN SD of all the chromosomes and an overall concordance, thus the average of all chromosomal concordances.

Cut-off value for overall concordance:  $\leq 0.5$

Cut-off value for interchromosomal DS for embryos with karyotype 46, XX:  $\leq 0.18$

Cut-off value for interchromosomal DS for embryos with karyotype 46, XY:  $\leq 0.32$

### 3.1.4 RESULTS

In the first phase, all samples from fibroblasts cell lines showed a concordant diagnosis with the expected outcome, both on a per sample (n=20/20,100%;95%IC=83.16-100.00) and on a per chromosome basis (n=460/460,100%;95%CI=99.20-100.00) Table 6. Sensitivity and specificity were 100% (n=11/11;95%IC=71.51-100.00) and 100%(n=449/449;95%IC=99.18-100.00) respectively. In the second phase, 117/123 biopsies analyzed in fourplex plates (95.1%;95%IC=89.68-98.12) produced a concordant result with TE biopsy previously

analyzed in duplex plates (Table 7). Only 4/41 samples (9.8%; 95%IC=2.72-23.13) corresponding to 6/123 biopsies (4.9%; 95%IC=1.81-10.32) produced discordant results, all due to single chromosome aneuploidy misdiagnosis (false negative). In this study, no false positive (overestimation of aneuploidies) cases were reported. Finally, 99.8% (n=2823/2829; 95%IC=99.54-99.92) of per chromosome concordance was obtained. Sensitivity and specificity were respectively 96.3% (n=156/162;95%IC=92.11-99.9) and a 100% (n=2667/2667; 95%IC=98.86-100.00) respectively.

This preliminary study on TE rebiopsies using 4-plex qPCR protocol, showed high levels of sensitivity and specificity both on cell lines and TE re-biopsies. Some of the discordant cases could be explained by a minimum level of biological variability within blastocysts. The introduction into clinical practice of this new enhanced throughput protocol will further reduce time and costs of individual analysis, enabling a growing number of patients to benefit from it.

Sample ID	Original karyotype	4-plex results
GM04435	48,XY,+16,+21	48,XY,+16,+21
GM02948	47,XY,+13	47,XY,+13
GM01359	47,XY,+18	47,XY,+18
GM00323	46,XY	46,XY
GM02067_38	47,XY,+21	47,XY,+21
GM11873_15	46,XY	46,XY
GM11872_13	46,XY	46,XY
GM03184_2	47,XY,+15	47,XY,+15
GM03184_1	47,XY,+15	47,XY,+15
GM01359_479	47,XY,+18	47,XY,+18
GM01359_478	47,XY,+18	47,XY,+18
GM00323_404	46,XY	46,XY
GM00323_403	46,XY	46,XY
GM00323_402	46,XY	46,XY
GM00323_401	46,XY	46,XY
GM00980_9	46,XX	46,XX
GM00980_8	46,XX	46,XX
GM04626_30	47,XXX	47,XXX
GM01201_47	45,XX,-21	45,XX,-21
GM11875_7	46,XX	46,XX

**Table 6:** karyotype and sample type for each sample employed in the first phase of the validation procedure.

Sample ID	RMA NJ RESULT	Duplex result (B)	4-plex result (C)	4-plex result (D)	4-plex result (E)
48967_3	45,XX,-13	45,XX,-13	45,XX,-13	45,XX,-13	45,XX,-13
48822_1	45,XX,-15	45,XX,-15	45,XX,-15	45,XX,-15	45,XX,-15
49252_4	45,XX,-17	45,XX,-17	45,XX,-17	45,XX,-17	45,XX,-17
49262_15	45,XX,-19	45,XX,-19	45,XX,-19	45,XX,-19	45,XX,-19
49199_1	45,XX,-2	45,XX,-2	45,XX,-2	45,XX,-2	45,XX,-2
49200_2	45,XX,-22	45,XX,-22	45,XX,-22	45,XX,-22	45,XX,-22
48921_1	45,XX,-4	45,XX,-4	45,XX,-4	45,XX,-4	45,XX,-4
48973_1	47,XX,+10	47,XX,+10	47,XX,+10	47,XX,+10	47,XX,+10
49174_7	47,XX,+18	47,XX,+18	47,XX,+18	46,XX	47,XX,+18
49193_8	47,XX,+2	47,XX,+2	47,XX,+2	47,XX,+2	47,XX,+2
48820_8	47,XX,+21	47,XX,+21	47,XY,+21	46,XY	47,XY,+21
49253_1	47,XX,+7	47,XX,+7	47,XX,+7	47,XX,+7	47,XX,+7
49174_2	47,XX,+9	47,XX,+9	47,XX,+9	47,XX,+9	47,XX,+9
49012_11	47,XXX	47,XXX	46,XXX	46,XXX	46,XXX
48863_2	45,XY,-10	45,XY,-10	45,XY,-10	45,XY,-10	45,XY,-10
48831_11	45,XY,-14	45,XY,-14	45,XY,-14	46,XY,-14	45,XY,-14
49255_2	45,XY,-15	45,XY,-15	45,XY,-15	45,XY,-15	45,XY,-15
48995_1	45,XY,-16	45,XY,-16	45,XY,-16	45,XY,-16	45,XY,-16
48858_6	45,XY,-17	45,XY,-17	45,XY,-17	45,XY,-17	45,XY,-17
48849_3	45,XY,-21	45,XY,-21	45,XY,-21	45,XY,-21	45,XY,-21
48863_17	45,XY,-5	45,XY,-5	45,XY,-5	45,XY,-5	45,XY,-5
49177_30	45,XY,-9	45,XY,-9	45,XY,-9	45,XY,-9	45,XY,-9
48834_2	47,XY,+1	47,XY,+1	47,XY,+1	47,XY,+1	47,XY,+1
48973_3	47,XY,+13	47,XY,+13	47,XY,+13	47,XY,+13	47,XY,+13
48917_2	47,XY,+16	47,XY,+16	47,XY,+16	47,XY,+16	47,XY,+16
48917_11	47,XY,+16	47,XY,+16	47,XY,+16	47,XY,+16	47,XY,+16
49048_11	47,XY,+17	47,XY,+17	47,XY,+17	47,XY,+17	47,XY,+17
48837_6	47,XY,+21	47,XY,+21	47,XY,+21	47,XY,+21	47,XY,+21
48837_12	47,XY,+5	47,XY,+5	47,XY,+5	47,XY,+5	47,XY,+5
48837_27	47,XY,+9	47,XY,+9	47,XY,+9	47,XY,+9	47,XY,+9
49170_17	46,XX,+9,-21	46,XX,+9,-21	XX,+9,-21	XX,+9,-21	XX,+9,-21
48858_7	46,XX,-15,+19	46,XX,-15,+19	46,XX,-15,+19	46,XX,-15,+19	46,XX,-15,+19
48864_21	46,X,+3	46,X,+3	46,X,+3	46,X,+3	46,X,+3
49193_10	46,XX,-17,+22	46,XX,-17,+22	46,XX,-17,+22	46,XX,-17,+22	46,XX,-17,+22
49200_9	46,XX,-18,+22	46,XX,-18,+22	46,XX,-18,+22	46,XX,-18,+22	46,XX,-18,+22
49200_28	46,XY,+16,-22	46,XY,+16,-22	46,XY,+16,-22	46,XY,+16,-22	46,XY,+16,-22
48828_1	46,XY,-18,+22	46,XY,-18,+22	46,XY,-18,+22	46,XY,-18,+22	46,XY,-18,+22
48849_1	48,XY,+16,+19	48,XY,+16,+19	48,XY,+16,+19	48,XY,+16,+19	48,XY,+16,+19
49029_3	49,XX,+3,+10,+11	49,XX,+3,+10,+11	48,XX,+10,+11	48,XX,+10,+11	48,XX,+10,+11
49262_13	49,XX,+6,+8,+10	49,XX,+6,+8,+10	49,XX,+6,+8,+10	49,XX,+6,+8,+10	49,XX,+6,+8,+10
48752_9	47,XY,+11,-18,+21	47,XY,+11,-18,+21	47,XY,+11,-18,+21	46,XY,+11,-18	47,XY,+11,-18,+21

**Table 7:** karyotype and sample type for each sample employed in the second phase of the validation procedure.

## **3.2 VALIDATION OF THE NEW ION REPROSEQ PROTOCOL AND INTERPLATFORM COMPARISON BETWEEN Q-PCR AND NGS-BASED PGT-A**

### **3.2.1 Introduction and aim of the study**

In January 2018, we have introduced a new NGS based protocol performed on Ion S5 platform, for routine application in PGT-A in our laboratory. The new approach replaces the previously used 24-chromosome testing method based on qPCR (Treff *et al.*, 2012; Capalbo *et al.*, 2015). This transition was marked primarily by a higher capacity of multiplexing more samples at reduced cost and by the possibility to detect segmental aneuploidies in our PGT-A program. Of note, different resolution limits have been reported amongst different NGS platforms when segmental aneuploidies are considered, showing the potential of NGS-based detection methods to detect these alterations within a biopsy (Vera-Rodríguez *et al.*, 2016; Goodrich *et al.*, 2017). This suggests that each program would need to establish own personal technological performance validation. Furthermore, little data have been reported on inter-platform PGT-A comparison. This demonstrates the high reliability of whole chromosome aneuploidies prediction in blastocyst biopsy, using different comprehensive chromosome screening methods (Capalbo *et al.*, 2015).

The purpose of this study was to firstly perform an internal validation of the new protocol in order to verify the performance values provided by the manufacturer, prior to the introduction into our PGT-A program. Secondly the study focused on assessing the concordance rates between diagnostic results obtained from our laboratory after moving from a qPCR-based PGT-A approach to an NGS-based approach from large datasets generated during years of extensive PGT-A diagnostic program. In this phase, we have been able to define the marginal contribution of segmental aneuploidies detection in the clinical PGT-A practice by comparing two methodologies with different resolution toward segmental aneuploidies as well as providing inter-platform concordance data in PGT-A analysis.

### **3.2.2 Study design and outcome measure**

The study was designed as two phases. In the first phase, we have validated the new NGS based PGT-A protocol for whole chromosome aneuploidies on cell lines. In details, we performed an internal verification of the Thermo Fisher Scientific NGS Ion ReproSeq™ platform using Ion Chef™ system plus the Ion S5™ XL Sequencer in our laboratory, to be used for PGT-A. Consistency of the cell line samples with the expected karyotype for 24-chromosome copy number predictions (previously established by the Coriell Cell Repository

by conventional karyotyping) was evaluated at the level of individual chromosome copy numbers and for the entire 24 chromosomes set of each sample tested. Sensitivity was calculated as the percentage of samples which were predicted as normal or abnormal for the correct karyotype (TP/TP+FN), while specificity was defined as the percentage of samples where euploidy was predicted for all the chromosomes expected to be normal (TN/TN+FP).

In the second phase we have compared the clinical diagnostic results obtained in 4425 consecutive TE biopsies analysed with the new NGS protocol with a qPCR-based group of results coming from our historical blastocyst stage PGT-A program (N=5166 clinical TE biopsy) (Capalbo *et al.*, 2017a). This has allowed inter-platform comparison and assessment of the relative contribution of de novo segmental aneuploidies to the overall aneuploidy rate of clinical TE samples. With the aim of verifying the clinical consistency of the new NGS-based PGT-A protocol and to evaluate the potential impact of a higher resolution system on our laboratory diagnostic routine, NGS-based PGT-A results obtained at Igenomix Italia laboratory, between February 2018 and February 2019 (n=4425, mean female age=37.85; 95%IC= 37.74-37.96) were collected and compared with a qPCR-based dataset of results previously obtained from the same laboratory during the previous year (February 2017-2018; n=5166, mean female age=38.6; 95%IC= 38.56-38.73 95%IC). Embryos were defined as normal/euploid in the absence of any alteration with respect to the reference base line, while aneuploid group contains embryos exhibiting single or multiple whole chromosome aneuploidies in the uniform range only (threshold for uniform euploid/aneuploid was established respectively at <30% and >70% of variation from the baseline). In addition, NGS results containing single or multiple segmental aneuploidies (deletion and duplication above 10 Mb), either alone or in concomitance with whole chromosome uniform aneuploidies, were classified as aneuploid. Aneuploidy rates were compared and reported at the individual chromosomal level as well as considering their global incidence across the board of female age for both technologies. Although studies on cell lines have shown the capability of NGS based protocols to increase the resolution toward chromosome copy number value variations, the diagnostic approach employed here did not consider a mosaic classification category because technical and biological variations on clinical TE NGS profiles cannot be distinguished in the absence of prospective non-selection clinical studies (Capalbo and Rienzi, 2017; Capalbo *et al.*, 2017c). Therefore, our classification scheme followed a binary approach for whole chromosome and segmental aneuploidies, disomic or uniform aneuploid.

### 3.2.3 MATERIAL AND METHODS

#### 3.2.3.1 Samples included in the verification of the Ion Reproseq PGT-A protocol

Eight commercial fibroblast cell lines and three genomic DNAs purchased from Coriell (NJ, USA), were used to validate the detection of whole chromosome aneuploidies. Single-cell fibroblast were analyzed to mimic day-3 embryo biopsies and 5-6 cells were analyzed to mimic day-5 or day-6 embryo biopsies. Genomic DNA was used at a final concentration of 30 pg/ul. In total, 48 samples were included in the validation and 2 separate experiments were performed (Table 8 A,B).

RUN A ITPGS-12042017A-VALIDATION				RUN B ITPGS-12062017A-VALIDATION			
Barcode	Sample identification	Karyotype	Sample type	Barcode	Sample identification	Karyotype	Sample type
1	NA10135_1	47, +22	genomic DNA	25	NA10135_1	47, +22	genomic DNA
2	NA10135_2	47, +22	genomic DNA	26	NA10135_2	47, +22	genomic DNA
3	NA07408_1	47, +20	genomic DNA	27	NA07408_1	47, +20	genomic DNA
4	NA07408_2	47, +20	genomic DNA	28	NA07408_2	47, +20	genomic DNA
5	NA03576_1	48, +2,+21	genomic DNA	29	NA03576_1	48, +2,+21	genomic DNA
6	NA03576_2	48, +2,+21	genomic DNA	30	NA03576_2	48, +2,+21	genomic DNA
7	GM04626_SINGLE	47, XXX	Single cell	31	GM04626_SINGLE	47, XXX	Single cell
8	GM04626_POOL	47, XXX	Pool	32	GM04626_POOL	47, XXX	Pool
9	GM03102_SINGLE	47, XXY	Single cell	33	GM03102_SINGLE	47, XXY	Single cell
10	GM03102_POOL	47, XXY	Pool	34	GM03102_POOL	47, XXY	Pool
11	GM09326_SINGLE	47, XYY	Single cell	35	GM09326_SINGLE	47, XYY	Single cell
12	GM09326_POOL	47, XYY	Pool	36	GM09326_POOL	47, XYY	Pool
13	GM03330_SINGLE	47, +13	Single cell	37	GM03330_SINGLE	47, +13	Single cell
14	GM03330_POOL	47, +13	Pool	38	GM03330_POOL	47, +13	Pool
15	GM01359_SINGLE	47, +18	Single cell	39	GM01359_SINGLE	47, +18	Single cell
16	GM01359_POOL	47, +18	Pool	40	GM01359_POOL	47, +18	Pool
17	GM04592_SINGLE	47, +21	Single cell	41	GM04592_SINGLE	47, +21	Single cell
18	GM04592_POOL	47, +21	Pool	42	GM04592_POOL	47, +21	Pool
19	NORMAL_XX_SINGLE	46, XX	Single cell	43	NORMAL_XX_SINGLE	46, XX	Single cell
20	NORMAL_XX_POOL	46, XX	Pool	44	NORMAL_XX_POOL	46, XX	Pool
21	NORMAL_XY_SINGLE	46, XY	Single cell	45	NORMAL_XY_SINGLE	46, XY	Single cell
22	NORMAL_XY_POOL	46, XY	Pool	46	NORMAL_XY_POOL	46, XY	Pool
23	NA03576_3	48, +2,+21	genomic DNA	47	NA10135_3	47, +22	genomic DNA
24	NA03576_4	48, +2,+21	genomic DNA	48	NA10135_4	47, +22	genomic DNA

**Table 8 A,B:** karyotype and sample type for each sample employed in the validation procedure.

### 3.2.3.2 Cell lysis and DNA extraction

A master mix was prepared according to the proportions specified in Table 9. 7.5 µl of freshly prepared master mix were added to each sample and the control.

Cell Extraction Buffer	Extraction Enzyme Dilution Buffer	Extraction Enzyme
2.5 µl	4.8 µl	0.2 µl

**Table 9:** lysis and extraction master mix components and quantities

The samples were incubated in a PCR thermo-cycler with the lid preheated to 95° C prior to starting the reaction, using the following program settings:

N° of cycles	Temperature of cycle	Incubation time
1	75° C	10 min
1	95° C	4 min
1	22° C	Hold

**Table 10:** thermic profile of lysis reaction

### 3.2.3.3 Pre-amplification

A master mix was prepared according to the proportions specified in table 11.

Pre-amplification Buffer	Pre-amplification Enzyme
4.8 µl	0.2 µl

**Table 11:** preamplification master mix components and quantities

5 µl of freshly prepared master mix were added to each sample and the control. The samples were taken in cold rack and incubated in a PCR thermo-cycler with the lid preheated to 99° C (for 1h 10 min) using the following program settings:

Number of cycles	Temperature of cycle	Incubation time
1	95° C	2 min
12	95° C	15 sec
	15° C	50 sec
	25° C	40 sec
	35° C	30 sec
	65° C	40 sec
	75° C	40 sec
1	4° C	Hold

**Table 12:** thermic profile of pre-amplification reaction



### 3.2.3.4 Amplification

A master mix was prepared according to the proportions specified in table 13.

Nuclease free-water	Amplification Buffer	Amplification Enzyme
2.5 $\mu$ l	27 $\mu$ l	0.5 $\mu$ l

**Table 13:** amplification master mix components and quantities

30  $\mu$ l of freshly prepared master mix were added to each sample and the control. 5  $\mu$ l of each of the SingleSeq Barcode Adapters were pipetted to the corresponding samples. The samples were taken in a cold rack and incubated in a PCR thermo-cycler with the lid preheated to 99° C using the following program settings:

Number of cycles	Temperature of cycle	Incubation time
1	95° C	3 min
4	95° C	20 sec
	50° C	25 sec
	72° C	40 sec
12	95° C	20 sec
	72° C	55 sec
1	4° C	Hold

**Table 14:** thermic profile of amplification reaction

The PCR tubes were placed into a cold rack and checked for sample amplification by agarose gel electrophoresis using Flash gel cassette 1.2% agarose (Lonza).

### 3.2.3.5 Library pooling and purification

1. A total of 5  $\mu$ L of each library were added to a new 1.5-mL tube to create an equi-volume pool. For a 530 chip up to 96 samples can be pooled together. For a 520 chip up to 24 samples can be pooled together.

2. Then 40  $\mu$ L of the library were transferred to a 0.2mL tube and heated in a thermal cycler according to the following program:

N° of cycles	Temperature of cycle	Incubation time
1	70° C	2 min
1	22° C	Hold

**Table 15:** thermic profile of library denaturation step

3. An equal volume of AMPure™ XP beads were added to the tube (40  $\mu$ L) and purification was performed according to the manufacturer instruction (Pub.no: MAN0016712).

### 3.2.3.6 Library quantification and dilution

The Ion SingleSeq library pool was quantified with the Qubit™ dsDNA HS (High Sensitivity) Assay Kit using the User Guide (Pub.no.MAN0002326).

According to the concentration of the library pool, a final dilution of 80pM was prepared.

### 3.2.3.7 Library preparation and sequencing

A volume of 50 µL of the 80pM pooled library was pipetted into the library Sample Tube (barcoded tube) from position A of the Ion S5 ExT Chef Reagents cartridge.

The sequencing chip was loaded into a centrifuge bucket and the Ion Chef™ S5 Series Chip Balance was loaded into position 2 of the Chip-loading centrifuge. When the run was completed the Ion Chef™ System was unload and the chip was sequenced immediately.

### 3.2.3.8 Data analysis and interpretation

The Ion Torrent™ dataflow (Figure 5) involves the transfer of raw sequencing data from the Ion S5™ Sequencer to the Torrent Server for analysis and reporting. The Ion sequencers output raw sequencing data in the form of DAT files. The raw measurements are the conversion of the raw pH value in a well to a digital representation of the voltage. These raw data are transferred to the Torrent Server for analysis pipeline processing. The analysis pipeline converts the raw signal measurements into incorporation measures and, ultimately, into base-calls for each read.

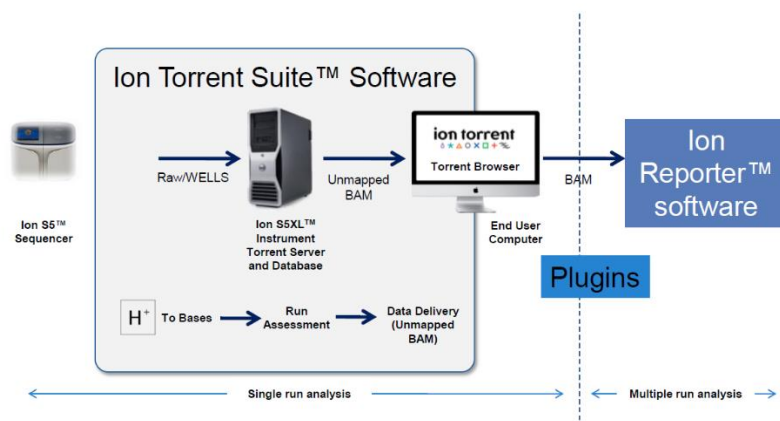
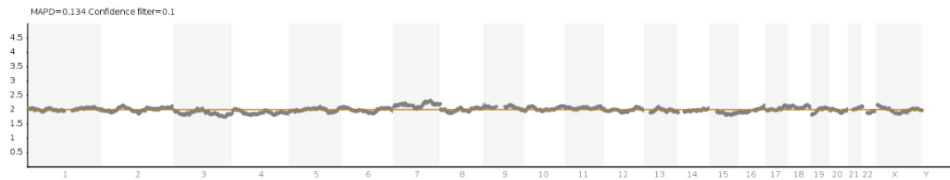


Figure 5: dataflow on Ion S5 system

Sequencing data obtained by the sequencer were processed and sent to Ion Reporter software 5.4 version for data analysis. This software uses the bioinformatic tool Represeq PGS w1.1 to detect 24 chromosomes aneuploidies from a single whole-genome sample with low coverage (minimum 0.01x). Normalization was done using the bioinformatics baseline RepreSeq Low-Coverage Whole-Genome Baseline (5.4) generated from multiple normal samples. Ion

Reporter software generates a graph representing the copy number variation (CNV) of the sample analyzed compared to the reference bioinformatics baseline. An embryo was considered as normal when it had no deviations from the reference bioinformatics baseline for any of the 24 chromosomes (Figure 6).



**Figure 6:** PGT-A profile from normal female embryo

An embryo was considered as abnormal by the presence of aneuploidy (chromosome gains or losses) when there are bins that are diverted into the upper (gain +) or lower part (-) of the graph (Figure 7).

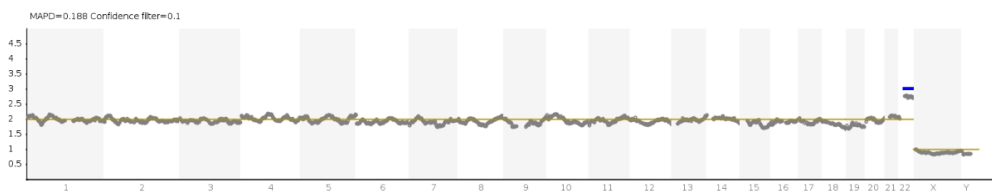


**Figure 7:** PGT-A profile from an aneuploid male embryo, showing a trisomy of chromosome 22.

The aneuploidies could be for a full chromosome, when all the bins covering a chromosome are gained or lost, or partial aneuploidies, when the bins gained or lost represent only part of the chromosome. These abnormalities are usually called deletions or duplications. The presence of aneuploidies for most of the chromosomes on the same specimen is interpreted as a complex abnormal embryo (Figure 8).

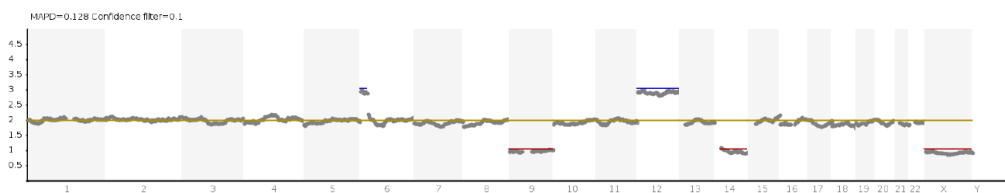


**Figure 8:** PGT-A profile from a complex aneuploid embryo, showing a partial duplication of chromosome 6, deletions of chromosomes 9, 14 and X and duplication of chromosome 12.

With this technique was not possible to identify deletions and duplications smaller than the limit of resolution of the platform used (10Mb as internal validation), balanced structural abnormalities, mosaic aneuploidy in low grade and defects affecting the complete set of chromosomes (haploidy, triploidy, etc).

### 3.2.3.9 Quality parameters

There are several quality criteria that should be met to emit a diagnosis. In details two relevant points were evaluated accordingly to the optimal values reported in table 16 :

- 1) the run (where all the embryos are analyzed);
- 2) the analysis of each embryo independently

QUALITY PARAMETERS NGS-PGT-A	
Run parameters	Optimal value
Loading	>70%
Life ISPS	>98%
Usable Reads	>30%
Policlonality	<50%
Sample parameters	Optimal value
Duplicated reads	<30%
MAPD*	<0.35
Reads per sample	>70.000

**Table 16:** Quality control parameters and related optimal values for Reproseq protocol on Ion torrent S5 platform.

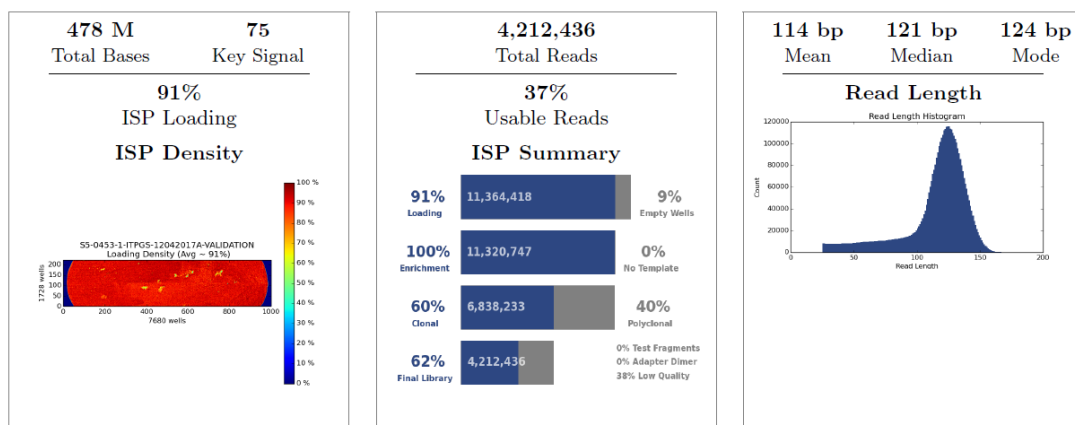
## 3.2.4 RESULTS

### 3.2.4.1 Validation of the new Reproseq protocol for routine application

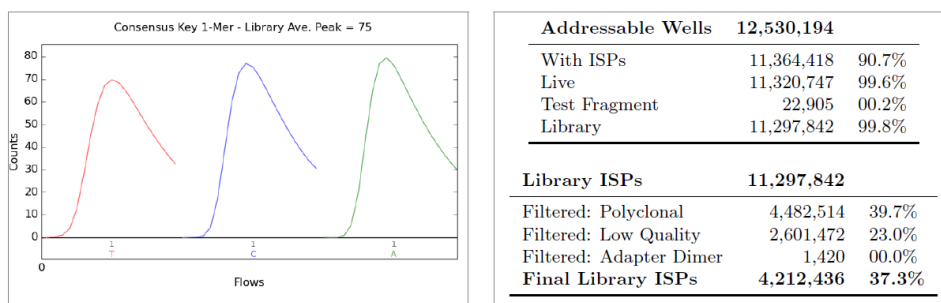
Before the evaluation of NGS results, quality control values for the run and for each single sample were firstly validated accordingly to the optimal values. One of the most relevant parameters is “loading” which represent the percentage of wells (out of all potentially addressable wells on the chip) loaded with an Ion Sphere™ Particle (ISP). Another important factor is “life ISPS”, the percentage of wells (out of total wells) that contain an ISP with a signal of enough strength and composition to be associated with the library or Test Fragment key. The “usable reads” is the percentage of Library ISPs that pass the polyclonal, low quality, and primer dimer filters. Finally, “policlonality” represents the percentage of ISP with “mixed” reads: even if the presence of polyclonal products is minimized during enrichment steps, they will always be present in the sample. Considering these relevant quality control parameters, we reported that both sequencing experiments, performed during the validation, reached the optimal quality control values, allowing to validate the overall “run”. Figures 9 and 10 summarize the most interesting parameters values obtained for both validation runs. Regarding optimal quality control values related to each single sample analysed, the percentage of duplicated reads, the total number of reads per sample and the

MAPD value were considered. In details ‘MAPD’ is used to assess sample variability and define whether the data are useful for copy number analysis. Considering these parameters, we reported that all samples included in the validation have passed the acceptable quality values to be able to emit a reliable diagnostic result. Individual reports of quality control analysis are summarized in appendix 1 and 2.

A



B



Alignment Summary (aligned to *Homo sapiens*)

C

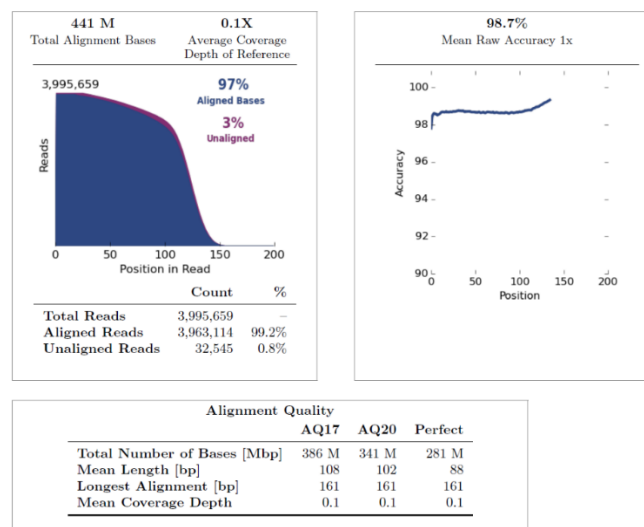
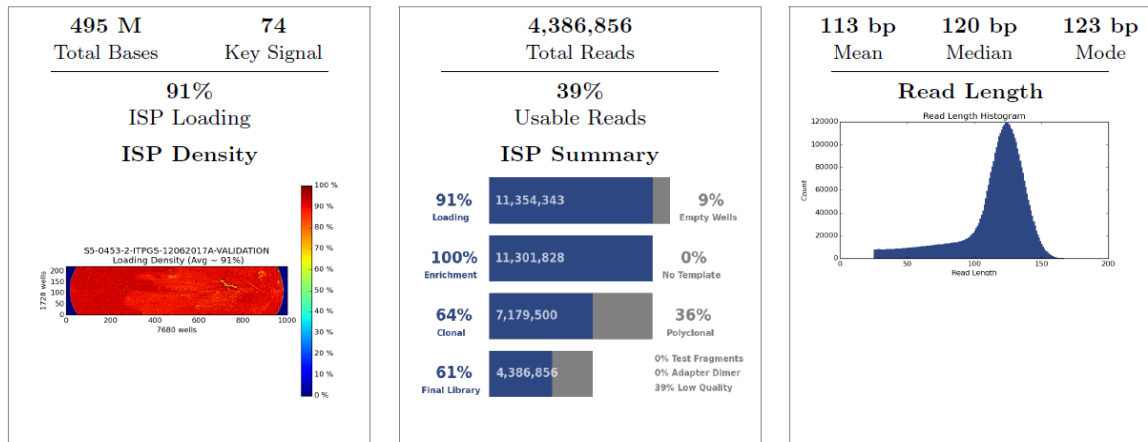
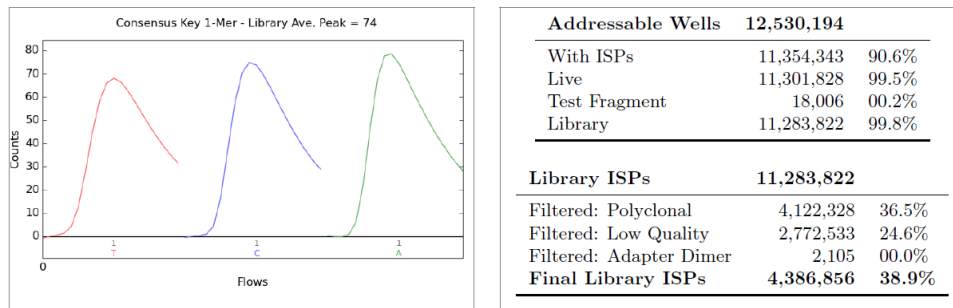


**Figure 9: A,B,C Run Report for ITPGS-12042017A (Run1)**

A



B



**Alignment Summary (aligned to *Homo sapiens*)**

C

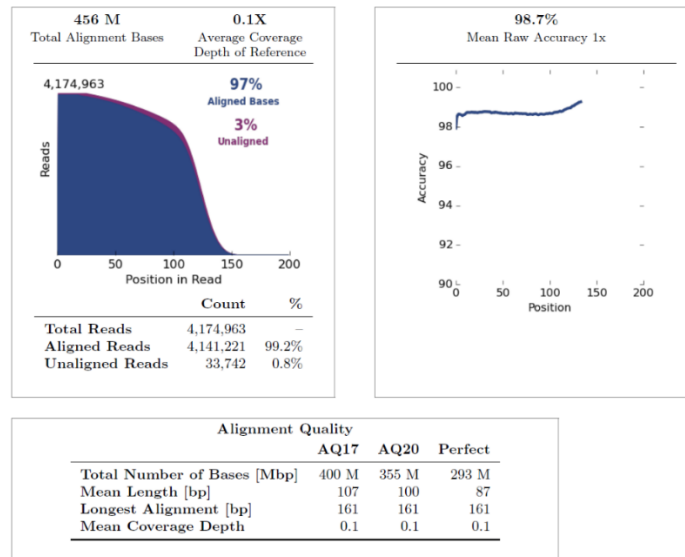


**Figure 10: A,B,C Run Report for ITPGS-12062017AR (Run2)**

Following the evaluation of Ion Reporter profiles we recorded the karyotype and relative values of quality for each sample. These data are summarized in tables 17 and 18.

Barcode	Sample identification	Karyotype	ION CHEF + S5 RESULTS	READS	MAPD
1	NA10135_1	47, +22	47, +22	191,690	0.146
2	NA10135_2	47, +22	47, +22	193,168	0.149
3	NA07408_1	47, +20	47, +20	145,459	0.162
4	NA07408_2	47, +20	47, +20	161,303	0.16
5	NA03576_1	48, +2,+21	48, +2,+21	206,235	0.142
6	NA03576_2	48, +2,+21	48, +2,+21	146,702	0.163
7	GM04626_SINGLE	47, XXX	47, XXX	191,553	0.146
8	GM04626_POOL	47, XXX	47, XXX	158,018	0.159
9	GM03102_SINGLE	47, XXY	47, XXY	176,303	0.19
10	GM03102_POOL	47, XXY	47, XXY	173,232	0.141
11	GM09326_SINGLE	47, XYY	47, XYY	229,748	0.14
12	GM09326_POOL	47, XYY	47, XYY	92,464	0.196
13	GM03330_SINGLE	47, +13	47, +13	154,963	0.164
14	GM03330_POOL	47, +13	47, +13	92,623	0.192
15	GM01359_SINGLE	47, +18	47, +18	171,875	0.176
16	GM01359_POOL	47, +18	47, +18	142,992	0.156
17	GM04592_SINGLE	47, +21	47, +21	160,188	0.162
18	GM04592_POOL	47, +21	47, +21	135,325	0.172
19	NORMAL_XX_SINGLE	46, XX	46, XX	145,428	0.169
20	NORMAL_XX_POOL	46, XX	46, XX	212,568	0.131
21	NORMAL_XY_SINGLE	46, XY	46, XY	173,466	0.16
22	NORMAL_XY_POOL	46, XY	46, XY	211,861	0.144
23	NA03576_3	48, +2,+21	48, +2,+21	172,647	0.148
24	NA03576_4	48, +2,+21	48, +2,+21	153,313	0.159

**Table 17:** RUN A ITPGS-12042017A-VALIDATION results

Barcode	Sample identification	Karyotype	ION CHEF + S5 RESULTS	READS	MAPD
25	NA10135_1	47, +22	47, +22	205,168	0.143
26	NA10135_2	47, +22	47, +22	211,714	0.14
27	NA07408_1	47, +20	47, +20	222,030	0.128
28	NA07408_2	47, +20	47, +20	200,551	0.139
29	NA03576_1	48, +2,+21	48, +2,+21	224,145	0.142
30	NA03576_2	48, +2,+21	48, +2,+21	237,787	0.134
31	GM04626_SINGLE	47, XXX	47, XXX	129,491	0.174
32	GM04626_POOL	47, XXX	47, XXX	152,358	0.176
33	GM03102_SINGLE	47, XXY	47, XXY	163,214	0.218
34	GM03102_POOL	47, XXY	47, XXY	140,940	0.17
35	GM09326_SINGLE	47, XYY	47, XYY	183,140	0.147
36	GM09326_POOL	47, XYY	47, XYY	141,553	0.157
37	GM03330_SINGLE	47, +13	47, +13	135,030	0.17

38	GM03330_POOL	47, +13	47, +13	141,076	0.164
39	GM01359_SINGLE	47, +18	47, +18	179,381	0.161
40	GM01359_POOL	47, +18	47, +18	125,481	0.182
41	GM04592_SINGLE	47, +21	47, +21	135,749	0.195
42	GM04592_POOL	47, +21	47, +21	111,040	0.186
43	NORMAL_XX_SINGLE	46, XX	46, XX	193,936	0.143
44	NORMAL_XX_POOL	46, XX	46, XX	234,345	0.138
45	NORMAL_XY_SINGLE	46, XY	46, XY	208,501	0.187
46	NORMAL_XY_POOL	46, XY	46, XY	155,989	0.153
47	NA10135_3	47, +22	47, +22	173,663	0.151
48	NA10135_4	47, +22	47, +22	168,681	0.158

**Table 18:** RUN B ITPGS-12062017A-VALIDATION results

The comparison between PGT-A results obtained from each single cell line and the expected karyotype resulted in 100% of per chromosome concordance (n=1104/1104; 95%CI=99.75-99.95) and 100% of per sample concordance (n=48/48;95%CI=93.41-98.24). Sensitivity per chromosome was 100.0% (n=46/46;95%CI=92.29-100.00) and specificity 100% (n=1058/1058;95%CI=99.65-100.00)

#### **3.2.4.2 qPCR and NGS based aneuploidy testing: inter-platform comparison**

Once the internal validation of the new protocol was concluded, NGS-based technology was introduced into clinical practice and routinely applied to perform PGT-A. NGS-based diagnostic results reported between January 2018 and January 2019 were evaluated and compared with a q-PCR-based group of results. In the clinical PGT-A setting, the overall aneuploidy rate from trophoctoderm biopsy analysed with NGS was 56.6% (n=2505/4425; IC95%=55.13-58.08). In details, the percentage of results with at least one segmental aneuploidy was 5.45% (n=241/4425; IC95%=4.80-6.16), while the percentage of embryos carrying a segmental alteration alone was 2.64% (n=117/4425; IC95%=2.19-3.16). NGS-based aneuploidy rate turned out to be not significantly different from the qPCR-based aneuploidy rate (55.30%, n=2857/5166;IC95%=53.9-56.7; P=0.201), suggesting that the inclusion of segmental aneuploidies detection does not affect the pool of abnormal embryos compared to lower resolution qPCR method (Figure 11).



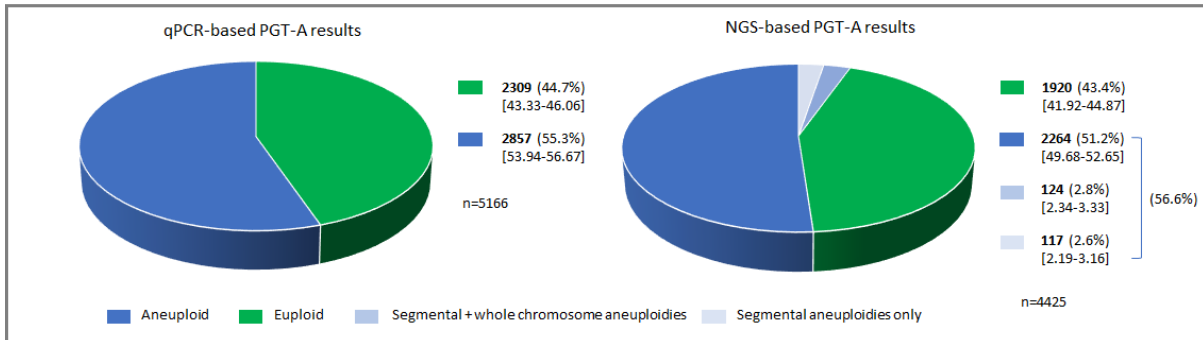


**Figure 11:** comparison of the PGT-A results between qPCR and NGS-based platform.

Focusing on the distribution of aneuploidies with respect to which chromosome was involved, we reported an overlapping trend between the two groups of results (Fig 12A). In details whole chromosome aneuploidies mainly involved smaller chromosomes, with higher rates reported for chromosomes 15, 16, 21 and 22 for both groups. These data perfectly match aneuploidy rates and trend previously reported in other studies (Rubio *et al.*, 2017). Considering the total number of abnormal chromosomes detected with NGS-based PGT-A, 43.3% of alterations were uniform whole chromosome monosomies, 50.9% were uniform trisomies and 5.8% were segmental aneuploidies (Figure 13A). Comparison between the percentage of all chromosome losses (whole chromosome and segmental) detected with NGS (47.04%) and qPCR (44.46%) didn't show significant differences ( $P = 0.16$ ). Similarly, no significant differences were observed in the percentage of all chromosome gains between the two platforms (52,96% for NGS vs 55,54% for qPCR,  $P = 0.16$ ). Another important parameter evaluated was the percentage of aneuploidies reported according to maternal age. As expected, aneuploidy rates increase at increasing maternal age for both groups of results but without differences between the two technologies ( $P = \text{Not Significant}$ ; Figure 12B).

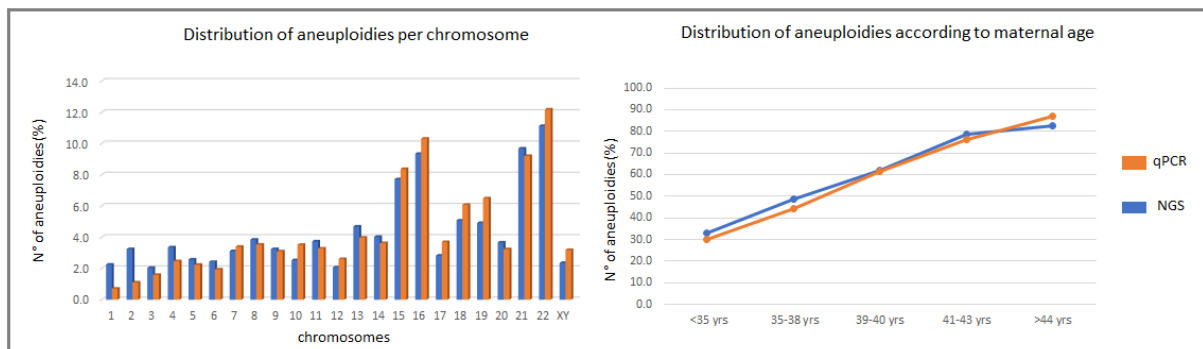


**Figure 12:** comparison of the PGT-A results between qPCR and NGS-based platform: **A:** distribution of aneuploidies per chromosome. **B:** prevalence of aneuploidy according to maternal age.

Finally, considering segmental aneuploidies category identified only with NGS approach, we evaluated their distribution among different chromosomes and the type of alteration involved. Our data showed that segmental alterations occurred more frequently as deletions in the long arms of larger chromosomes (Figure 13B).

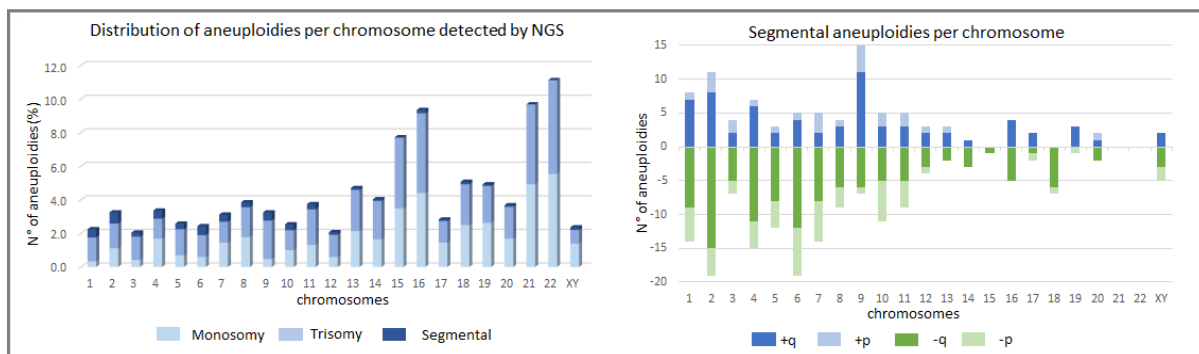


**Figure 13:** Distribution of aneuploidies detected by NGS **A:** Distribution of monosomies, trisomies and segmental aneuploidies per chromosome. **B:** Distribution of segmental aneuploidies according to chromosome carrier and types (losses on the small or large chromosome-arm: -p, -q, respectively; or gains on the small or large chromosome-arm: +p, +q, respectively).

### **3.3 SEGMENTAL ANEUPLOIDIES CHARACTERIZATION AND PREDICTIVE VALUE ANALYSIS**

#### **3.3.1 Introduction and aim of the study**

Once the internal validation of the new platform was concluded and Ion Reproseq protocol was implemented to perform PGT-A, the upgrade in the resolution capabilities became evident with the increased detection of segmental aneuploidies. Despite their relative low frequency in preimplantation embryos, from our PGT-A clinical data we reported an overall frequency of 5.45%. However, it is not yet clear whether the higher detection of these abnormalities is a consequence of the methodology employed for analysis or a true biological finding. Because of the unknown origin and impact of segmental aneuploidies on embryo development they are generally considered as evidence of embryo aneuploidy and documented in the diagnostic report to the clinics and patients and these embryos are discarded and not used for transfer. Additionally, a definitive assessment of their incidence and origin has yet to be determined. Considering lack of knowledge regarding these types of alteration, reporting segmental aneuploidy in PGT-A cycles without further knowledge of their origin or evidence of their true detection and biological presence can be seen as a potentially risk procedure.

With the aim of producing more meaningful data on segmental aneuploidies and generating more robust data regarding their overall incidence in preimplantation embryos, we used clinical TE re-biopsies and blastocysts donated for research (euploid and with segmental aneuploidies) showing a segmental aneuploidy in the clinical TE biopsy to evaluate the positive and negative diagnostic predictive values on remaining embryos. This has allowed to evaluate biological mechanisms responsible for segmental aneuploidies observation at the blastocyst stage and to assess the clinical predictive values considering also potential important variables for enhancing the confirmation of the aneuploidy finding.

#### **3.3.2 Study design and outcome measure**

A cohort study blinded to the geneticist was carried out to assess positive and negative predictive values for segmental aneuploidy detection in TE biopsies. To this aim we analysed with Ion Reproseq PGT-A protocol two different group of samples. Firstly, 51 blastocysts known to carry segmental aneuploidies, either in concomitance or not with whole chromosome aneuploidies, were warmed, allowed to re-expand subjected to a second clinical TE re-biopsy to evaluate confirmation rates in a clinical setting, where only one additional TE biopsy can be safely obtained to further evaluate an original PGT-A results (Cimadomo et

al., 2018). In details a total of the 102 samples were collected at GENERA centre for reproductive medicine Italy under IRB approval and informed consent form. In this set of data, concordance was established when in the TE re-biopsy we observed the same segmental finding (fully concordant) or a different chromosomal abnormality involving the same chromosome (partially concordant). In the case of reciprocal events in the rebiopsies, a mitotic origin could be confirmed. In case of confirmation failure on a second TE biopsy, mosaicism or technical artefact could not be distinguished and were considered concomitantly as possible explanations. Next, a second subset of blastocysts donated for research from Bahceci clinic in Cyprus with normal and abnormal (at least one segmental error detected in the uniform range) PGT-A result detected by NGS on clinical TE biopsies. The investigative approach involved multifocal analysis of both several portions of the TE tissue and the ICM. 25 normal and 53 abnormal embryos known to carry segmental aneuploidies (either in concomitance or not with whole chromosome aneuploidies) were warmed, allowed to re-expand and subjected to ICM isolation and multiple TE biopsies using a previously described and validated methodology (Capalbo *et al.*, 2013). In the multifocal analysis, concordance rates were calculated comparing overall PGT-A results from all TE biopsies from the same blastocyst and the correspondent ICM. In details, from the overall comparison, the result was considered concordant when the abnormality, found in the clinical biopsy of TE, was present in the ICM and in all TE biopsies. These outcomes were considered consistent with a pattern of meiotic origin. Results were also confirmed when one of the TE biopsies showed the same segmental finding or a different aneuploidy pattern on the same chromosome (reciprocal or whole chromosome). In this case, the aneuploidy was considered to be originating as a consequence of mitotic error leading to mosaicism. Furthermore, the aneuploidy was considered confined to TE when was uniformly detected in all TE samples but not in the ICM. As opposite, results were considered as not confirmed when the alteration found in clinical TE biopsy was not detected in ICM sample and in any of the remaining TE biopsies. This last scenario was interpreted as consistent with a pattern of low mosaicism or as technical artefact (not confirmed). When ICM result was not available, the overall comparison between all TE samples was considered using same principle for classification.

### 3.3.3 MATERIAL AND METHODS

#### 3.3.3.1 Samples included

In the table below are reported the total number of samples included in the study.

**Table 19:** summary of samples included in the double clinical TE and multifocal blastocyst analysis

	Clinical TE (1)	ICM	Second clinical TE biopsy (2)	TE biopsy (3)	TE biopsy (4)
Group 1	51		51		
Group 2	78	78	78	78	78
Total number of samples	129	78	129	78	78

#### 3.3.3.2 PGT-A analysis

Embryo culture and clinical TE biopsies were performed as previously described (Capalbo, 2014). For NGS based PGT-A, clinical TE biopsies were subjected to genomic DNA extraction and WGA using Ion Reproseq PGS kit (ThermoFisher). Template preparation and chip loading was performed with Ion Chef system according to manufacturer instructions. Chip was then loaded and sequenced on Ion S5<sup>TM</sup> XL Sequencer<sup>TM</sup>.

#### 3.3.3.3 Interpretation of sequencing data and diagnosis

Sequencing data obtained by the S5<sup>TM</sup> XL Sequencer are processed and sent to the Ion Reporter software for data analysis. Aneuploidies and copy number variations are analysed with the Ion Reporter<sup>TM</sup> Software version 5.4 (Thermo Fisher Scientific). This software uses the bioinformatic tool ReproSeq Low-pass whole-genome aneuploidy workflow v1.1 to detect 24 chromosomes aneuploidies from a single whole-genome sample with low coverage (minimum 0.01x). Data obtained from the Ion Reporter files for each embryo are analysed by Igenomix proprietary algorithm to release an automated result including detection of segmental aneuploidies (Rubio *et al.*, 2019b). Segmental aneuploidies >10Mb are manually identified if only a fragment of the chromosome deviates from the standard threshold for disomy.

#### 3.3.3.4 Statistical analysis

In this study, categorical variables are shown as percentages with 95% confidence interval (CI), and continuous variables as mean  $\pm$  standard deviation (SD). Statistical analysis was conducted using two-tailed Chi square test for categorical variables and ANOVA with Bonferroni's correction for continuous variables. In order to define sensitivity and specificity toward ICM ploidy status prediction, we firstly classified each segmental aneuploidy as true positive (TP, abnormal ICM and abnormal TE), true negative (TN, normal ICM and normal TE), false positive (FP, normal ICM and abnormal TE), false negative (FN, abnormal ICM

and normal TE). Sensitivity was calculated as the percentage of abnormal chromosome correctly predicted as aneuploid, while specificity was defined as the percentage of euploid chromosomes detected for all chromosomes expected to be normal. Positive (PPV) and negative predictive values (NPV) were calculated as the proportion of positive and negative results that were true positive and true negative [PPV=TP/(TP+FP); NPV=TN/(TN+FN)]. To assess the diagnostic reliability of segmental detection on a single clinical TE over the remaining embryo, concordance measures were calculated as described above but considering as confirmation the presence of at least one additional biopsy showing the same or an alternative aneuploidy pattern for the same chromosomal segment.

A logistic regression model was built to identify potential additional variables to enhance segmental aneuploidy predictive values. To this end, a multivariate analysis where the independent variable was the confirmation state on the re-biopsies was conducted including as main covariates female age, sperm quality, male age, segmental size, chromosome involved, embryo morphology and day of biopsy. Recursive partitioning analysis was used to stratify the samples according to predictive variables on confirmation outcome. Accordingly, a decision-making model was computed. P-value <0.05 was considered statistically significant.

### **3.3.4 RESULTS**

#### **3.3.4.1 Segmental aneuploidies characterization and predictive value analysis in clinical conditions**

In the double clinical biopsies model, the comparison between clinical TE and TE re-biopsy PGT-A results showed that only 51.7% (n=31/60; 95%CI=38.39-64.77) of the total segmental alterations detected in 51 biopsies were confirmed in the second TE analysis (Figure 14A). In particular, 31.7% (n=19/60; 95%CI=20.26-44.96) of paired samples showed the same alteration, suggesting a meiotic origin and 20.0% (n=12/60; 95%CI=10.78-32.33) showed a different aneuploidy pattern. In detail, 11.7% (n=7/60; 95%CI=4.82-22.57) showed the corresponding whole chromosome aneuploidy and 8.3% (n=5/60; 95%CI=2.76-18.39) carried the reciprocal segmental aneuploidy of the same chromosome fragment (Figure 14A). These findings suggest that a significant proportion of TE segmental alterations are present in a mosaic constitution, consistent with mitotic origin. Differently from segmental aneuploidies, uniform whole chromosome aneuploidies showed high intra-blastocyst concordance rate (96.08%; n=49/51; 95%CI=86.54-99.52 per sample concordance; 99.8%;

n=1171/1173; 95%CI=99.39-99.98 per chromosome concordance) (Figure 14B). Karyotypes for each sample included in this phase are reported in Table 20. Considering the high rate of mosaic pattern identified for segmental aneuploidies in this study model, we decided to carry out a more detailed investigation by analysing aneuploidy configuration across the whole blastocyst including the ICM.

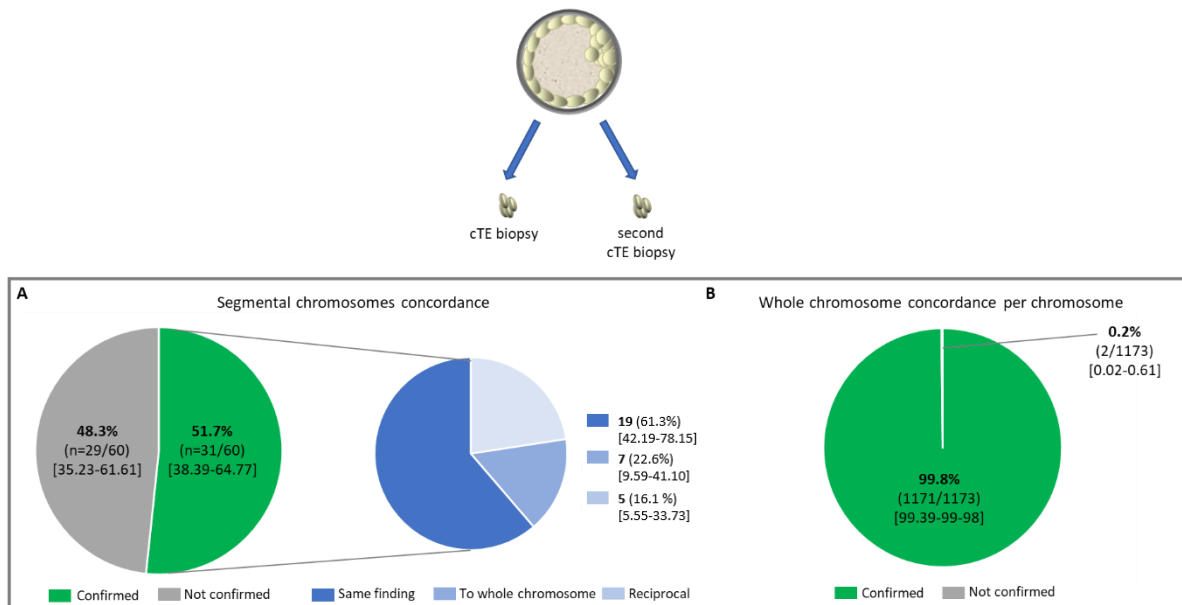


**Figure 14:** summary of double clinical TE biopsy comparison results. **A:** segmental chromosomes concordance  
**B:** whole chromosome concordance

### 3.3.4.2 Segmental aneuploidies characterization in multifocal analysis

To further investigate the prevalence and configuration of segmental aneuploidies in blastocysts, 25 euploid and 53 aneuploid embryos with a segmental alteration detected in the clinical TE were disaggregated in 5 sections (4 TE and 1 ICM biopsies) and blindly analysed. The percentage of confirmed results, showing the same segmental alteration or alternative patterns involving the same chromosome in the ICM or in at least one additional TE biopsy was 60.4% (n=32/53; 95%CI=46.00-73.55; Figure 15A). In this group of confirmed samples, 53.1% (n=17/32; 95%CI=34.74-70.91) showed uniform presence of the same segmental alteration in all biopsies, suggesting defective chromosome segregation of meiotic origin. In the remaining embryos a mosaic pattern was observed. In particular, the same segmental aneuploidy was confirmed in at least 1 TE specimens in 21.9% of samples (n=7/32; 95%CI=9.28-39.97), whilst reciprocal patterns were observed in multiple biopsies in 9.4% of samples (n=3/32; 95%CI=1.98-25.02) or the same segmental aneuploidy was detected in all TE biopsies (15.6% of samples; n=5/32; 95%CI=5.28-39.97) but not in ICM biopsies,

highlighting an aneuploidy pattern fully confined to the trophectoderm tissue. In contrast, segmental aneuploidies were detected only in the clinical TE biopsy in 39.6% of cases (n=21/53; 95%CI=26.45-54.00) (Figure 15A), suggesting an aneuploidy pattern consistent with low-grade mosaicism or the presence of a technical artefact in the initial PGT-A analysis. From the overall comparison between PGT-A results obtained from each single TE biopsy and the correspondent ICM we reported 99.3% of per chromosome concordance (n=7125/7176; 95%CI=99.07-99.47) and 83.6% of per sample concordance (n=261/312; 95%CI=79.07-87.58). Considering that the portion of cells included in a TE biopsy fragment is randomly chosen, we calculated PPV and NPV of all TE biopsies, both from normal and abnormal blastocysts analysed, in relation to their ICM chromosomal status. When considering segmental aneuploidies only, PPV per chromosome and per sample was 70.8% (n=97/137;95%CI=62.43-78.25) while NPV were 99.8% (n=7028/7039; 95%CI=99.72-99.92) and 93.7% (n=164/175; 95%CI=89.03-96.82) respectively.


























A Segmental aneuploidies configurations from aneuploid samples in cTE						
Sample concordance	ICM	cTE	scTE	TE2	TE3	Total blastocyst: n,(%),[95%CI]
Uniform concordance						17, (53.1) [34.74-70.91]
Partial concordance 4/7, 1 discordant sample; 2/7, 2 discordant samples; 1/7, 3 discordant samples						7, (21.9) [9.28-39.97]
Reciprocal segmental						3, (9.4) [1.98-25.02]
Confined to TE 2/5, 4 TE segmental; 3/5, 3 TE segmental;						5, (15.6) [5.28-32.79]
Low grade mosaic or artefact						21, (39.6) [26.45-54.00]
						32, (60.4) [46.00-73.55]
						<b>Mitotic or mosaic configurations</b> 15, (28.3) [16.79-42.35]
B Segmental aneuploidies configurations from euploid samples in cTE						
Uniform concordance						24, (96.0) [79.65-99.90]
Partial concordance						1, (4.0) [0.10-20.35]

**Figure 15:** Overview of segmental aneuploidies configurations **A:** segmental aneuploidies configuration in blastocyst with single segmental aneuploidy in cTE **B:** segmental aneuploidies configuration in blastocyst with euploid cTE

Regarding whole chromosome aneuploidies, comparison between PGT-A results obtained from each single TE biopsy and the correspondent ICM resulted in 99.9% of per chromosome concordance (n=7171/7176; 95%CI=99.84-99.98) and 98.7% of per sample concordance



(n=308/312; 95%CI=96.75-99.65). For whole chromosome aneuploidies PPV per chromosome and per sample were 97.2% (n=69/71; 95%CI=90.19-99.66) and 95.2% (n=40/42; 95%CI=83.84-99.42) respectively, while NPV were 100.0% (n=7102/7105; 95%CI=99.88-99.99) and 100.0% (n=270/270; 95%CI=98.64-100.0) respectively. Considering the overall comparison between all biopsies from segmental aneuploid embryos, 98.1% (n=52/53; 95%CI=89.93-99.95) of samples showed uniform concordant profile among all biopsy specimens. Differently from segmental aneuploidies, only 1 blastocyst (1.9%, n=1/53; 95%CI=0.5-10.07) showed non-concordant results between 2 TE specimens and the ICM for 3 whole chromosome aneuploidies (Figure 16 A,B). These data highlight that whole chromosome aneuploidies are almost always consistently detected in the blastocyst and incidence of mosaicism is very low. Karyotypes for each sample included in this phase are reported in Table 21.

<b>A</b> Whole chromosome aneuploidies configurations from segmental aneuploid samples in cTE						
Sample concordance	ICM	cTE	TE1	TE2	TE3	Total blastocyst: n,(%),[95%CI]
Uniform concordance						<b>9</b> (17.0) [8.07-29.80]
						
Partial concordance						<b>1</b> (1.9) [0.5-10.07]
<b>52</b> (98.1) [89.93-99.95]						
<b>B</b> Whole chromosome aneuploidies configurations from euploid samples in cTE						
Uniform concordance						<b>23</b> (92.0) [73.97-99.02]
Partial concordance						<b>2</b> (8.0) [0.98-26.03]

**Figure 16:** Overview of whole chromosome aneuploidies configurations **A:** whole chromosome aneuploidies configuration in blastocyst with single segmental aneuploidy in cTE **B:** whole chromosome aneuploidies configuration in blastocyst with euploid cTE.

### 3.3.4.3 Segmental aneuploidies length and confirmation outcome

Considering that only one TE biopsy is generally obtained in clinical PGT-A settings, we sought to investigate the predictivity of the segmental finding with respect to the ICM status and whether certain clinical and embryological parameters could enhance predictivity. For the purpose of this analysis all segmental alterations were divided into two groups according to confirmation outcome (confirmed and not confirmed in ICM). Logistic regression analysis

revealed that the segmental size and confirmation in the second clinical TE biopsy (scTE, possible clinical procedure) are the only variables associated a true identification of a segmental aneuploidy in the first TE biopsy. Mean segmental length was higher in confirmed diagnoses ( $67.0 \pm 38.5$  vs  $50.6 \pm 30.9$ , for confirmed and not confirmed, respectively; Figure 17A) and the presence of the same or alternative aneuploid pattern in the second clinical TE was the strongest prognostic factor for confirmation in the ICM. Indeed, 84.0% ( $n=21/25$ ; 95%CI=63.92-95.46) of cases showing a positive second clinical TE showed the same/alternative pattern in the relative ICM for that chromosome (Figure 17B). There was no difference in the ICM confirmation rate according to the TE biopsy analysed (P=not significant). Indeed, excluding cases where the segmental was only detected in the cTE, ICM confirmation ranged from 84.4% for cTE and TE3 ( $n=27/32$ ; 95%IC=67.21-94.72) to 75.0% for TE4 ( $n=24/32$ ; 95%IC=56.60-88.54) and 68.8% for scTE ( $n=22/32$ ; 95%IC=49.99-83.88) (Figure 17C), suggesting equal representation for the different TE biopsies toward the ICM.

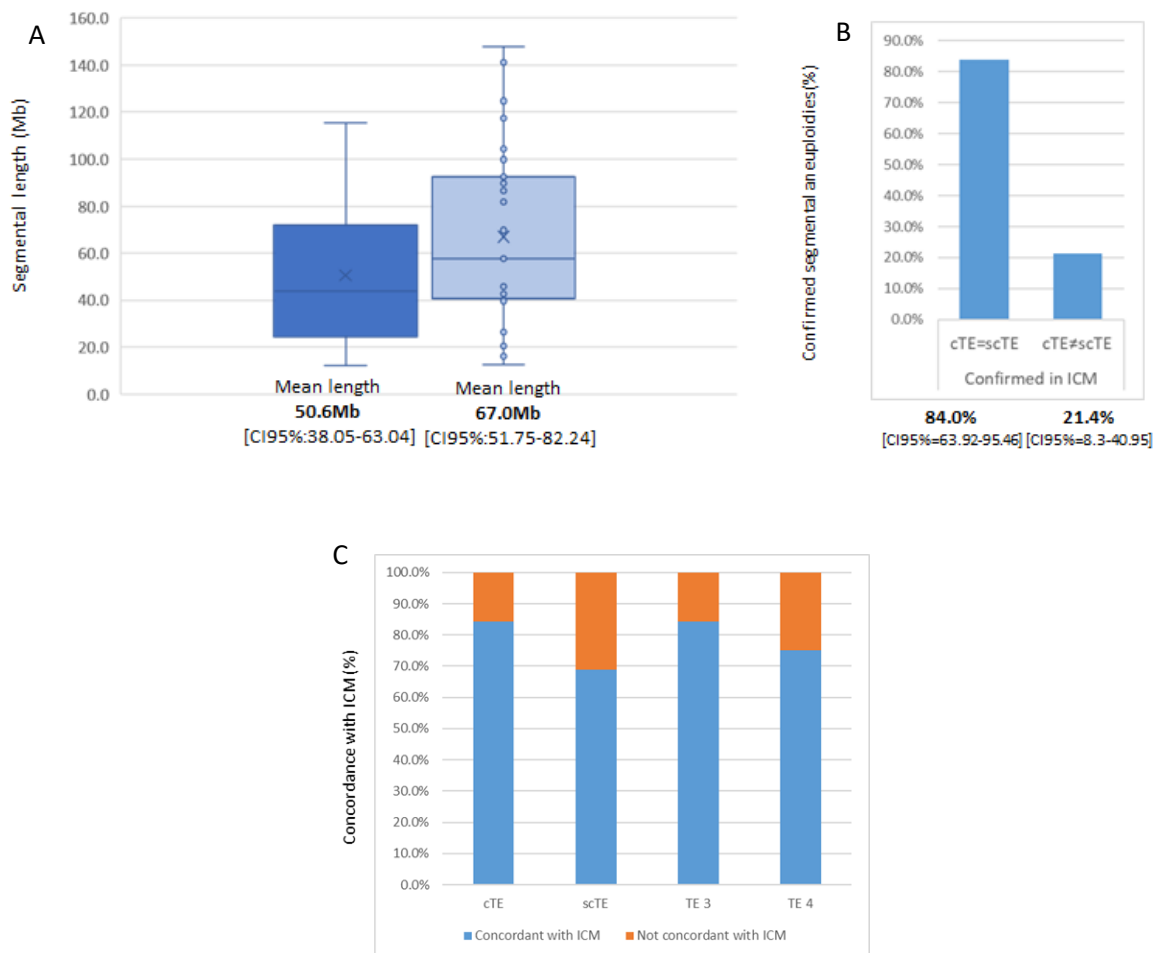
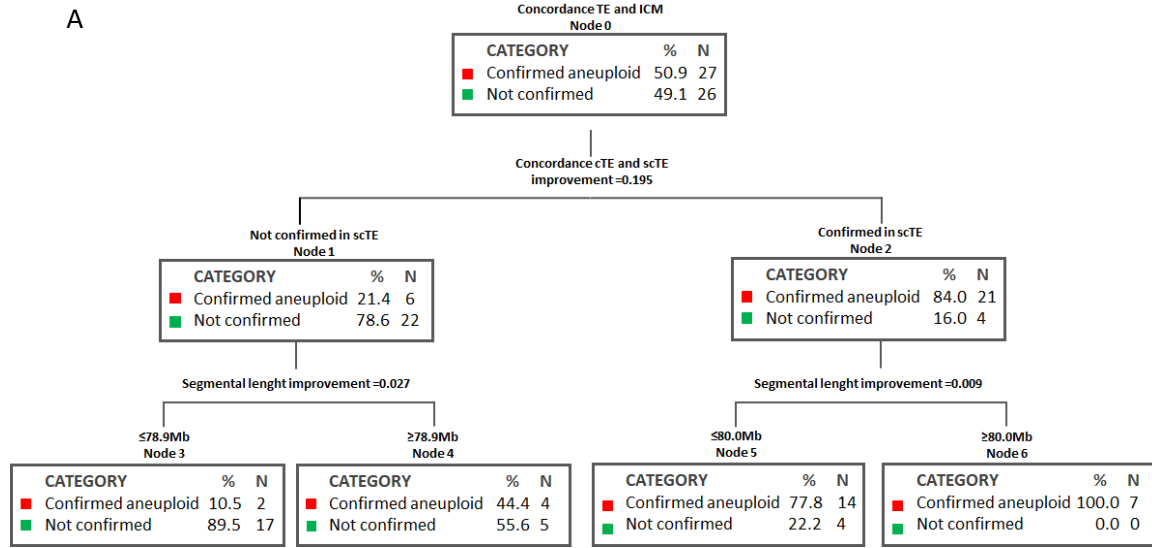


**Figure 17:** predictivity of confirmation rate in ICM from blastocysts showing segmental aneuploidies in their clinical TE sample. **A):** Mean segmental length according to confirmation outcome. **B):** confirmation rate according to scTE outcome **C):** confirmation rate according to TE biopsy.

By recursive partitioning analysis, a general intuitive model has been developed, able to predict the likelihood of the segmental aneuploidy presence in the ICM. As shown in Figure 18A, when considering the availability of a second cTE biopsy, confirmation in ICM increases from 21.4% to 84% when the scTE tests positive. In case of euploid scTE biopsy, detecting a segmental aneuploidy smaller than 78.94Mb reduces the risk of segmental ICM aneuploidy from 21.4% to 10.5% (Figure 18A). In the absence of information gathered from the scTE, the first risk stratification is observed for segments larger than 116Mb where the segmental aneuploidies are confirmed in all cases. ICM confirmation rate decreases for segmental aneuploidies shorter than 116Mb. In this low risk group, a second stratification point is detectable at 37Mb, with shorter segmental aneuploidies being confirmed in 31.2% of ICMs (Figure 18B).

**Decisional tree analysis based on confirmation in scTE biopsy and segmental aneuploidy length.**



**Decisional tree analysis based on segmental aneuploidy length.**

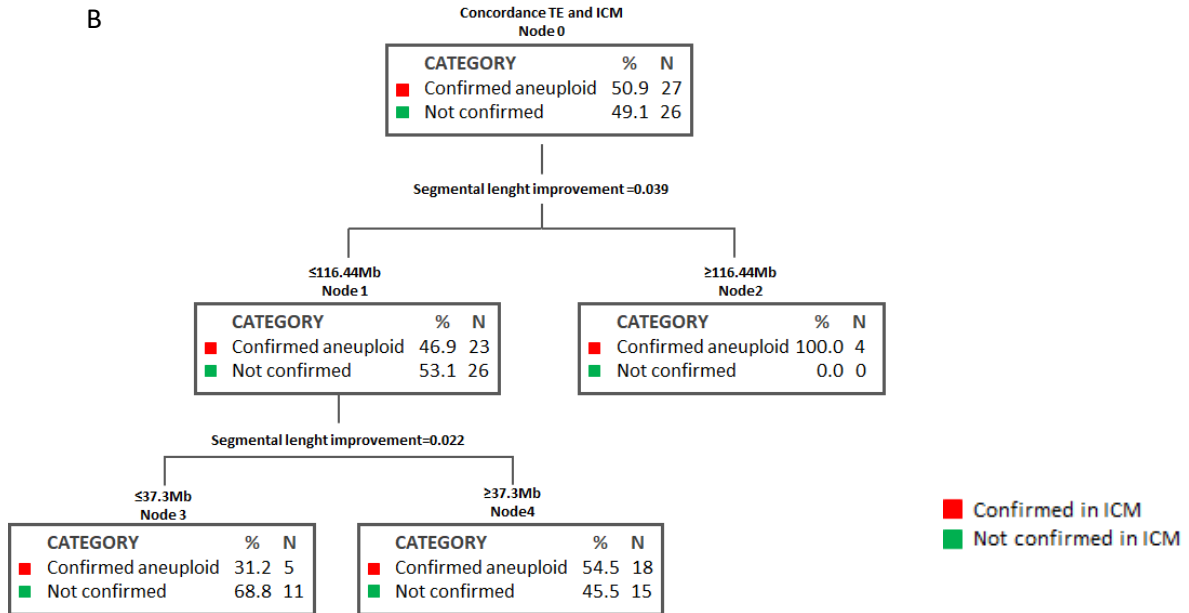


**Figure 18:** Decision-making model based on recursive partitioning analysis. **A:** Mean segmental length according to confirmation outcome, **B:** segmental length .

**Table 20:** PGT-A resulting karyotype obtained in the double clinical biopsy model: for each embryo, morphological grade and segmental length are reported.

Embryo ID	Embryo grade	PatientAge	Clinical TE biopsy	Second clinical TE biopsy	Segmental length (Mb)
G01	C22	38	unbalanced,XY,del(9)(p12q34.3)	unbalanced,XY,del(9)(q21.11q34.3)	99.73-70.31
G02	C11	33	unbalanced,XX,del(7)(q11.21q36.3)	unbalanced,XX,del(7)(q11.21q36.3)	97.16
G03	B32	38	unbalanced,XX,del(3)(q22.1q29)	unbalanced,XX,del(3)(q13.33q29)	68.29-78.34
G04	C33	39	unbalanced,XX,+19,del(11)(p15.5p11.12)	unbalanced,XX,+19,del(11)(p15.5p11.12)	50.72
G05	A22	44	unbalanced,XY,-4,+5,-6,del(8)(q24.13q24.3)	unbalanced,XY,-4,+5,-6,del(8)(q24.13q24.3)	22.58
G06	C11	41	unbalanced,XY,+11,del(8)(p23.3p11.1),dup(8)(q11.1q24.3)	unbalanced,XY,+11,del(8)(p23.3p11.1),dup(8)(q11.1q24.3)	43.78-98.47
G07	C23	38	unbalanced,XY,-8,del(11)(p15.5p14.1),dup(11)(q24.1q25)	unbalanced,XY,del(11)(p15.5p14.1)	30.89- 12.16
G08	C22	39	unbalanced,XX,+13,del(4)(q24q35.2)	unbalanced,XX,+13,del(4)(q24q35.2)	83.70
G09	C11	36	unbalanced,XY,del(5)(q33.1q35.3)	unbalanced,XY,del(5)(q33.1q35.3)	29.84
G010	C22	41	unbalanced,XY,del(2)(q34q37.3)	unbalanced,XY,del(2)(q34q37.3)	29.14
G011	C33	38	unbalanced,XY,+9,+19,del(8)(q13.1q24.3)	unbalanced,XY,+9,+19,del(8)(q13.1q24.3)	78.61
G012	C22	37	unbalanced,XY,del(7)(p22.3p15.2)	unbalanced,XY,del(7)(p22.3p15.2)	26.04
G013	C23	41	unbalanced,XX,del(X)(q26.3q28)	unbalanced,XX,del(X)(q26.3q28)	17.28
G014	C33	30	unbalanced,XX,del(4)(q25q35.2)	unbalanced,XX,del(4)(q25q35.2)	77.72
G015	C33	38	unbalanced,XX,+4,del(7)(q31.1q36.3)	unbalanced,XX,+4,del(7)(q31.1q36.3)	50.64
G016	C21	35	unbalanced,XX,del(1)(q32.1q44)	unbalanced,XX,del(1)(q21.2q44)	42.42- 99.39
G017	C12	41	unbalanced,XY,del(6)(p25.3p22.3)	unbalanced,XY,del(6)(p25.3p22.3),dup(6)(p22.3p11.2)	18.00-40.01
G018	C11	34	unbalanced,XX,del(6)(q12q27)	unbalanced,XX,dup(6)(p25.3q12),del(6)(q12q27)	102.18-68.03
G019	C11	32	unbalanced,XX,del(X)(q26.3q28)	unbalanced,X0	21.19
G020	C22	38	unbalanced,XY,dup(16)(p13.3p12.3),del(16)(p12.3q24.3)	unbalanced,XY,-16	18.37-71.86
G021	C33	34	unbalanced,XX,del(X)(p22.33p21.1)	unbalanced,X0	30.35
G022	B22	36	unbalanced,XY,del(7)(p22.3q22.1)	unbalanced,XY,-7	98.28
G023	C11	36	unbalanced,XX,dup(20)(p13p11.1)	unbalanced,XX,-20	26.25
G024	C12	38	unbalanced,XY,dup(4)(q24q35.2)	unbalanced,XY,-4	87.69

G025	C32	37	unbalanced,XX,dup(7)(p22.3p11.1)	unbalanced,XX,-7	57.77
G026	C23	42	unbalanced,XX,+2,-15,del(11)(q13.3q25)	unbalanced,XX,+2,-15,del(11)(p15.5q13.2),dup(11)(q13.2q25)	66.97- 67.91
G027	C33	41	unbalanced,XY,-22,dup(11)(q23.1q25)	unbalanced,XY,-22,del(11)(q23.1q25)	24.32
G028	C12	36	unbalanced,XX,del(7)(p22.3p11.1)	unbalanced,XX,dup(7)(p22.3p11.1)	57.77
G029	C12	35	unbalanced,XX,dup(1)(q21.1q44),dup(4)(q27q35.2)del(5)(q11.1q35.3),del(18)(p11.32p11.1)	unbalanced,XX,del(4)(q27q35.2)	104.09-69.75- 131.49-15.40
G030	C11	40	unbalanced,XX,del(8)(q11.23-q24.3)	unbalanced,XX,dup(8)(q11.1q24.3)	90.53-98.47
G031	C12	37	unbalanced,XX,-16,dup(7)(p22.3p11.1)	unbalanced,XX,-16	57.77
G032	C22	41	unbalanced,XY,-22,dup(10)(q22.1q26.3)	unbalanced,XY,-22	63.96
G033	C32	42	unbalanced,XY,+18,dup(3)(q11.1q29)	unbalanced,XY,+18	104.45
G034	C32	42	unbalanced,XY,+15,-16,-17,-19,dup(2)(p25.3p22.2)	unbalanced,XY,+15,-16,-17,-19	37.28
G035	C33	41	unbalanced,XY,+22,dup(1)(q21.1q44)	unbalanced,XY,+22	104.09
G036	C33	41	unbalanced,XX,-7,-21,+22,dup(1)(q21.1q44),dup(12)(p13.33p11.1)	unbalanced,XX,-7,-21,+22	104.09-34.71
G037	C33	39	unbalanced,XX,-18,del(2)(q31.1q37.3),del(X)(q11.1q28)	unbalanced,XX,-18	73.26-93.20
G038	C22	37	unbalanced,XX,+22,del(11)(q11q25)	unbalanced,XX,+22	80.25
G039	C11	41	unbalanced,XY,+9,-13,dup(4)(q26q35.2)	unbalanced,XY,+9	75.73
G040	C22	42	unbalanced,XY,+9,dup(16)(q11.2q24.3)	unbalanced,XY,+9	43.90
G041	C22	39	unbalanced,XX,+21,del(2)(p25.3p22.3)	unbalanced,XX,+21	33.25
G042	C12	38	unbalanced,XY,dup(16)(q11.2q24.3),dup(X)(p22.33p21.2)	balanced,XY	43.90-28.32
G043	C11	34	unbalanced,XX,del(6)(q24.1q27)	balanced,XX	30.64
G044	C12	35	unbalanced,XY,dup(1)(q21.1q44)	balanced,XY	104.09
G045	C22	31	unbalanced,XX,del(16)(q11.2q24.3)	balanced,XX	43.90
G046	C12	40	unbalanced,XX,dup(15)(q21.3q26.3)	balanced,XX	49.48
G047	C12	37	unbalanced,XX,del(3)(q24q29)	balanced,XX	54.23
G048	C12	35	unbalanced,XX,del(2)(q14.1q37.3)	balanced,XX	125.93
G049	C11	32	unbalanced,XX,dup(16)(p13.3p12.2)	balanced,XX	22.20
G050	C11	39	unbalanced,XX,dup(4)(q21.22q35.2)	balanced,XX	107.62
G051	C11	39	unbalanced,XY,dup(17p13.3p11.1)	balanced,XY	21.17

**Table 21:** PGT-A resulting karyotypes obtained in the multifocal analysis: for each embryo, morphological grade and segmental length are reported.

Embryo ID	Embryo grade	Patient Age	ICM biopsy	Clinical TE biopsy	Segmental length (Mb)	Te rebiopsy 1	TE rebiopsy 2	TE rebiopsy 3
C01	5AB	25	unbalanced,XX,-4	unbalanced,XX,del(4)(p16.3q31.1)	141.21-49.82	unbalanced,XX,del(4)(q31.1q35.2)	unbalanced,XX,del(4)(q31.1q35.2)	unbalanced,XX,-4
C02	5AA	28	unbalanced,XY,dup(9)(p24.3q22.2)	unbalanced,XY,dup(9)(p24.3q22.2)	92.33	unbalanced,XY,dup(9)(p24.3q22.2)	unbalanced,XY,dup(9)(p24.3q22.2)	unbalanced,XY,dup(9)(p24.3q22.2)
C03	5AB	33	unbalanced,XX,del(9)(p24.3p13.1)	unbalanced,XX,del(9)(p24.3p13.1)	39.6	unbalanced,XX,del(9)(p24.3p13.1)	unbalanced,XX,del(9)(p24.3p13.1)	unbalanced,XX,del(9)(p24.3p13.1)
C04	5BB	39	unbalanced,XY,-17,dup(20)(p13p11.1)	unbalanced,XY,-17,dup(20)(p13p11.1)	26.260	unbalanced,XY,-17,dup(20)(p13p11.1)	unbalanced,XY,-17,dup(20)(p13p11.1)	unbalanced,XY,-17,dup(20)(p13p11.1)
C05	5BB	32	unbalanced,XY,del(3)(q11.1q29)	unbalanced,XY,del(3)(q11.1q29)	104.46	unbalanced,XY,del(3)(q11.1q29)	unbalanced,XY,del(3)(q11.1q29)	unbalanced,XY,del(3)(q11.1q29)
C06	5AA	32	unbalanced,XY,del(2)(p25.3p11.2)	unbalanced,XY,del(2)(p25.3p11.2)	89.62	unbalanced,XY,del(2)(p25.3p11.2)	unbalanced,XY,del(2)(p25.3p11.2)	unbalanced,XY,del(2)(p25.3p11.2)
C07	5AA	32	unbalanced,XY,dup(2)(q11.1q37.3)	unbalanced,XY,dup(2)(q11.1q37.3)	147.78	unbalanced,XY,dup(2)(q11.1q37.3)	unbalanced,XY,dup(2)(q11.1q37.3)	unbalanced,XY,dup(2)(q11.1q37.3)
C08	5AA	24	unbalanced,XY,del(6)(q25.3q27)	unbalanced,XY,del(6)(q25.3q27)	12.59	unbalanced,XY,del(6)(q25.3q27)	unbalanced,XY,del(6)(q25.3q27)	unbalanced,XY,del(6)(q25.3q27)
C09	5BB	40	unbalanced,XX,del(4)(p16.3p13)	unbalanced,XX,del(4)(p16.3p13)	41.55	unbalanced,XX,del(4)(p16.3p13)	unbalanced,XX,del(4)(p16.3p13)	unbalanced,XX,del(4)(p16.3p13)
C10	5BB	23	unbalanced,XY,del(8)(p23.3p11.1)	unbalanced,XY,del(8)(p23.3p11.1)	43.78	unbalanced,XY,del(8)(p23.3p11.1)	unbalanced,XY,del(8)(p23.3p11.1)	unbalanced,XY,del(8)(p23.3p11.1)
C11	5BC	33	unbalanced,XY,del(4)(q27q35.2)	unbalanced,XY,del(4)(q27q35.2)	69.75	unbalanced,XY,del(4)(q27q35.2)	unbalanced,XY,del(4)(q27q35.2)	unbalanced,XY,del(4)(q27q35.2)
C12	5BB	37	unbalanced,XX,del(9)(p24.3p12)	unbalanced,XX,del(9)(p24.3p12)	42.60	unbalanced,XX,del(9)(p24.3p12)	unbalanced,XX,del(9)(p24.3p12)	unbalanced,XX,del(9)(p24.3p12)
C13	5BB	26	unbalanced,XX,del(3)(p26.3p25.1)	unbalanced,XX,del(3)(p26.3p25.1)	16.023	unbalanced,XX,del(3)(p26.3p25.1)	unbalanced,XX,del(3)(p26.3p25.1)	unbalanced,XX,del(3)(p26.3p25.1)
C14	6AB	40	unbalanced,XY,+15,del(8)(q22.3q24.3)	unbalanced,XY,+15,del(8)(q22.3q24.3)	40.59	unbalanced,XY,+15,del(8)(q22.3q24.3)	unbalanced,XY,+15,del(8)(q22.3q24.3)	unbalanced,XY,+15,del(8)(q22.3q24.3)
C15	5CB	22	unbalanced,XY,del(5)(p15.33p14.1)	unbalanced,XY,del(5)(p15.33p14.1)	27.86	unbalanced,XY,del(5)(p15.33p14.1)	unbalanced,XY,del(5)(p15.33p14.1)	unbalanced,XY,del(5)(p15.33p14.1)
C16	3BB	26	unbalanced,XY,del(18)(q12.1q23)	unbalanced,XY,del(18)(q12.1q23)	45.68	unbalanced,XY,del(18)(q12.1q23)	unbalanced,XY,del(18)(q12.1q23)	unbalanced,XY,del(18)(q12.1q23)
C17	4AA	39	unbalanced,XY,+16,dup(11)(p15.5p12)	unbalanced,XY,+16,dup(11)(p15.5p12)	40.80	unbalanced,XY,+16,dup(11)(p15.5p12)	unbalanced,XY,+16,dup(11)(p15.5p12)	unbalanced,XY,+16,dup(11)(p15.5p12)
C18	4BB	43	unbalanced,XX,+1,-4,-6,+22	unbalanced,XX,+1,-6,+22,del(4)(q25q35.2)	81.71	unbalanced,XX,+1,+22	unbalanced,XX,-4,-6,+22	unbalanced,XX,+1,-4,-6,+22
C20	5AB	33	unbalanced,XX,dup(9)(p12q34.3)	unbalanced,XX,dup(9)(p12q34.3)	99.74	unbalanced,XX,dup(9)(p12q34.3)	unbalanced,XX,dup(9)(p12q34.3)	balanced,XX
C21	5AA	39	unbalanced,XX,+15,+16,del(8)(q24.13q24.3)	unbalanced,XX,+15,+16,dup(8)(q24.13q24.3)	20.57-20.57	unbalanced,XX,+15,+16	unbalanced,XX,+15,+16,del(8)(q24.13q24.3)	unbalanced,XX,+15,+16,del(8)(q24.13q24.3)
C22	5AA	31	unbalanced,XX,del(7)(q11.23q36.3)	unbalanced,XX,del(7)(q11.23q36.3)	86.537	balanced,XX	unbalanced,XX,del(7)(q11.23q36.3)	unbalanced,XX,del(7)(q11.23q36.3)
C23	5AB	21	unbalanced,XY,dup(17)(q12q25.3)	unbalanced,XY,dup(17)(q12q25.3)	46.46	balanced,XY	unbalanced,XY,dup(17)(q12q25.3)	balanced,XY
C24	5BB	29	unbalanced,XX,del(3)(q13.11q29)	unbalanced,XX,del(3)(q13.11q29)	92.40	balanced,XX	unbalanced,XX,del(3)(q13.11q29)	balanced,XX
C25	5AA	39	unbalanced,XX,+15,+16,dup(8)(p23.3q24.13)	unbalanced,XX,+15,+16,del(8)(p23.3q24.13)	124.74-124.74	unbalanced,XX,+15,+16	unbalanced,XX,+15,+16	unbalanced,XX,+15,+16
C26	5AB	26	unbalanced,XY,del(1)(q21.1q44)	unbalanced,XY,del(1)(q31.1q44)	104.09-59.10-44.99	unbalanced,XY,del(1)(q31.1q44)	unbalanced,XY,del(1)(q31.1q44),dup(1)(q21.1q31.1)	unbalanced,XY,del(1)(q31.1q44)
C27	5BB	39	unbalanced,XX,del(7)(q22.3q36.3)	unbalanced,XX,dup(7)(p22.3p11.1)	50.64-57.77-97.16	unbalanced,XX,del(7)(q31.1q36.3)	unbalanced,XX,del(7)(q31.1q36.3)	unbalanced,XX,-7
C29	5CB	26	unbalanced,XX,del(4)(q27q35.2)	unbalanced,XX,del(4)(p16.3q26)	69.754-117.29-113.30	unbalanced,XX,del(4)(q27q35.2)	unbalanced,XX,dup(4)(p16.3q25)	unbalanced,XX,-4
C30	5AB	29	balanced,XY	unbalanced,XY,del(5)(p15.33p11)	46.40	unbalanced,XY,del(5)(p15.33p11)	unbalanced,XY,del(5)(p15.33p11)	unbalanced,XY,del(5)(p15.33p11)
C31	5BB	37	balanced,XX	unbalanced,XX,del(1)(p36.33p36.11)	25.12	unbalanced,XX,del(1)(p36.33p36.11)	unbalanced,XX,del(1)(p36.33p36.11)	unbalanced,XX,del(1)(p36.33p36.11)
C32	5BB	32	balanced,XY	unbalanced,XY,dup(4)(q13.3q35.2)	115.59-93.66	unbalanced,XY,del(4)(q22.3q35.2)	balanced,XY	unbalanced,XY,-4
C33	6BB	26	balanced,XX	unbalanced,XX,dup(9)(q21.11q34.3)	70.32	unbalanced,XX,dup(9)(q21.11q34.3)	balanced,XX	unbalanced,XX,dup(9)(q21.11q34.3)
C34	5AA	30	balanced,XY	unbalanced,XY,del(12)(q21.31q24.33)	52.28	unbalanced,XY,del(12)(q21.31q24.33)	unbalanced,XY,del(12)(q21.31q24.33)	balanced,XY
C35	5AA	37	balanced,XX	unbalanced,XX,dup(7)(p22.3p14.1)	40.07	balanced,XX	balanced,XX	balanced,XX
C36	5BB	29	balanced,XX	unbalanced,XX,dup(4)(q21.22q35.2)	107.62	balanced,XX	balanced,XX	balanced,XX
C37	5BB	29	balanced,XX	unbalanced,XX,dup(8)(p23.3p22)	14.11	balanced,XX	balanced,XX	balanced,XX
C39	5AB	37	unbalanced,XX,+21	unbalanced,XX,+21,del(4)(q32.1q35.2)	33.88	unbalanced,XX,+21	unbalanced,XX,+21	unbalanced,XY,+21
C40	5AB	21	balanced,XY	unbalanced,XY,dup(X)(q24q28)	34.86	balanced,XY	balanced,XY	balanced,XY
C41	5AA	28	balanced,XX	unbalanced,XX,dup(4)(q34.3q35.2)	11.96	balanced,XX	balanced,XX	balanced,XX
C42	5BB	29	balanced,XX	unbalanced,XX,dup(11)(q13.3q25)	65.17	balanced,XX	balanced,XX	balanced,XX
C43	5AB	29	balanced,XY	unbalanced,XY,dup(1)(p36.33p36.13)	16.60	balanced,XY	balanced,XY	balanced,XY
C44	5BB	45	unbalanced,X0,-9,+12,-14	unbalanced,X0,-9,+12,-14,dup(6)(p25.3p22.3)	22.01	unbalanced,X0,-9,+12,-14	unbalanced,X0,-9,+12,-14	unbalanced,X0,-9,+12,-14
C45	5AB	39	balanced,XX	unbalanced,XX,del(8)(q11.23q24.3)	90.53	balanced,XX	balanced,XX	balanced,XX
C46	5AB	25	unbalanced,XY,+2	unbalanced,XY,+2,del(1)(p36.33p36.13)	16.60	unbalanced,XY,+2	unbalanced,XY,+2	unbalanced,XY,+2
C47	5AA	22	balanced,XY	unbalanced,XY,dup(9)(p24.3p2)	13.88	balanced,XY	balanced,XY	balanced,XY
C48	5AA	22	balanced,XY	unbalanced,XY,del(10)(q25.1q26.3)	27.76	balanced,XY	balanced,XY	balanced,XY
C49	5AB	26	balanced,XX	unbalanced,XX,dup(16)(q11.2q24.3)	43.91	balanced,XX	balanced,XX	balanced,XX
C50	3BB	26	balanced,XY	unbalanced,XY,dup(9)(q21.11q34.3)	70.31	balanced,XY	balanced,XY	balanced,XY
C51	5AA	36	balanced,XX	unbalanced,XX,dup(16)(q11.2q24.3)	43.90	balanced,XX	balanced,XX	balanced,XX
C52	6BC	21	balanced,XY	unbalanced,XY,dup(17)(q22q25.3)	30.65	balanced,XY	balanced,XY	balanced,XY
C53	5BB	32	balanced,XY	unbalanced,XY,dup(3)(p26.3p11.1)	90.44	balanced,XY	balanced,XY	balanced,XY

C054	5BB	35	unbalanced,XX,-22	unbalanced,XX,-22,dup(6)(q14.1q27)	94.30	unbalanced,XX,-22	unbalanced,XX,-22	unbalanced,XX,-22
C055	5BB	29	balanced,XX	balanced,XX,dup(10)(q22.2q26.3)	59.94	balanced,XX	balanced,XX	balanced,XX
C056	5AB	29	balanced,XX	balanced,XX,dup(X)(q21.1q28)	76.18	balanced,XX	balanced,XX	balanced,XX
C057	6BB	36	balanced,XY	balanced,XY		balanced,XY	unbalanced,XY,+8	balanced,XY
C058	5AA	23	balanced,XY	balanced,XY		balanced,XY	balanced,XY	balanced,XY
C059	5AA	23	balanced,XY	balanced,XY		balanced,XY	balanced,XY	balanced,XY
C060	5BA	23	balanced,XY	balanced,XY		balanced,XY	balanced,XY	balanced,XY
C061	5AA	23	balanced,XY	balanced,XY		balanced,XY	balanced,XY	balanced,XY
C062	5BB	36	balanced,XX	balanced,XX		balanced,XX	balanced,XX	balanced,XX
C063	5AB	23	balanced,XY	balanced,XY		balanced,XY	balanced,XY	balanced,XY
C064	5AA	23	balanced,XY	balanced,XY		balanced,XY	balanced,XY	balanced,XY
C065	5AA	31	balanced,XX	balanced,XX		balanced,XX	balanced,XX	balanced,XX
C066	5AB	36	balanced,XX	balanced,XX		balanced,XX	balanced,XX	balanced,XX
C067	4BB	31	balanced,XX	balanced,XX		balanced,XX	balanced,XX	balanced,XX
C068	5AB	36	balanced,XX	balanced,XX	60.51	balanced,XX	unbalanced,XX,dup(6)(6q21q27)	unbalanced,XX,del(6)(6q21q27)
C069	5AA	38	balanced,XY	balanced,XY		balanced,XY	balanced,XY	balanced,XY
C070	4AA	26	balanced,XX	balanced,XX		balanced,XX	balanced,XX	balanced,XX
C072	4BB	25	balanced,XY	balanced,XY		balanced,XY	balanced,XY	balanced,XY
C073	4AA	25	balanced,XX	balanced,XX		balanced,XX	balanced,XX	balanced,XX
C074	5BB	34	balanced,XX	balanced,XX		balanced,XX	balanced,XX	balanced,XX
C075	5AA	34	balanced,XX	balanced,XX		balanced,XX	balanced,XX	balanced,XX
C076	5BC	33	balanced,XX	balanced,XX		balanced,XX	balanced,XX	unbalanced,XX,+14
C077	5BC	33	balanced,XX	balanced,XX		balanced,XX	balanced,XX	balanced,XX
C077	5AB	33	balanced,XX	balanced,XX		balanced,XX	balanced,XX	balanced,XX
C079	5AB	34	balanced,XX	balanced,XX		balanced,XX	balanced,XX	balanced,XX
C080	5AB	34	balanced,XY	balanced,XY		balanced,XY	balanced,XY	balanced,XY
C081	5AB	34	balanced,XX	balanced,XX		balanced,XX	balanced,XX	balanced,XX
C082	5AB	34	balanced,XX	balanced,XX		balanced,XX	balanced,XX	balanced,XX



## **4 PREIMPLANTATION GENETIC TEST FOR MONOGENIC CONDITIONS**

### **4.1 EVALUATION OF A NOVEL NON-INVASIVE PGT-M PROTOCOL USING BLASTOCOEL FLUID AND SPENT EMBRYO CULTURE MEDIA**

#### **4.1.1 Introduction**

In the last decade, the number of PGT-M cases has rapidly increased worldwide and PGT is now widely employed in IVF cycles to select unaffected embryos from couples carrier of specific mutations. Therefore, the study and selection of embryos prior to transfer is a key step for the birth of an unaffected child in assisted reproduction. Despite its extensive application, one of the biggest challenges of the PGT methodology is the requirement of biopsy samples collected from an embryonic specimen, a procedure that entails both technical and economic challenges. In this regard, TE biopsy is considered generally safe, and it is the technique with the least impact on the embryo (Cimadomo *et al.*, 2016). Nonetheless, the high degree of technical skill required to obtain these samples and the costs associated with both the equipment (i.e., laser) and operator training remain a bottleneck for wider implementation of this strategy. In fact, although TE biopsy has been proven safe, suboptimal embryo biopsies may undermine embryo developmental and reproductive competence (SA *et al.*, 2016). However, the process of embryo biopsy requires specific equipment and trained personnel that add cost and risks to the diagnostic workflow. Thus, non-invasive or ‘liquid biopsy’ approaches are sought as an alternative. Recently, blastocoel fluid (BF) was suggested as a source of embryonic DNA for PGT purposes (Poli *et al.*, 2013; Gianaroli *et al.*, 2014). The fluid can be aspirated from the embryo using an injection needle through a procedure described by Poli *et al.* as blastocentesis (Poli *et al.*, 2012). Using this technique, the sampling of embryo-derived compounds is less invasive compared with biopsies, avoiding the removal of trophoblast cells from the developing embryo. Nonetheless, blastocentesis entails minimal invasiveness to the embryo. To develop a completely noninvasive, inexpensive and easily implementable methodology for PGT purposes, several investigators proposed the use of spent culture medium, where the embryo was incubated until the time of transfer or freezing, collected at blastocyst stage (SBM) (Shamonki *et al.*, 2016; Feichtinger *et al.*, 2017; Hammond *et al.*, 2017). In daily routine, this media is discarded after finishing the culture of the embryo. Nevertheless, embryo culture media contains traces of embryonic cell-free DNA that can represent the genetic load of the embryo (Hammond *et al.*, 2016). However, recent studies underline the presence of contaminating DNA in spent culture media, probably derived from maternal cumulus cells or

other embryo-associated structures, leading to high rate of false negative results (Hammond *et al.*, 2017).

#### 4.1.2 Aim of the study and study design

The study focused on assessing the suitability of BF and SBM specimens as PGT-M analysis templates, in order to develop a completely non-invasive procedure for PGT-M analysis. To do so, we determined the diagnostic rate of PGT-M when applied to TE, BF, and SBM samples, also providing details on amplification failure (AF) and ADO rates of alleles of maternal and paternal origin. In this context, genotyping analysis offered the unique possibility to obtain important information about the nature and origin of DNA amplified from BF and SBM samples in standard clinical conditions.

A total of 267 samples were collected from 26 patients and enrolled in the study in order to evaluate the application of PGT-M protocols on TE, spent blastocyst media (SBM), and blastocoel fluid (BF) specimens (221 samples from 14 consenting couples who were referred to the clinic as carriers of an inheritable genetic condition; Figure 19). The samples included in the studies were obtained from patients undergoing PGT-M and consenting to the use of SBM. Of the total 221 samples, 80 were TE biopsies, 69 were BF samples, and 72 were SBM samples (specifically, 61 triads BF-TE-SBM, 8 pairs BF-TE and 11 pairs TE-SBM; Figure 19).

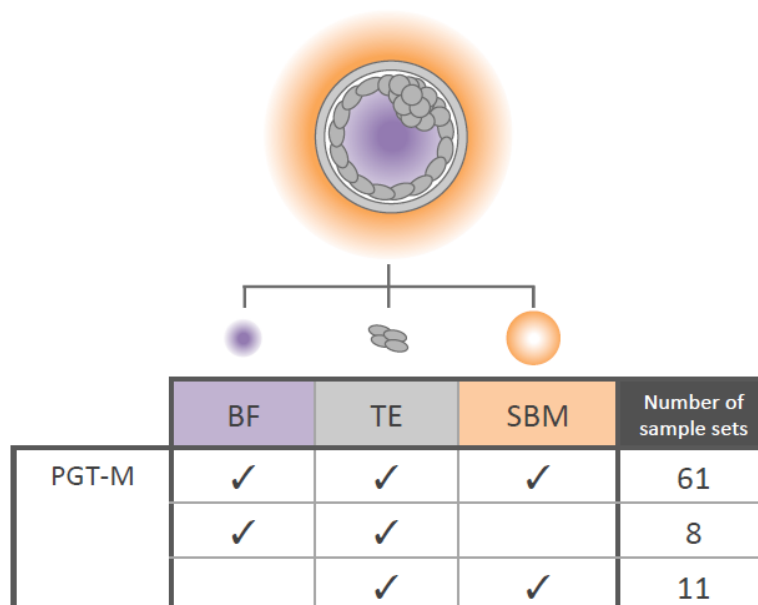


**Figure 19:** Study design and sample size. (Capalbo *et al.* *Fertil Steril* 2018)

All 221 samples were subsequently analyzed using PGT-M protocols specific for the parental mutation in order to genotype the embryo (Zimmerman *et al.*, 2016). Additionally,

a subset of these samples (70 loci carrying the pathologic mutation, 39 of paternal origin, and 31 of maternal origin) were analyzed to assess the relationship between test concordance and origin of the investigated locus. Because SNPs are common genomic variations in the population, their exclusion from the analysis rules out the potential interference of exogenous/environmental contamination. Instead, the exclusive analysis of the genetic mutations that are rare variants and specific for each trio considered, allows the precise assessment of parental contribution in fluidic samples. For both phases, results from trophectoderm biopsy and the other specimens were compared, considering that the results obtained from the trophectoderm biopsy are more reliable as a higher amount of genetic material is processed, and for this reason the trophectoderm biopsy were considered as the gold standard.

#### **4.1.3 Outcome measure**

In all PGT-M cases the amplification rates were calculated based on the detection of the target loci sequences tested. The results were deemed concordant across specimens (BF/SBM/TE) if they showed the same allele variant. Discordant results were considered artefacts if the allele showed an unexpected genotype, or allele drop-in (ADI) if they showed the alternative parental allele variant, not present in the embryo. Finally, the presence of a single allele in a sample expected to be heterozygous for that locus was counted as allele drop-out ADO. When the relationship between the efficiency in detecting the correct locus variant and its parental inheritance was investigated, all SNPs used for linkage analysis were removed from the data set to minimize biases potentially introduced by exogenous DNA contamination (including those cases where diagnosis was not possible via direct mutation and linkage analysis was used to produce a diagnosis). Also, to precisely assess allelic origin (maternal or paternal), those cases where the same mutation was present in both parents were removed, and only triads derived from embryos presenting mutation sites in heterozygosis or compound heterozygotes were analysed.

#### **4.1.4 MATERIALS AND METHODS**

##### **4.1.4.1 BF and SBM Specimen Collection**

**Blastocoel.** Fully expanded blastocysts were placed in a 10 µl drop of HEPES buffered medium and overlaid with warmed mineral oil. A conventional ICSI needle was gently pushed through the zona pellucida and TE cell wall to reach the centre of the cavity. Light negative pressure was applied to allow the aspiration of the fluid. Once the blastocoelic cavity reached around 10% of its initial volume, the needle was retracted from the embryo,

and the retrieved specimen was released in a 5  $\mu$ l drop of the same medium plated next to the biopsy drop used. The medium drop containing the BF was then collected and placed in a 0.2-mL sterile PCR tube stored at  $-80^{\circ}\text{C}$  to be processed as described in the genetic analysis section. The TE biopsy was performed immediately after the BF aspiration.

**Spent blastocyst media.** Once the embryos reached the blastocyst stage, they were moved to a biopsy/blastocentesis dish, and the spent culture medium was collected immediately after, as previously described (Capalbo *et al.*, 2016). TE biopsy strategy used didn't entail any kind of extra embryonic manipulation before the biopsy stage, thus providing culture media samples more representative of those obtained in standard IVF treatments. Blank culture media drops were collected from the stock and after 3 and 5 days of culture as negative controls.

#### **4.1.4.2 Genetic analysis: PGT-M by qPCR (TE, BF, SBM)**

The TE biopsies were processed by alkaline lysis. The embryonic origin of the DNA sourced from BF and SBM, and the possibility of genotyping the embryo from these specimens was assessed using protocols of qPCR analysis customized for the specific disorder investigated. Quantitative PCR is based on the use of TaqMan allelic discrimination assays (ThermoFisher Scientific) for direct mutation and indirect linked marker PGT-M analysis as described elsewhere (Zimmerman *et al.*, 2016). Each protocol was previously validated on individually isolated cells from each parent and relatives.

#### **4.1.4.3 Statistical Analysis**

Either two-tailed chi-square or two-tailed Fisher's exact tests were employed to assess statistical significance. All confidence intervals (CI) were calculated at 95%.

### **4.1.5 RESULTS**

#### **4.1.5.1 PGT-M amplification rates for TE biopsy, BF and SBM samples**

In this set of experiments, we assessed the embryonic origin of the DNA detected in specimens of TE, BF, and SBM. We also estimated the diagnostic concordance across specimens derived from the same embryo. To do this, we accurately genotyped each specimen using a qPCR-based approach (TaqMan Genotype Assay) targeted at the combined detection of both mutation sites and multiple informative single nucleotide polymorphisms (SNPs) surrounding the mutation. In total, 405 loci were tested in 80 TE samples, 347 loci in 69 BF samples, and 378 loci in 72 SBM samples (Table 22).

PATHOLOGY (GENE)	N° OF PROBES	MUTATION-SPECIFIC PROBES				N° OF PROBES	INFORMATIVE SNP PROBES
CYSTIC FIBROSIS (CFTR)	3	C.1521_1523DELCTT (P.PHE508DELPHE)	C.1584+18672BPA>G (P.GLY1244GLU)	C.1657C>T (P.ARG553X)		9	rs172507; rs4148699; rs1896887; rs17569137; rs41741; rs17139625; rs39310; rs6978581; rs39745
ADRENOLEUKODYSTROPHY (ABCD1)	1	C.1202G>A (P.ARG401GLN)				4	rs2226983; rs5970441; rs6571296; rs1734787
DB MUSCULAR DYSTROPHY	-	LINKAGE ANALYSIS				6	rs2692986; rs5971587; rs5927928; rs5971628; rs1546885; rs10522007
BETA THALASSEMIA (HBB)	4	C.93-21 G>A (IVS I-110)	C.92 G>C (CODON 30)	C.92+1 G>A (IVS I-1)	C.118 C>T (CODON 39)	10	rs2219231; rs10837540; rs11036238; rs4910550; rs10838092; rs3824949; rs1378738; rs6578588; rs2855123; rs1566282
NON-SYNDROMIC HEARING LOSS (GJB2)	1	C.35DELG (P. GLY12VALFSXZ)				4	rs17074497; rs9315353; rs4770022; rs9509266
DM1 MYOTONIC DYSTROPHY	-	LINKAGE ANALYSIS				11	rs16979595; rs7251736; rs4884; rs12460033; rs314661; rs12461093; rs2889490; rs238404; rs12972158; rs1008591; rs1363759
MARFAN SYNDROME (FBN1)	1	C.376 G>T (P.GLY126X)				2	rs8027003; rs2118181
NOONAN SYNDROME (SOS1)	1	C.806T>C (P.MET269THR)				2	rs10495881; rs10208929
HEMOPHILIA (F8)	1	C.5476 G>A (P.ASP1759ASN)				4	rs4898348; rs5945109; rs2051161; rs35296872
HUNTINGTON'S DISEASE (HTT)	-	LINKAGE ANALYSIS				4	rs1203790; rs231707; rs3182; rs11940152
SCID (JAK3)	2	C.2125 T>A (P.TRP709ARG)	C.1796 T>G (P.VAL599GLY)			4	rs10419511; rs8106359; rs8112975; rs11086101

**Table 22:** Probes used for both the mutations-specific and the informative SNPs. (Capalbo et al, *Fertility and Sterility* 2018)

Amplification failure occurred in 0, 252 (72.6%), and 39 loci (10.3%) for TE, BF, and SBM samples, respectively ( $P<0.001$ ) (Table 23). In TE samples, 99.8% of the tests produced concordant results, showing the presence of the expected allele; a single ADO occurred in one sample. Overall, loci amplification in SBM samples performed statistically significantly better than in the BF samples ( $P<0.001$ ) (Table 23).

Probes	N	TE		BF		SBM	
		N	% (95% CI)	N	% (95% CI)	N	% (95% CI)
All	405			347		378	
Amplification failure	0/405		0.0 (0.0–9.1)	252/347	72.6 (67.6–77.3)	39/378	10.3 (7.4–13.8)
Concordant genotype	404/405		99.8 (98.6–99.9)	46/347	13.3 (9.9–17.3)	225/378	59.5 (54.4–64.5)
Discordant genotype	1/405		0.25 (0.01–1.4)	49/347	14.1 (10.6–18.2)	114/378	30.2 (25.6–35.1)
ADO	1/405		0.25 (0.01–1.4)	44/347	12.7 (9.4–16.7)	76/378	20.1 (16.2–24.5)
Materna	1/1		100.0 (2.5–100.0)	14/44	31.8 (19.9–46.6)	28/76	36.8 (26.1–48.7)
Paternal	0/1		0.0 (0.0–97.5)	30/44	68.2 (52.4–81.4)	48/76	63.2 (51.3–73.9)
Artifact	0/405		0.0 (0.0–9.1)	5/347	1.4 (0.5–3.3)	38/378	10.1 (7.2–13.5)
Mutation-specific only	76			65		69	
Amplification failure	0/76		0.0 (0.0–4.7)	49/65	75.4 (63.1–85.2)	11/69	15.9 (8.2–26.7)
Concordant genotype	75/76		98.7 (92.9–100.0)	8/65	12.3 (5.5–22.8)	40/69	58.0 (45.5–69.8)
Discordant genotype	1/76		1.3 (0.03–7.1)	8/65	12.3 (5.5–22.8)	18/69	26.1 (16.3–38.1)
ADO	1/76		1.3 (0.03–7.1)	8/65	12.3 (5.5–22.8)	12/69	17.4 (9.3–28.4)
Maternal	1/1		100.0 (2.5–100.0)	0/8	0.0 (0.0–36.9)	5/12	41.7 (15.2–72.3)
Paternal	0/1		0.0 (0.0–97.5)	8/8	100.0 (63.1–100.0)	7/12	58.3 (27.7–84.8)
Artifact	0/76		0.0 (0.0–4.7)	0/65	0.0 (0.0–5.5)	6/69	8.7 (3.3–18.0)

**Table 23:** Preimplantation genetic testing for monogenic diseases results in trophectoderm TE, BF and SBM samples (Capalbo et al, *Fertility and Sterility* 2018).

Additionally, among successfully amplified loci, the SBM samples were more frequently concordant with the control compared with the BF samples (n=225 of 339,66.4% vs. 46 of 95, 48.4%;P=0.002). Among the successfully amplified loci, ADO was more frequently detected for alleles of paternal origin compared with the ones of maternal origin in both BF (n=30 of 95, 31.6% vs. n=14 of 95, 14.7%, respectively; P=0.01) and SBM samples (n=48 of 339, 14.2% vs. n=28 of 339, 8.3%, respectively; P=0.02). This finding is consistent with the lower levels of paternally derived DNA in the BF and SBM samples.

#### **4.1.5.2 Loci amplification and concordance rates based on maternal and paternal inheritance**

Data from mutation loci analysis were also investigated in regards of parental inheritance. In this part of the study, to precisely assess the allelic origin only triads where embryos showed mutation sites in heterozygosis were analysed. In the selected cases, the mutation was present in only one of the parents, and it was possible to perform direct mutation detection (no linkage analysis).

**Identification of the mutated genes of paternal origin in BF and SBM samples.** In this selected cohort, BF and SBM were characterized by high paternal ADO rate (Table 24). In the BF samples, eight out of the nine successfully amplified loci (amplification failure: n=10 of 19, 52.6%) produced discordant genotypes, all due to paternal ADO (89%; 95%CI: 51.8–99.7) (Figure 20A). Of the 14 successfully amplified SBM samples (amplification failure: n=2 of 16, 12.5%) (Table 24), 7 (50.0%) produced discordant genotypes due to ADO, 6 of which involved paternal alleles (85.7% of the ADO events and 43% of successfully amplified loci; 95%CI, 17.7–71.1) (Figure 20A). No mutation was detected in either BF or SBM samples of the wild-type embryos. This is consistent with the absence of paternal genome contamination in the blastocyst fluidic samples.

Parent-specific mutation probes	TE		BF		SBM	
	n	% (95% CI)	n	% (95% CI)	n	% (95% CI)
<b>Paternal</b>						
Total	39		35		32	
Heterozygous (informative)	20		19		16	
Amplification failure	0/20	0.0 (0.0–16.8)	10/19	52.6 (28.9–75.5)	2/16	12.5 (1.6–38.4)
Concordant genotype	20/20	100.0 (83.2–100.0)	1/19	5.3 (0.1–26.0)	7/16	43.8 (19.8–70.1)
Discordant genotype	0/20	0.0 (0.0–16.8)	8/19	42.1 (20.3–66.5)	7/16	43.8 (19.8–70.1)
ADO	0/20	0.0 (0.0–16.8)	8/19	42.1 (20.3–66.5)	7/16	43.8 (19.8–70.1)
Maternal	0/0	0.0	0/8	0.0 (0.0–36.9)	1/7	14.3 (0.36–57.9)
Paternal	0/0	0.0	8/8	100.0 (63.1–100.0)	6/7	85.7 (42.1–99.6)
Artifact	0/20	0.0 (0.0–16.8)	0/19	0.0 (0.0–17.6)	0/0	0.0
<b>Maternal</b>						
Total	31		27		31	
Heterozygous (informative)	19		18		19	
Amplification failure	0/19	0.0 (0.0–17.7)	16/18	88.9 (65.3–98.6)	3/19	15.8 (3.4–39.6)
Concordant genotype	18/19	94.7 (74.0–99.9)	2/18	11.1 (1.4–34.7)	11/19	57.9 (33.5–79.8)
Discordant genotype	1/19	5.3 (0.1–26.0)	0/18	0.0 (0.0–18.5)	5/19	26.3 (9.2–51.2)
ADO	1/19	5.3 (0.1–26.0)	0/18	0.0 (0.0–18.5)	5/19	26.3 (9.2–51.2)
Maternal	1/1	100.0 (2.5–100)	0/0	0.0 (0.0–0.0)	4/5	80.0 (28.4–99.5)
Paternal	0/1	0.0 (0.0–97.5)	0/0	0.0 (0.0–0.0)	1/5	20.0 (0.5–71.6)
Artifact	0/19	0.0 (0.0–17.7)	0/18	0.0 (0.0–18.5)	0/19	0.0 (0.0–17.7)

**Table 24:** Preimplantation genetic testing for monogenic diseases results in TE, BF and SBM samples divided between paternal- and maternal-specific probes (Capalbo et al, *Fertility and Sterility* 2018).

**Identification of mutated genes of maternal origin in BF and SBM samples.** The analysis of maternally inherited mutations showed the presence of extra-embryonic DNA contamination in BF samples and of maternal DNA contamination in the SBM samples. In the SBM samples collected from heterozygote embryos (amplification failure: n=3 of 19, 15.8%) (Table 24), 5 of the 16 successfully amplified loci produced discordant genotypes due to ADO (31.3%, 95%CI, 11.0–58.7), 4 of which involving the maternal allele (80% of the ADO events, and 25.0% of the successfully amplified loci; 95%CI, 7.3–52.4). The mutated alleles were potentially masked by the excess of the wildtype variant deriving from the degenerating first polar body or by extra embryonic DNA (Figure 20B). Importantly, in four cases, where the embryo showed homozygosity for the wild type allele, the mutated allele was detected in the SBM sample (n=4 of 12, 33% of the cases; 95% CI, 9.9–65.1) showing direct evidence of maternal DNA contamination (Figure 20C). Results from combined maternal and paternal mutation loci data sets confirmed the higher amplification rates in SBM compared with BF samples (n= 30 of 35, 85.7% vs. n=11 of 37, 29.7%; P<0.001) (Table 24). However, in this subset of targets there was no difference in concordance rate between the SBM and BF results when the TE results were used as the standard (n =18 of 30, 60.0% vs. n=3 of 11, 27.3%; P= not statistically significant) (Table 24). Additionally, among successfully amplified loci in both BF and SBM, ADO occurred more frequently for alleles of paternal origin compared with maternal ones (n=14 of 23,

60.9% vs. n=4 of 18, 22.2%; P=0.03) (Table 24), suggesting a higher amount of maternal genomic DNA compared to paternal genomic DNA.

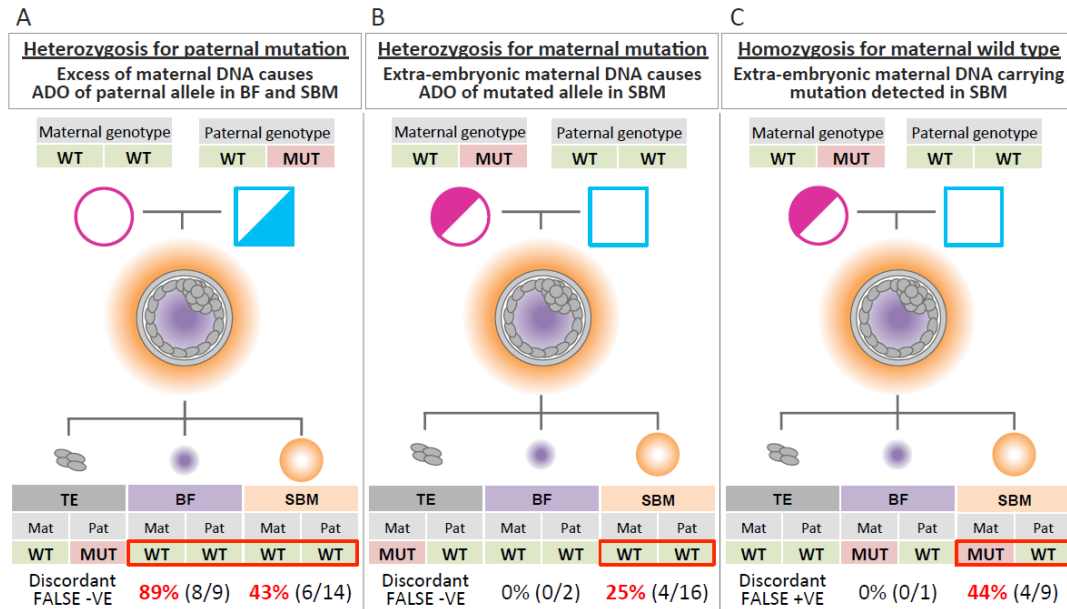


**Figure 20:** Summary of PGT-M results is indicative of contamination derived from maternal DNA in spent blastocyst medium and/or blastocoel fluid. **A:** excess of maternal WT DNA causes paternal ADO in BF and SBM in cases of heterozygosis for paternal mutation in the TE. **B:** maternal WT DNA causes ADO of mutated allele in the SBM in cases of heterozygosis for maternal mutation in the TE. **C:** maternal DNA carrying the mutation detected in the SBM in cases of homozygosis of maternal WT in the TE. The detection rates of these events are reported below each section of the picture. -ve, negative; +ve, positive. (Capalbo et al, *Fertility and Sterility* 2018).

PGT-M diagnostic rates for TE biopsy, BF and SBM samples for monogenic disorders diagnosis was performed using both probes for the mutation site and for informative SNP sites flanking the mutation site. Overall, it was possible to generate consistent embryonic haplotypes in 100% of the TE samples (Table 25). In the BF and SBM groups, respectively, only 2.9% and 20.8% of samples allowed whole haplotype generation that was fully concordant with the corresponding TE sample (P=0.001; Table 25).



	TE	BF	SBM
	N% (95%CI)	N% (95%CI)	N% (95%CI)
<b>Overall PGT-M diagnostic rate</b>	80/80 <b>100%</b> (95.5-100.0)	2/69 <b>2.9%</b> (0.4-10.1)	15/72 <b>20.8%</b> (12.2-32.0)
Pathology	N% (95%CI)	N% (95%CI)	N% (95%CI)
Cystic Fibrosis	4/4 <b>100%</b> (39.8-100.0)	0/4 <b>0%</b> (0.0-60.2)	0/4 <b>0%</b> (0.0-60.2)
Adrenoleukodystrophy	7/7 <b>100%</b> (59.0-100.0)	0/5 <b>0%</b> (0.0-52.2)	3/7 <b>42.9%</b> (9.9-81.6)
DB muscular dystrophy	3/3 <b>100%</b> (29.2-100.0)	0/3 <b>0%</b> (0.0-70.8)	2/3 <b>66.7%</b> (9.4-99.2)
Beta thalassemia	12/12 <b>100%</b> (73.5-100.0)	1/10 <b>10%</b> (0.3-44.5)	2/12 <b>16.7%</b> (2.1-48.4)
Nonsyndromic hearing loss	6/6 <b>100%</b> (54.1-100.0)	0/3 <b>0%</b> (0.0-70.8)	1/6 <b>16.7%</b> (0.4-64.1)
DM1 myotonic dystrophy	17/17 <b>100%</b> (80.5-100.0)	0/15 <b>0%</b> (0.0-21.8)	1/16 <b>6.3%</b> (0.2-30.2)
Marfan syndrom	15/15 <b>100%</b> (78.2-100.0)	0/13 <b>0%</b> (0.0-24.7)	3/10 <b>30%</b> (6.7-65.3)
Noonan syndrom	5/5 <b>100%</b> (47.8-100.0)	1/5 <b>20%</b> (0.5-71.6)	1/3 <b>33.3%</b> (0.8-90.6)
Hemophilia	5/5 <b>100%</b> (47.8-100.0)	0/5 <b>0%</b> (0.0-52.2)	1/5 <b>20%</b> (0.5-71.6)
Huntington's disease	3/3 <b>100%</b> (29.2-100.0)	0/3 <b>0%</b> (0.0-70.8)	1/3 <b>33.3%</b> (0.8-90.6)
SCID	3/3 <b>100%</b> (29.2-100.0)	0/3 <b>0%</b> (0.0-70.8)	0/3 <b>0%</b> (0.0-70.8)

**Table 25:** PGT-M diagnostic rates in TE, BF and SBM (Capalbo et al, *Fertility and Sterility* 2018).

## 4.2 VALIDATION OF A NEW TECHNOLOGY TO PERFORM PGT-M USING INFINIUM KARYOMAPPING PROTOCOL AND ILLUMINA NEXTSEQ 550 PLATFORM

### 4.2.1 Introduction and aim of the study

Karyomapping is a comprehensive method for genome-wide linkage-based analysis of single gene defects, recently developed and commercialized (Handyside *et al.*, 2010). By Mendelian analysis of the SNP genotypes of the parents and a close relative of known disease status (termed a trio), for example an existing child (termed the reference), this method allows to identify informative loci for each of the four parental haplotypes across each chromosome and map the inheritance of these haplotypes and the position of any crossovers in the proband. The resulting ‘karyomap’, identifies the parental and grandparental origin of each chromosome (Figure 21). The test can be performed on a single cell or few cells from an embryo (day 3 and day 5 embryos) and the main advantage of this platform for PGT-M applications is that it is applicable to almost any familial single-gene disorder, or any combination of loci, within the chromosome regions covered by informative SNP loci, eliminating the need for developing patient- or disease-specific tests. The aim of this study was to verify a new SNP-array based approach to perform PGT-M on TE biopsies using Infinium karyomapping protocol and Illumina NextSeq550 platform.

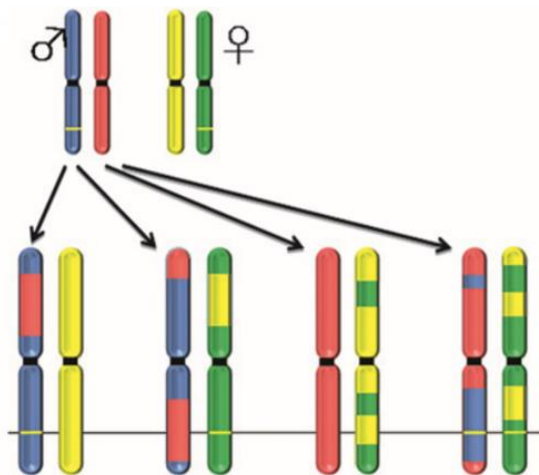


**Figure 21:** Linkage based diagnosis of inheritance of single gene defects. The two pairs of parental chromosomes (top row) are each colour coded to represent the two parental haplotypes inherited from the grandparents; the two paternal chromosomes in blue and red and the two maternal chromosomes in yellow and green. The parental haplotypes and the position of any crossovers for each paternal (left) and maternal (right) chromosomes inherited by the four children is identified and represented as a karyomap (Handyside *et al.*, 2010).

### 4.2.2 Study design and outcome measure

The verification procedure of the new protocol was performed using trophoctoderm re-biopsies from clinical PGT-M cases, where all embryos were previously analysed using linkage analysis and TaqMan genotyping in real-time PCR (Zimmerman *et al.*, 2016). In addition, all embryos were previously subjected to PGT-A analysis using a qPCR approach

validated and described elsewhere (Treff *et al.*, 2012). All embryos included in the validation were previously reported as affected by the disease for which the PGT-M was performed or aneuploid after 24 chromosome screening analysis, thus they were excluded from the transfer. Furthermore, the genomic DNA of the parents and the genomic DNA of a reference sample with known disease status, "related to the tested embryos", were analysed in the same experiment. Each sample was karyomapped, the disease status of the embryo was analysed blind, and the results were compared for concordance with the original diagnosis based on TaqMan allelic discrimination assays and indirect linked marker PGT-M analysis. In this phase we have been able to produce interesting data on inter-platform comparison and on the reliability and applicability of PGT-M to exclude inherited genetic diseases. Finally, all samples included in the verification were also blindly analysed in an independent laboratory providing useful data on the determination of the performance of karyomapping test at Igenomix laboratory (proficiency test) by inter-laboratory comparison. The aim of this study was to develop and validate a new SNP-array based approach to perform PGT-M on TE biopsies using Infinium karyomapping protocol and Illumina Next Seq 550 platform.

To evaluate the new PGT-M approach and to introduce it as a possible clinical procedure, all the main steps involved in the protocol were tested during the verification procedure:

- amplification of the entire genome using REPLI-g Advanced DNA Single Cell Kit (Qiagen);
- BeadArray analysis using the HumanKaryomap-12 DNA analysis kit;
- chip scanning with the NextSeq550 system;
- data analysis using the BlueFuse Multi software.

### **4.2.3 MATERIAL AND METHODS**

#### **4.2.3.1 Samples included in the verification**

A total of 11 samples belonging to two different PGT-M clinical cases were included in the verification. In details both families have a specific indication for Spinal Muscular atrophy (SMA), an autosomal recessive neuromuscular disease characterized by degeneration of alpha motor neurons in the spinal cord, resulting in progressive proximal muscle weakness and paralysis. This disease is caused by homozygous mutations of the survival motor neuron 1 (SMN1) gene, and the diagnostic test demonstrates in most patients the homozygous deletion of the SMN1 gene, generally showing the absence of SMN1 exon 7.

In these PGT-M cases, both members of the couples are carriers of exon 7 and 8 deletion in SMN1 gene. For each case DNA from parents and the reference, affected by the disease (trios), were included. Additional trophectoderm biopsy was performed on embryos not suitable for transfer, due to the presence of both parental mutation (affected embryos) or whole chromosome aneuploidies (Table 26).

CASE	SAMPLES	DISEASE AND MUTATIONS TESTED	DISEASE STATUS	PGT-A RESULTS
CASE 1	GX15/00678 Female partner	SPINAL MUSCULAR ATROPHY Exons 7-8 deletion	Carrier of the mutation	
	GX15/00679 Male partner	SPINAL MUSCULAR ATROPHY Exons 7-8 deletion	Carrier of the mutation	
	GX15/00742 Reference	SPINAL MUSCULAR ATROPHY Exons 7-8 deletion	Affected child	
	GM1119_3 Embryo n°3	SPINAL MUSCULAR ATROPHY Exons 7-8 deletion	Normal	Aneuploid: Monosomy 19
	GM1119_15 Embryo n°15	SPINAL MUSCULAR ATROPHY Exons 7-8 deletion	Carrier of maternal mutation	Aneuploid: Trisomy 22
	GM1119_16 Embryo n°16	SPINAL MUSCULAR ATROPHY Exons 7-8 deletion	Carrier of paternal mutation	Aneuploid: Monosomy 16
CASE 2	GX15/01736 Female partner	SPINAL MUSCULAR ATROPHY Exons 7-8 deletion	Carrier of the mutation	
	GX15/01737 Male partner	SPINAL MUSCULAR ATROPHY Exons 7-8 deletion	Carrier of the mutation	
	SMA3977 Reference	SPINAL MUSCULAR ATROPHY Exons 7-8 deletion	Affected child	
	GM1282_6SC Embryo n°6SC	SPINAL MUSCULAR ATROPHY Exons 7-8 deletion	Carrier of maternal mutation	Aneuploid: XXX
	GM1282_10SC Embryo n°10SC	SPINAL MUSCULAR ATROPHY Exons 7-8 deletion	Carrier of maternal mutation	Aneuploid: Monosomy 16, X0

**Table 26:** summary of samples included in the validation

#### 4.2.3.2 Whole genome amplification of trophectoderm biopsies

Whole genome amplification was performed using REPLI-g Advanced DNA Single Cell Kit (Qiagen). The method is based on Multiple Displacement Amplification (MDA) technology, which carries out isothermal genome amplification utilizing a uniquely processive DNA polymerase capable of replicating up to 100 kb without dissociating from the genomic DNA template. All samples were treated with 3 µl of buffer D2, prepared with

1 µl of DDT and 11 µl di buffer DLB, and incubated 10 min at room T to perform cell lysis and denaturation under isothermal alkaline conditions. After denaturation 3 ul of stop solution were added. Amplification was performed adding 40 µl of master mix, prepared following the instruction in Table 27.

REAGENTS	VOLUME/REACTION
Water, SC	9 µl
REPLI-g SC Reaction Buffer	29 µl
REPLI-g SC DNA Polymerase	2 µl
Total volume	40 µl

**Table 27:** amplification master mix components and quantities

Samples were taken in a cold rack and incubated in a PCR thermo-cycler with the lid preheated to 75°C and the isothermal amplification reaction was performed using the following program settings:

Number of cycles	Temperature of cycle	Incubation time
1	30°C	120 min
1	65°C	3 min
1	4°C	hold

**Table 28:** thermic profile of amplification reaction

Samples amplification was checked by agarose gel electrophoresis: 2 µl of MDA products, with 3 µl of water and 5 µl of 2x loading dye were electrophoresed 60 minutes at 120 V in a 0.8% 1xTBE agarose gel.

#### 4.2.3.3 Preparation and incubation of MSA3 plate

In this phase 8 µl (50 ng/µl) of gDNA from parents and reference, followed by 8 µl of TE biopsies amplified with MDA, were transferred to the corresponding wells of the MSA3 plate. Samples were treated with 40 µl of MA1 and 8 µl of NaOH 0.1M and incubated 10 minutes at room T. After incubation 68 µl MA2 and 76 µl MSM were added into each well of the MSA3 plate. Amplification was performed incubating the plate in the heat block for 2 hours at 37°C. DNA fragmentation was performed adding 50 µl of FMS and incubating the plate at 37°C for 30 minutes. All samples were then treated with 100 µl of PM1 and 310 µl 100% 2-propanol to obtain DNA precipitation.

#### 4.2.3.4 Hybridization of DNA to the BeadChip

DNA pellet was resuspended adding 17  $\mu$ l RA1 and incubating the MSA3 plate for 15 min at 48°C in the Illumina Hybridization Oven. Samples were denatured at 95°C for 20 minutes. Finally, 15  $\mu$ l of each DNA sample were then loaded onto the appropriate BeadChip section (Figure 22) and the BeadChip was placed in Hyb Chamber and incubated at 48°C for least 12 hours.

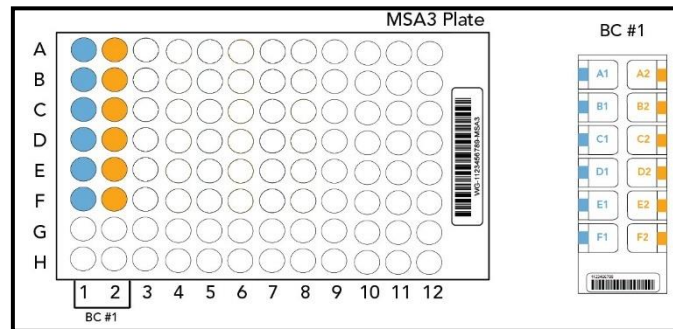


**Figure 22:** Chip loading

#### 4.2.3.5 Extend and Stain of BeadChips

After overnight incubation the chip was washed with PB1 and XC4 reagents. To wash unhybridized and nonspecifically hybridized DNA samples from the BeadChips, add labeled nucleotides to extend the primers hybridized to the DNA and stain the primers, the bead chip was treated alternately adding 250  $\mu$ l of STM and 250  $\mu$ l of ATM reagents. Before scanning the Beadchip was washed with PB1 and XC4 reagents and dried in a desiccator for 55 minutes applying a vacuum pressure of 675 mmHg (0.9 bar).

#### 4.2.3.6 BeadChip Scan

Decode Map (DMAP) files, a manifest file, and a cluster file for the BeadChip were loaded into the NextSeq550 Station. Then the Beadchip was scanned and Output files, available in a genotype call (GTC) file format, were collected from the instrument and employed for data analysis in BlueFuse Multi software.

#### 4.2.3.7 DATA ANALYSIS AND INTERPRETATION

The objective of Karyomapping data analysis is to determine whether each embryo in a case has inherited the same chromosomes from the parents as the selected reference. The outcome of the laboratory protocol is a set of genotype calls for each SNP on the array (~300000), included in *.gtc* files (Gen Train Call). These files are obtained from the Bead Chip, integrating information from *.dMap* files (Decode Map) which gives x,y location in the Bead chip, *.idat* files (Intensity Data), *.bpm* files (Bead Pool Manifest) which give information on

SNP sequence and *.egt* files (Electronic GenTrain) which contains cluster definition for each SNP (figure 23).

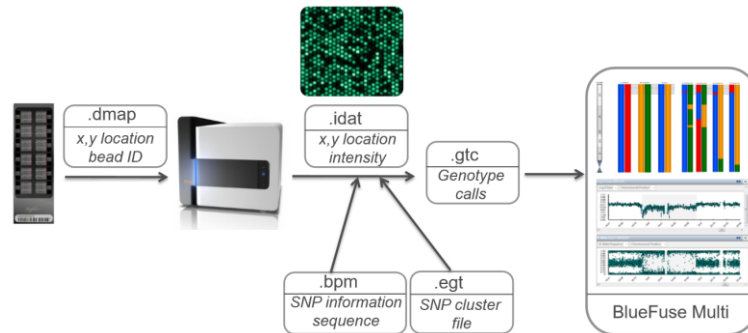


**Figure 23:** data flow from NextSeq550

Data analysis is performed from *.gvc* files using BlueFuse Multi v4.5 software (Illumina) through the following steps:

- **Informative SNPs identification:** a genotype can be assigned to 1 of the chromosomes inherited from the mother or inherited from the father. For a SNP to be informative 1 parent must have a heterozygous genotype and the other a homozygous genotype.
- **Phasing:** the informative allele is used to phase the SNPs in the embryo against the alleles of the reference. If the embryo and the reference both inherited or both did not inherit the informative allele, then they inherited the same chromosome from that parent (**in phase**). If either the embryo or the reference inherited the informative allele and the other did not, then they inherited different parental chromosomes (**out of phase**).
- **Key and Non-key SNPs:** allele drop-out (ADO) occurs when one of the alleles at a SNP fails to amplify. Key SNPs are SNPs in an embryo that contain the informative allele and ADO could not have affected their phasing. Non-key SNPs do not contain the informative allele thus there is no guarantee that they are genuinely homozygous; it is possible they have lost the informative allele through ADO and therefore had their phase altered.
- **Haploblocks generation:** paternally and maternally informative SNPs are phased for each embryo relative to the reference and represented as colored haploblocks in the

software. The Haploblock Chart shows the haploblock structure of a selected chromosome for every sample in the case reporting an ideogram of the selected chromosome, the paternal chromosome pair (P1-P2), the maternal chromosome pair (M1-M2), the reference chromosome pair (arbitrarily assigned), a pair of chromosomes for each embryo in the case, colored according to the phase predicted by Blue Fuse Multi.

Following the creation of a karyomapping case, BlueFuse Multi produces a Case Report that provides a summary of the data for a case, including the array performance and the supporting evidence for the phase of each embryo in a case. Overall each karyomapping case is assessed considering the QC measures reported in Table 29.

QC Measure	Description
<b>Call Rate</b>	The fraction of SNPs with a successfully called genotype
<b>AB Rate</b>	The fraction of called SNPs with an AB genotype
<b>ADO Rate</b>	The estimated fraction of SNPs affected by allele dropout. This rate is calculated from the proportion of loci where the embryo is homozygous but was expected to be heterozygous, based on the parental genotypes.
<b>Miscall Rate</b>	The estimated fraction of SNPs affected by genotyping errors. This rate is calculated from the proportion of loci where the embryo is heterozygous but was expected to be homozygous, based on the parental genotypes. The measured miscall rate is used to adjust the estimate of the ADO rate

**Table 29:** Main quality control parameters evaluated in karyomapping experiments.

The QC section in the case report includes metrics about the quality of the karyomapping data. The sample type has an influence on the call rate, AB rate, ADO and miscall rate. The following table lists the recommended values for good quality genomic DNA, often obtained from parental and reference samples (blood), and for amplified DNA from embryo biopsies (trophectoderm and blastomere biopsies).

Sample type	Call rate	AB rate	ADO	Miscall rate
Blood	95–99%	25–29%	~0%	~0%
Trophectoderm samples	85–99%	20–30%	0–80%	<5%

**Table 30:** optimal QC values for each type of sample.

In particular if the SNP call rates (the fraction of SNPs successfully assigned a genotype) in the parents or reference (Trio SNP call rates) are less than or equal to 0.8 is not recommended to proceed with a case. Moreover, if an embryo has a SNP call rate less than or equal to a



threshold of 0.6, BlueFuse Multi produces a Case Warning and no haplotype calls can be used for that embryo.

#### 4.2.4 RESULTS

##### CASE 1

Prior to the evaluation of diagnostic results for the specific PGT-M case, quality control parameters, recommended by the supplier, were checked from ‘Case Report’ of BlueFuse software. All the results for CASE 1 have passed the quality control parameters recommended:

1. The SNPs call rates were > 60% for embryos and > 80% for trio samples (Mother / Father / Reference)
2. AB rates for embryos and parents were all > 26%
3. ADO rates for embryos and trios were ~0%
4. Miscall rates were 0% for all samples

Quality control measure from case 1 are shown in table 31

Barcode	Array	Designation/Sample ID	Cell Type	Sign Off Status	Call					Mis- Call	Heterozygous Rate	X Call Rate	Y Call Rate
					Rate	AA	AB	BB	ADO				
201662330122	R03C01	Father GX15/00679	Blood	Not set	0.98	0.33	0.29	0.38			0.01	0.93	
201662330122	R02C01	Mother GX/00678	Blood	Not set	0.98	0.32	0.30	0.37			0.24	0.07	
201662330122	R04C01	Reference GX15/00742	Blood	Not set	0.98	0.33	0.29	0.38	0.00	0.00	0.01	0.93	
201662330122	R05C01	Embryo GM1119_3	Trophectoderm	Not set	0.95	0.34	0.26	0.40	0.03	0.00			
201662330122	R06C01	Embryo GM1119_15	Trophectoderm	Not set	0.96	0.33	0.28	0.39	0.00	0.00			
201666260034	R04C02	Embryo GM1119_16	Trophectoderm	Not set	0.96	0.33	0.28	0.39	0.03	0.00			

**Table 31:** case report, quality control measure

The most relevant information about Maternal and Paternal Informative SNPs in the main region of the gene SMN1 and in 3’ and 5’ flanking region are reported in figure 24.

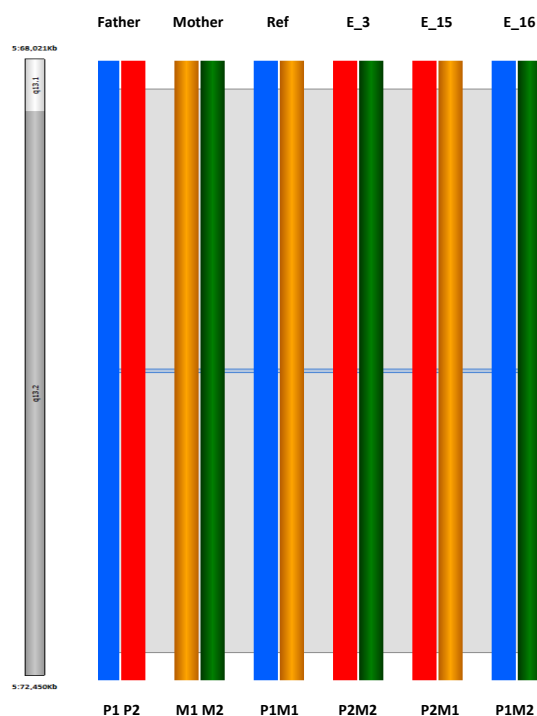
<b>Chromosome</b>	5	Disorder Type	Autosomal Recessive
<b>Band</b>	q13.2	Maternal Status	Heterozygous Carrier
<b>Start</b>	70220768	Paternal Status	Heterozygous Carrier
<b>End</b>	70249769	Reference Status	Homozygous Disease
<b>Size</b>	29.0 Kb		

Available Platform SNPs		Maternal Informative SNPs		Paternal Informative SNPs	
Left Flanking Region (5')	29	5'	7 / 29	5'	2 / 29
Main Region	0	Main	0 / 0	Main	0 / 0
Right Flanking Region (3')	91	3'	24 / 91	3'	13 / 91

**Figure 24:** case report, SMN1 region statistics

Haplotypes produced by karyomapping are relative to the reference, which had chromosome pair of reference (affected child) arbitrarily assigned as P1 from the father and M1 from the mother. In the haploblock chart blue and orange represent the paternal and maternal haplotypes, respectively, inherited by the reference. Red and green are the paternal and maternal haplotypes, respectively, that were not inherited by the reference. According to BlueFuse prediction Embryo GM1119\_3 inherited P2 chromosome from the father and M2 chromosome from the mother, meaning that the embryo inherited both different chromosome from parents with respect to the reference. Embryo GM1119\_15 inherited a different chromosome from the father (P2) but the same chromosome from the mother (M1) with respect to the reference. Embryo GM1119\_16 inherited the same paternal chromosome (P1) but different maternal chromosome (M2) with respect to the reference.



**Figure 25:** Haploblock chart for case 1 shows the haploblock structure of chromosome 5 for every sample in the case: parents, reference (ref), and each embryo (E\_3:GM1119\_3; E\_15:GM1119\_15; E\_16: GM1119\_16)

To decide on the final diagnosis of each embryo, a combination between the visualization of haploblock in the region of SMN1 gene and the individual region statistics listed in the Case Report were evaluated. For each embryo, case report contains 2 sections:

1. The predicted phase – M1 or M2, P1 or P2, listed with the supporting and opposing evidence.
2. The evidence that supports the predicted phase broken down into the number of key (strong evidence) and non-key (weaker evidence) SNPs for each phase.

The results from region statistics of the three embryos for CASE 1 are reported below:

Predicted Phase		M2, P2			
Supporting Evidence		11 key SNPs support M2			
		7 key SNPs support P2			
Contrary Evidence		0 key SNPs oppose M2			
		0 key SNPs oppose P2			
Maternal SNPs					
Region	Maternal-M1		Maternal-M2		
	Key	Non Key	Key	Non Key	
5'	0 / 6	0 / 1	1 / 1	6 / 6	
Main	0 / 0	0 / 0	0 / 0	0 / 0	
3'	0 / 10	0 / 14	10 / 14	10 / 10	
Paternal SNPs					
Region	Paternal-P1		Paternal-P2		
	Key	Non Key	Key	Non Key	
5'	0 / 2	0 / 0	0 / 0	2 / 2	
Main	0 / 0	0 / 0	0 / 0	0 / 0	
3'	0 / 5	0 / 8	7 / 8	5 / 5	

**Figure 26:** Case report: SNP phasing for embryo GM1119\_3

Predicted Phase		M1, P2			
Supporting Evidence		14 key SNPs support M1			
		4 key SNPs support P2			
Contrary Evidence		0 key SNPs oppose M1			
		0 key SNPs oppose P2			
Maternal SNPs					
Region	Maternal-M1		Maternal-M2		
	Key	Non Key	Key	Non Key	
5'	6 / 6	1 / 1	0 / 1	0 / 6	
Main	0 / 0	0 / 0	0 / 0	0 / 0	
3'	8 / 10	14 / 14	0 / 14	0 / 10	
Paternal SNPs					
Region	Paternal-P1		Paternal-P2		
	Key	Non Key	Key	Non Key	
5'	0 / 2	0 / 0	0 / 0	2 / 2	
Main	0 / 0	0 / 0	0 / 0	0 / 0	
3'	0 / 5	0 / 8	4 / 8	5 / 5	

**Figure 27:** Case report: SNP phasing for embryo GM1119\_15

Predicted Phase		M2, P1			
Supporting Evidence	15 key SNPs support M2				
	7 key SNPs support P1				
Contrary Evidence	0 key SNPs oppose M2				
	0 key SNPs oppose P1				
<b>Maternal SNPs</b>					
	Maternal-M1		Maternal-M2		
Region	Key	Non Key	Key	Non Key	
5'	0 / 6	0 / 1	1 / 1	6 / 6	
Main	0 / 0	0 / 0	0 / 0	0 / 0	
3'	0 / 10	0 / 14	14 / 14	10 / 10	
<b>Paternal SNPs</b>					
	Paternal-P1		Paternal-P2		
Region	Key	Non Key	Key	Non Key	
5'	2 / 2	0 / 0	0 / 0	0 / 2	
Main	0 / 0	0 / 0	0 / 0	0 / 0	
3'	5 / 5	8 / 8	0 / 8	0 / 5	

**Figure 28:** Case report, SNP phasing for embryo GM1119\_16

Considering all the information from haploblock visualization and automatic SNP phasing, karyomapping results for the three embryos analyzed in CASE 1 were reported and compared with the previous diagnosis, obtained with qPCR at Igenomix Italy laboratory. In addition, all karyomapping results were independently confirmed by a second external laboratory. The results are reported in Table 32.

<b>Samples</b>	<b>qPCR results (Igenomix Italy)</b>	<b>Karyomapping run 1 (Igenomix Italy)</b>	<b>Karyomapping run 2 (external laboratory)</b>
GM1119_3	Not affected	Not affected	Not affected
GM1119_15	Carrier of maternal mutation	Carrier of maternal mutation	Carrier of maternal mutation
GM1119_16	Carrier of paternal mutation	Carrier of paternal mutation	Carrier of paternal mutation

**Table 32:** summary results for CASE 1 embryos

In this verification experiment all embryo diagnosis for Spinal Muscular Atrophy, performed with karyomapping approach, were concordant with previously reported qPCR-based results and with the second karyomapping experiment performed by an external certified laboratory.

## CASE 2

Prior to the evaluation of diagnostic results for the specific PGT-M case, quality control parameters, recommended by the supplier, were checked from 'Case Report' of BlueFuse software. All the results for CASE 2 have passed the quality control parameters recommended:

1. The SNPs call rates were > 60% for embryos and > 80% for trio samples (Mother / Father / Reference)
2. AB rates for embryos and parents were all > 28%
3. ADO rates for embryos and trios were ~0%

4. Miscall rates were 0% for all samples

Quality control measure from case 2 are shown in Table 33.

Barcode	Array	Designation/Sample ID	Cell Type	Sign Off Status	Call Rate	Call				Mis-ADO Call	Heterozygous Rate	X Call Rate	Y Call Rate
						AA	AB	BB	ADO				
201662330122	R02C02	Father GX15/01737	Blood	Not set	0.98	0.33	0.29	0.38			0.01	0.93	
201662330122	R01C02	Mother GX15/01736	Blood	Not set	0.98	0.32	0.30	0.37			0.23	0.06	
201662330122	R04C02	Reference SMA3977	Blood	Not set	0.98	0.33	0.29	0.38	0.00	0.00	0.01	0.92	
201666260034	R05C01	Embryo GM1282_10sc	Trophectoderm	Not set	0.96	0.33	0.28	0.39	0.01	0.00			
201666260034	R01C02	Embryo GM1282_6sc	Trophectoderm	Not set	0.97	0.33	0.29	0.38	0.00	0.00			

**Table 32:** summary results for CASE 1 embryos

The most relevant information about Maternal and Paternal Informative SNPs in the main region of the gene SMN1 and in 3' and 5' flanking region are reported in figure 29.

<b>Chromosome</b>	5	<b>Disorder Type</b>	Autosomal Recessive		
<b>Band</b>	q13.2	<b>Maternal Status</b>	Heterozygous Carrier		
<b>Start</b>	70220768	<b>Paternal Status</b>	Heterozygous Carrier		
<b>End</b>	70249769	<b>Reference Status</b>	Homozygous Disease		
<b>Size</b>	29.0 Kb				
<b>Available Platform SNPs</b>					
Left Flanking Region (5')	29	<b>Maternal Informative SNPs</b>		<b>Paternal Informative SNPs</b>	
Main Region	0	5'	1 / 29	5'	2 / 29
Right Flanking Region (3')	91	Main	0 / 0	Main	0 / 0
		3'	11 / 91	3'	24 / 91

**Figure 29:** case report, SMN1 region statistics

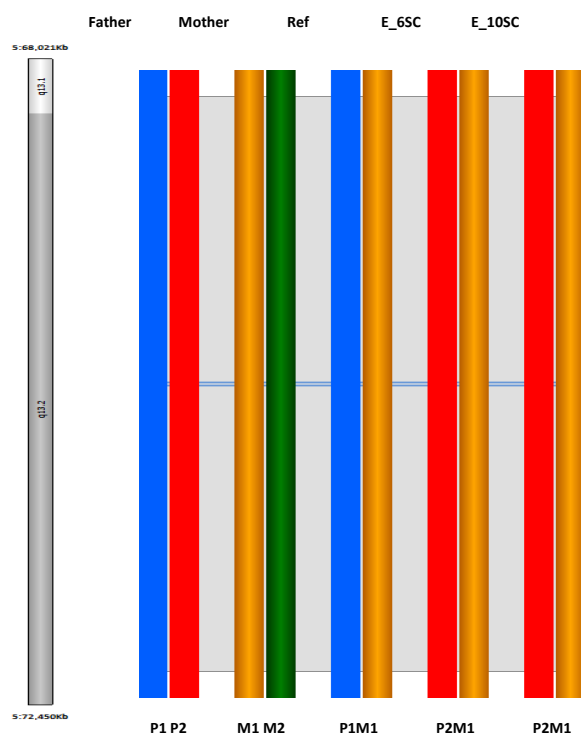


**Figure 30:** Haploblock chart for case 2 shows the haploblock structure of chromosome 5 for every sample in the case: parents, reference (ref), and each embryo. (E\_6SC: GM1282\_6SC; E\_10SC: GM1282\_10SC)

In the haploblocks, chart blue and orange represent the paternal and maternal haplotypes, respectively, inherited by the reference. Red and green are the paternal and maternal haplotypes, respectively, that were not inherited by the reference. According to BlueFuse prediction both embryos GM1282\_6SC and GM1282\_10SC inherited a different chromosome from the father (P2, red) but the same chromosome from the mother (M1, orange) with respect to the reference. Embryo phasing, in the region of SMN1 gene, was performed combining information from the individual region statistics listed in the Case Report and the visualization of haploblock were evaluated. The results from region statistics of the two embryos for CASE 2 are reported below.

<b>Predicted Phase</b>	<b>M1, P2</b>			
Supporting Evidence	7 key SNPs support M1			
	12 key SNPs support P2			
Contrary Evidence	0 key SNPs oppose M1			
	0 key SNPs oppose P2			
<b>Maternal SNPs</b>				
	<b>Maternal-M1</b>		<b>Maternal-M2</b>	
<b>Region</b>	<b>Key</b>	<b>Non Key</b>	<b>Key</b>	<b>Non Key</b>
5'	1 / 1	0 / 0	0 / 0	0 / 1
Main	0 / 0	0 / 0	0 / 0	0 / 0
3'	6 / 6	5 / 5	0 / 5	0 / 6
<b>Paternal SNPs</b>				
	<b>Paternal-P1</b>		<b>Paternal-P2</b>	
<b>Region</b>	<b>Key</b>	<b>Non Key</b>	<b>Key</b>	<b>Non Key</b>
5'	0 / 0	0 / 2	2 / 2	0 / 0
Main	0 / 0	0 / 0	0 / 0	0 / 0
3'	0 / 14	0 / 10	10 / 10	14 / 14

**Figure 31:** Case report: SNP phasing for embryo GM1281\_6sc

<b>Predicted Phase</b>	<b>M1, P2</b>			
Supporting Evidence	6 key SNPs support M1			
	12 key SNPs support P2			
Contrary Evidence	0 key SNPs oppose M1			
	0 key SNPs oppose P2			
<b>Maternal SNPs</b>				
	<b>Maternal-M1</b>		<b>Maternal-M2</b>	
<b>Region</b>	<b>Key</b>	<b>Non Key</b>	<b>Key</b>	<b>Non Key</b>
5'	1 / 1	0 / 0	0 / 0	0 / 1
Main	0 / 0	0 / 0	0 / 0	0 / 0
3'	5 / 6	5 / 5	0 / 5	0 / 6
<b>Paternal SNPs</b>				
	<b>Paternal-P1</b>		<b>Paternal-P2</b>	
<b>Region</b>	<b>Key</b>	<b>Non Key</b>	<b>Key</b>	<b>Non Key</b>
5'	0 / 0	0 / 2	2 / 2	0 / 0
Main	0 / 0	0 / 0	0 / 0	0 / 0
3'	0 / 14	0 / 10	10 / 10	14 / 14

**Figure 32:** Case report: SNP phasing for embryo GM1281\_10sc

Considering all the information from haploblock visualization and automatic SNP phasing, karyomapping results for the two embryos analyzed in CASE 2 were reported and compared with the previous diagnosis, obtained with qPCR at Igenomix Italy laboratory (Table 34). In addition, all karyomapping results were independently confirmed by a second external laboratory.

<b>Samples</b>	<b>qPCR results (Igenomix Italy)</b>	<b>Karyomapping run 1 (Igenomix Italy)</b>	<b>Karyomapping run 2 (external laboratory)</b>
GM1282_6SC	Carrier of maternal mutation	Carrier of maternal mutation	Carrier of maternal mutation
GM1282_10SC	Carrier of maternal mutation	Carrier of maternal mutation	Carrier of maternal mutation

**Table 34:** summary results for CASE 2 embryos.

## 5 DISCUSSION AND CONCLUSIONS

Preimplantation genetic testing is a methodology designed to assess the genetic complement of embryos generated during in vitro fertilization treatments. During the years, improvements in culture systems and cryopreservation protocols employed in IVF allowed the production of more robust results from genetic testing and additional analytical flexibility and costs reduction. PGT-A has been introduced in clinical routine practice to improve pregnancy rates in sub-fertile couples, since aneuploidy has been reported as the single most important cause of implantation failure and miscarriage in humans (Hassold and Hunt, 2001). Later, large datasets from comprehensive aneuploidy testing of preimplantation embryos have demonstrated that over half of embryos produced by in vitro fertilization are aneuploid (Rabinowitz *et al.*, 2012; Fragouli *et al.*, 2013; Franasiak *et al.*, 2014) and maternal age is the major factor that influences aneuploidy. Indeed, Harton *et al.* (Harton *et al.*, 2013) demonstrated that implantation rates remain stable across all age groups if euploid embryos are transferred; therefore, aneuploidy is the predominant cause of age-related decline in fertility. Today, the use of comprehensive chromosome screening tools for PGT-A (24 chromosomes), allows the identification and exclusion for treatment of abnormal embryos carrying whole chromosome aneuploidy, thus avoiding the transfer of embryos destined to developmental arrest or miscarriage soon after implantation. Additionally, the use of PGT-A drastically reduces the risk of transferring embryos carrying chromosomal abnormalities compatible with life but associated with severe syndromes (i.e., involving chromosomes 13, 18, 21 and X).

Over the years, several methodologies have been employed for PGT-A analysis, including array comparative genomic hybridization, single-nucleotide polymorphism array, quantitative real-time PCR and, more recently, NGS. The need of producing reliable and faster results, combined with the increasingly spread of PGT, have increased the processivity of recent technologies compared to the previous approaches, allowing the reduction of both costs and time associated to the analysis. This technological evolution has allowed the optimisation of molecular protocols and our laboratory workflow. In the first part of this project, we evaluated two different protocols both characterized by the possibility of increasing the number of samples analysed, respect to the first protocol employed. In details we firstly designed and validated a novel plate layout for the simultaneous analysis of 2 additional embryos per run, following the first standard protocol base on real time qPCR, employed for



routine PGT-A analysis. The validation of this new experimental layout has reached high levels of concordance and diagnostic reliability, both on cell lines and multiple trophoctoderm biopsies from the same embryo. Despite its potential advantage with respect to the first layout, qPCR-based PGT-A was replaced with a novel NGS-based approach. The last platform was characterised by high throughput and processing capacity allowing the simultaneous analysis of up to 96 samples per run. Moreover, a significant improvement in automatization of library's clonal amplification using Ion Chef System, has allowed the reduction of hands-on time. The protocol perfectly fits with laboratory workflow due its scalability of 24 or 96 samples/run, rapid turnaround time and easy-to-use data analysis software. The clinical application of Ion Reproseq protocol and Ion Torrent platform was preceded by extensive technical validation performed in two independent sequencing runs. The validation procedure of whole chromosome aneuploidies detection reached high levels of accuracy and the precision obtained in both sequencing runs gave us enough confidence to use Ion ReproSeq™ platform for the 24-chromosome aneuploidy screening in PGT-A.

Moreover, the higher resolution of new NGS platforms has the potential to enable the detection of not only whole chromosome aneuploidies, but also sub-chromosomal abnormalities (segmental aneuploidies) and the presence of embryonic mosaicism. Thus moving from a qPCR approach, typically producing a binary result (euploid/aneuploid), NGS based platforms have introduced novel diagnostic categories: partial aneuploid with one portion of a chromosome missing or duplicated in all cells, mosaic containing two different cell lines within the same embryo (often one euploid cell line and one aneuploid cell line), or partial mosaic with one euploid cell line and one partial aneuploid cell line. Unfortunately, the clinical management of these type of alterations is still limited by their unclear biological and prognostic significance. Thus, in this part of the study we lastly focused on clarifying the biological and clinical significance of segmental aneuploidies in preimplantation embryos. We first compared the diagnostic results obtained from the two main platforms employed for routine PGT-A analysis in our laboratory, qPCR and NGS, which are characterised by different resolution toward segmental aneuploidies. Despite different analytical resolution, we did not report significant difference in the overall aneuploidy rate between qPCR and NGS-based results. Since qPCR-based technology targets only 4 regions on each chromosome, it is possible that some large segmental aneuploidies are reported as whole chromosome aneuploidy by qPCR. When focusing on the general contribution of sub-

chromosomal aneuploidies, only 2.65% of samples analysed with NGS technology displayed single or multiple segmental aneuploidies as the only alteration. Remarkably, contrary to whole chromosome aneuploidies, segmental aneuploidies were primarily affecting larger chromosomes. This pattern of incidence is consistent with those reported in other works (Zhou *et al.*, 2018), and clearly supports the hypothesis that molecular mechanisms leading to segmental aneuploidy are likely to be distinct from those responsible for whole chromosome aneuploidies. Because segmental aneuploidies incidence was not correlated with female age, their minimal contribution to NGS-based aneuploidy rate did not affect the global maternal age dependent increase. These data are thus confirming high inter-platform concordance of PGT-A results when working in standardized conditions and a relatively low clinical incidence of segmental aneuploidies in the general PGT-A practice with NGS, providing higher capability for aneuploidy discrimination.

In terms of single TE biopsy predictivity of whole embryo ploidy status, our data from multifocal analysis of TE and ICM specimens revealed high predictivity only when uniform whole chromosome aneuploidies are considered. Indeed, whole chromosomal alterations were consistently detected across all blastocyst sections, showing minimal evidence of karyotype discordance and mosaicism incidence in human blastocyst stage embryos. In particular, only 4 out of 390 (1%) ICM/TE biopsies showed a different aneuploidy pattern compared to the expected profile. It is important to stress that the observed discordance rate for these 4 TE biopsies (1%) accounts for the combination and sum of both true biological variations (e.g. mosaicism for whole chromosomes) and false positive analytical error rate. The high reliability of whole chromosome aneuploidies detection was also confirmed in an independent clinical dataset of double TE biopsies comparison, when single TE re-biopsy was performed in clinical conditions. These results are in line with previous studies showing high concordance rates for whole chromosome aneuploidies between TE re-biopsies and ICM from the same blastocyst when only uniform aneuploidies are reported (Popovic *et al.*, 2018; Victor *et al.*, 2019) or more stringent and narrow range for mosaicism classification is applied (Lawrenz *et al.*, 2019). These results highlight the high reliability and representativeness of blastocyst stage PGT-A analysis when performed with standardized criteria for aneuploidy classification (Capalbo *et al.*, 2016).

In contrast, comparing PGT-A results obtained from different TE biopsies and ICM, showed low confirmation rates for segmental aneuploidies and highlighted their true mitotic origin.

Indeed, contrary to whole chromosome aneuploidies, a significant proportion of segmental alterations are not uniformly present in the whole blastocyst, reducing both their positive and negative predictive values in blastocyst stage PGT-A cycles. In fact, approximately half of the segmental aneuploidies detected in clinical TE biopsies are not confirmed when a second biopsy was collected or when the entire embryo was disaggregated and reanalysed. Interestingly, our results showed both different aneuploidies patterns and reciprocal segmental alterations in independent biopsies, revealing clear evidence of mitotic non-disjunction events. In particular, 47% of disaggregated blastocysts where the aneuploidy was confirmed in at least one additional biopsy, showed a pattern consistent with true mosaicism. The fact that different TE portions showed discordant PGT-A profiles raises several issues regarding technical and biological limitations of single cTE biopsy analysis in detecting biological heterogeneity of the whole blastocyst for both research studies and clinical PGT-A application. On the research side, it is clear that forthcoming studies focusing on PGT-A predictivity will need to consider segmental aneuploidies separately from whole chromosome analysis. Indeed, since segmental aneuploidy frequently originate as a consequence of mitotic errors during preimplantation development, the observation of discordant intra-blastocyst results should be considered as an expected outcome (Lawrenz *et al.*, 2019).

From a clinical standpoint, these data suggest that a diagnosis of segmental aneuploidy on a single TE biopsy is not sufficient to correctly predict the ICM chromosomal constitution or the clinical implication of the observed aneuploidy. The clinical management of embryos showing segmental aneuploidy as the only abnormality in the cTE biopsy is extremely challenging at present as the transfer of these embryos can be seen as a potentially risky procedure. In our study, 32% of all segmental aneuploidies detected were of meiotic origin, while in an additional 28% of cases the aneuploidy was detected in mosaic constitution but still involving the ICM. Considering the potentially harmful effect of transferring embryos with segmental aneuploidies (Capalbo *et al.*, 2017b) and the limited clinical data available, our findings suggest extreme caution when evaluating their clinical use. At present, no clinical data are available to assess the reproductive potential of embryos showing uniform segmental aneuploidies. Only two retrospective studies have reported clinical data following the transfer of embryos showing mosaic segmental aneuploidies in cTE biopsies (Fragouli *et al.*, 2017; Munné *et al.*, 2019). Both these studies showed that blastocysts with segmental mosaicism have reduced reproductive potential, higher miscarriage rate but retain the ability

to result in live birth (8/14, 57% implantation rate, (Fragouli *et al.*, 2017); 26/65, 40% live-birth rate, (Munné *et al.*, 2019). Unfortunately, these retrospective studies are both based on a very small sample size (60 embryos transferred collectively), on the analysis of putative mosaic segmental aneuploidies (not uniform) and affected by selection bias where segmental mosaic embryos are transferred as last option in patients who had already failed with previous euploid embryo transfers. Thus, the clinical relevance and the possibility to translate these data for clinical evaluation remains very limited and further prospective non-selection studies are required. In this study, additional parameters were evaluated to improve the predictive value of segmental alterations in TE biopsies. As shown above, the segmental length and the confirmation of the segmental finding in an independent scTE biopsy are valuable parameters for tailoring patient's counselling after a segmental aneuploidy is detected during clinical treatment. In particular, failure to confirm the same chromosome segmental alteration in a second clinical TE biopsy lowers the risk of ICM involvement from 50% to 21%. Additionally, in this low risk group, the occurrence of a segmental abnormality shorter than 80Mb was able to further reduce the risk down to 10% of ICM involvement. On the contrary, the confirmation of the aneuploidy on a scTE in the presence of a segmental alteration larger than 80 Mb was always associated with ICM involvement. Thus, at current state of knowledge, both confirmation result from second biopsy and fragment length can be suggested as valuable parameters for evaluation of transfer of embryos showing only a segmental aneuploidy in the original cTE biopsy. This approach would particularly benefit poor prognosis patients showing few or no euploid embryos for transfer following PGT-A. Of note, a second round of TE biopsy and cryopreservation is not expected to reduce implantation outcome or increase pregnancy complications (Cimadomo *et al.*, 2018).

In terms of negative predictive value of segmental aneuploidies detected in cTE biopsies, in our cohort of 25 euploid embryos, only one showed evidence for a reciprocal segmental aneuploidy involving 2 of the 4 TE samples and none of the 25 ICM biopsies analysed. Thus, in euploid embryo transfer cycles a very low residual risk can be predicted for segmental aneuploidies, as indeed observed by Product Of Conception (POC) analysis and PND following PGT-A cycles.

In conclusion, our results support and confirm optimal performance of TE-based PGT-A analysis in diagnosing uniform whole chromosome aneuploidies, with almost perfect concordance rate toward the ICM. Accordingly, for the main and primary purpose of PGT-A

of detecting meiotically derived aneuploidies, the performance is consistently within the expectations and standards. We have further characterized that segmental aneuploidies are often mitotic posing challenges for interpretation and clinical management. While a second TE analysis was shown the best available approach to enhance predictivity and clinical management, the different patterns (i.e., mosaic distribution, involvement of ICM) are impossible to be distinguished based on a single observation and careful consideration is required when reporting this information in PGT-A cycles. Although their relative contribution to PGT-A cycles is low, involving less than 3% of the blastocysts, future non-selection studies will need to investigate the clinical predictive values of segmental abnormalities detected in single or double clinical TE biopsy and their impact on embryonic reproductive potential and gestational risks.

In the second part of this project we focused on two different approaches for the application of PGT to the diagnosis of monogenic conditions in the embryo. Recently the explosion of preconception carrier screening for couples with no family history of specific genetic disease as a result of best practice guidelines, reduced cost, and improved access to pan-ethnic expanded carrier screening have increased further the number of PGT-M cases and the conditions for which PGT-M is applied. According to the latest ESHRE PGD consortium data the most common indications, involving the presence of two mutated copies from each healthy carrier parent, are cystic fibrosis, spinal muscular atrophy, and hemoglobinopathies. (De Rycke *et al.*, 2015). For autosomal dominant conditions myotonic dystrophy type 1, neurofibromatosis, and Huntington's disease are the most frequently requested indications. More recently cancer predisposition, HLA matching and isoimmunisation are novel indications for PGT-M. As a consequence, thanks to improving technologies and best practice guidelines, PGT-M analysis has reached a high level of accuracy and has enabled also the possibility of performing multiple diagnoses from the same sample. Two main issues in the field of PGT still require further evaluation and improvements. Firstly, despite trophoctoderm biopsy provides the most robust and reliable source of embryonic DNA for the analysis of embryo's genetic features without affecting embryo's reproductive potential, there is increasing interest in reducing or completely avoid intervention on the embryo for diagnostic purposes, developing non-invasive procedures to collect embryo-derived DNA for the subsequent genetic assessment. (Poli *et al.*, 2019). Secondly, the majority of current PGT-

M methodologies requires a preliminary patient-specific custom SET-UP phase, which increases the time the patient has to wait before starting IVF procedures. In this project both these aspects were considered and evaluated. Focusing on non-invasive PGT-M, in the last 5 years many studies have been published on the efficacy of these strategies for PGT-A and/or PGT-M, however different methodologies applied to culture systems, samples collection and DNA analysis have produced different concordant rates (or inconsistent results compared to the gold standard) (Feichtinger *et al.*, 2017; Hammond *et al.*, 2017; Vera-Rodriguez *et al.*, 2018). With our in home protocol based on SNP genotyping analysis with TaqMan assay we have been able to develop a minimal invasive protocol for blastocoel fluid and non-invasive protocol for spent culture media assessment, without changing the standard operating procedures (Capalbo *et al.*, 2018). Interestingly, we have sought not only to assess the embryonic origin of the DNA from each sample type, but also to evaluate concordance rates in assigning a genotype to the corresponding embryo. Indeed, embryos' genotypes were generated during PGT-M cycles and compared across the different specimens, considering TE biopsy as the gold standard. Although inferior compared with the TE samples, the SBM samples performed statistically significantly better than the BF samples in terms of diagnostic rate. Despite its diagnostic potential, SBM showed high detection of artefacts or ADI, which occurred in 10.1% of all loci investigated. This notable rate of detectable nonembryonic DNA material has several potential origins including the presence of exogenous DNA in the culture media (Hammond *et al.*, 2017; Vera-Rodriguez *et al.*, 2018). Although this type of DNA contamination is negligible and possibly harmless in conventional IVF treatments, it can be easily detected when SNP genotyping is employed on culture media samples. It is interesting that the ADO rates were statistically significantly higher for paternal alleles than maternal ones in both BF and SBM samples. This preliminary observation suggested an imbalance in DNA representation in favour of maternal DNA over paternal DNA. It is thus probable that genetic material from the cumulus complex or polar bodies is still present in the culture system and that it is collected and analysed together with embryonic DNA. In the SBM samples, this hypothesis was further supported by the detection of the mutated allele of maternal origin where the corresponding TE showed homozygosity for the wild-type allele. These data provided clear evidence about the substantial presence of maternal DNA in SBM samples. Recent studies have suggested the clinical use of SBM for PGT-M (Wu *et al.*, 2015), but our results highlight the needs for further investigations before this diagnostic

approach can be considered in clinical settings. Several strategies could be adopted to increase the fraction of embryonic DNA and prevent nonembryonic DNA carryover. An interesting example is given in the study recently performed by Rubio and colleagues (Rubio *et al.*, 2019a) where some technical improvements in the culture conditions of IVF laboratory were introduced, to reduce the time of contact between the embryo and the collected spent culture media. In details, on day 4, each compacted embryo was thoroughly washed in three sequential 20  $\mu$ l drops of culture media and finally moved to an individual 10  $\mu$ l drop. Once the embryos reached the fully expanded blastocyst stage on day 5–7, they were moved to a biopsy dish and the SBM were collected. Thus, the SBM corresponded to conditioned culture media collected after 1 day in culture (day 4 to day 5) or 2 or 3 days in culture (day 4 to day 6 or 7). Interestingly, they provided evidence that modification in the culture conditions can improve informativity and concordance rates decreasing the impact of maternal contamination in the accuracy of the diagnosis. In our data set, only a fraction (37.5%) of the amplified samples led to results concordant with those generated by TE biopsies, in agreement with published data by Tobler's and Werner's groups (53% and 72% of amplified samples matched the original embryo diagnosis, respectively). The biological bases of such discordances are extremely difficult to define in the absence of functional studies on the biological mechanisms of embryonic DNA release in the extracellular environment. Membrane-encapsulated DNA can derive from DNA-containing fragments originating from cells undergoing apoptosis, or self-corrective mechanisms in chromosome segregation processes during cell division or selective degeneration of abnormal cells in mosaic diploid/aneuploid embryos. This type of nonrepresentative DNA can provide serious contamination to the analytical sample, critically impairing the diagnostic accuracy. Thus, based on the standard methodologies adopted in this study, neither BF nor SBM genetic analysis offers consistent and sufficiently reliable diagnostic rates to justify their use in clinical PGT treatments. Due to the high risk of maternal contamination and subsequent misdiagnosis directly observed, SBM should not be used as specimens for the detection of single-gene mutations until these risk factors are properly assessed and prevented. To conclude, the presence of measurable cell-free DNA in the BF and spent culture media of human embryos is well demonstrated, nonetheless, future efforts to develop novel strategies for the enrichment of the embryonic DNA fraction in SBM samples are needed before accepting non-invasive PGT (Ni-PGT) as a reliable source of embryonic genomic information.

Another interesting diagnostic strategy recently proposed for PGT-M is Karyomapping. In this project we have verified the Infinium Karyomapping Bead Chip protocol provided by Illumina, which employed the karyomapping approach previously tested in a multicentre validation study including 218 embryos from 44 PGT-M cases (Natesan *et al.*, 2014a). The verification procedure was performed using TE rebiopsies belonging to clinical cases, where a previous diagnosis was established using the standard protocol for PGT-M and real time qPCR technology. Comparison of karyomapping with the current standard practice for identifying the inheritance of single gene disorders (SGD) has confirmed that karyomapping is highly accurate. Indeed, all original diagnosis were confirmed when the protocol was applied in our laboratory and then secondly confirmed, following the same protocol, in an external laboratory. The main advantage of this methodology is that PGT-M can be offered clinically without the need of customized patient- or disease-specific test development. As a result, the time patients have to wait to initiate their IVF cycle is dramatically reduced. As in the verification experiment, each case requires only the DNA from trios (mother, father and reference) which are analysed simultaneously with TE biopsies. Thus, theoretically can be applied to any familial SGD, within the chromosome regions covered by informative SNP loci. However, the major limitation of karyomapping is that it does not include direct mutation detection but only indirect linkage analysis. Thus, the strength of the diagnosis is completely due to the phasing procedure, by which parental haplotypes of both parents are defined, starting from heterozygous loci of the reference. In cases where insufficient informative SNPs markers are found in the region of interest (e.g., in some telomeric genes) or when pseudogenes are involved the diagnosis is challenging. Moreover, karyomapping cannot be performed without a reference, thus is not immediately applicable to de novo mutations where there's not a family history (Natesan *et al.*, 2014a). For these cases Karyomapping should be used in combination with direct mutation detection, for at least one embryo, to define the phase (Giménez *et al.*, 2015). Regarding the possibility of determining both monogenic diagnosis and aneuploidy detection, the high SNP coverage of each human chromosome provided by the HumanKaryomap-12 BeadChip allows the accurate identification of the region of interest containing the mutation and simultaneous high-resolution molecular cytogenetic analysis. Indeed, it has been reported that meiotic trisomies can be identified by the presence of both haplotypes from one parent in segments of the chromosome, resulting from the inheritance of two chromosomes with different patterns of



recombination, in combination with a single haplotype from the other parent. Moreover, monosomies or deletions can be identified by the absence of one of the parental haplotypes. Despite several studies reported, a clinical use of karyomapping (Natesan *et al.*, 2014b; Thornhill *et al.*, 2015) for both monogenic and chromosomal aneuploidies exclusion, there are still some technical limitations in detecting post-zigotic errors, such as mitotic and mosaic aneuploidies. It should be emphasized that, during this study, only the chromosome in which the gene of interest was located was assessed, nevertheless all the aneuploidies were correctly detected and identified using “karyotype charts”, confirming the high reproducibility of meiotic whole chromosome aneuploidies detection between different rebiopsies of the same embryo. In conclusion, considering that detecting chromosomal aneuploidies is not the main purpose of this technology, its use represents a significant advance over the current gold standard for PGT and will be a powerful tool to investigate parental origin and phase of origin of meiotic chromosome errors. Nevertheless, at present karyomapping is not commercially offered for chromosome screening and accurate validation is necessary before its clinical use. Regarding its application for PGT-M we can confirm the high accuracy of the protocol, even though only spinal muscular atrophy was evaluated during the verification. The protocol is feasible in 2 working days and avoids the time-consuming SET-UP phase, clearly reducing the time and costs to embryo diagnosis. Due to its limitations on direct mutation assessment, karyomapping is not use as the gold standard in our laboratory but represents a powerful tool to obtain genotyping data for parents, in order to select informative SNPs according to the disease investigated. SNP genotyping using TaqMan assay and real time PCR combined with linkage analysis remains the best approach that covers the largest number of SGD with different mode of transmission, with direct mutation assessment and indirect linkage analysis.

Recent genomics technological achievements and optimization in molecular protocols have allowed to generate reliable diagnostic conclusion both for chromosomes and single gene disorders testing. Our current PGT-A technology is well-integrated in the PGT workflow and allows our laboratory to handle high volumes of samples for CCS tests, providing a very valuable tool for couples of advanced reproductive age to benefit from PGT by avoiding the transfer of chromosomally impaired embryos. Nevertheless, current PGT approaches have margin for improvement, especially for what it concerns parallel PGT-A

and PGT-M analysis. Regarding non-invasive approaches, they represent an interesting field of development for PGT, especially if we consider that spent embryo culture media contains not only DNA from the embryo, but also small noncoding RNA, microRNAs (Cimadomo *et al.*, 2019) and other potential biomarkers for non-invasive embryo assessment. Nevertheless, based on our study PGT-M with non-invasive approaches is not ready to be offered as a commercial or clinical test and cannot replace embryo biopsy. Further improvements in SBM collection methods and analysis are clearly necessary to avoid maternal contamination and increase concordance rates.

## 6 REFERENCES

- Capalbo A, Hoffmann ER, Cimadomo D, Ubaldi FM, Rienzi L. Human female meiosis revised: New insights into the mechanisms of chromosome segregation and aneuploidies from advanced genomics and time-lapse imaging. *Hum Reprod Update* 2017a;.
- Capalbo A, Rienzi L. Mosaicism between trophectoderm and inner cell mass. *Fertil Steril* [Internet] 2017;**107**:1098–1106. Elsevier Inc.
- Capalbo A, Rienzi L, Cimadomo D, Maggiulli R, Elliott T, Wright G, Nagy ZP, Ubaldi FM. Correlation between standard blastocyst morphology, euploidy and implantation: An observational study in two centers involving 956 screened blastocysts. *Hum Reprod* 2014;**29**:1173–1181.
- Capalbo A, Rienzi L, Ubaldi FM. Diagnosis and clinical management of duplications and deletions. *Fertil Steril* [Internet] 2017b;**107**:12–18. Elsevier Inc.
- Capalbo A, Romanelli V, Patassini C, Poli M, Girardi L, Giancani A, Stoppa M, Cimadomo D, Ubaldi FM, Rienzi L. Diagnostic efficacy of blastocoel fluid and spent media as sources of DNA for preimplantation genetic testing in standard clinical conditions. *Fertil Steril* 2018;
- Capalbo A, Treff NR, Cimadomo D, Tao X, Upham K, Ubaldi FM, Rienzi L, Scott RT. Comparison of array comparative genomic hybridization and quantitative real-time PCR-based aneuploidy screening of blastocyst biopsies. *Eur J Hum Genet* [Internet] 2015;**23**:901–906. Nature Publishing Group.
- Capalbo A, Ubaldi FM, Cimadomo D, Noli L, Khalaf Y, Farcomeni A, Ilic D, Rienzi L. MicroRNAs in spent blastocyst culture medium are derived from trophectoderm cells and can be explored for human embryo reproductive competence assessment. *Fertil Steril* 2016;
- Capalbo A, Ubaldi FM, Rienzi L, Scott R, Treff N. Detecting mosaicism in trophectoderm biopsies: Current challenges and future possibilities. *Hum Reprod* 2017c;.
- Capalbo A, Wright G, Elliott T, Ubaldi FM, Rienzi L, Nagy ZP. FISH reanalysis of inner cell mass and trophectoderm samples of previously array-CGH screened blastocysts shows

high accuracy of diagnosis and no major diagnostic impact of mosaicism at the blastocyst stage. *Hum Reprod* 2013;**28**:2298–2307.

Cimadomo D, Capalbo A, Ubaldi FM, Scarica C, Palagiano A, Canipari R, Rienzi L. The Impact of Biopsy on Human Embryo Developmental Potential during Preimplantation Genetic Diagnosis. *Biomed Res Int* 2016;

Cimadomo D, Rienzi L, Giancani A, Alviggi E, Dusi L, Canipari R, Noli L, Ilic D, Khalaf Y, Ubaldi FM, *et al.* Definition and validation of a custom protocol to detect miRNAs in the spent media after blastocyst culture : searching for biomarkers of implantation. 2019;1–16.

Cimadomo D, Rienzi L, Romanelli V, Alviggi E, Levi-Setti PE, Albani E, Dusi L, Papini L, Livi C, Benini F, *et al.* Inconclusive chromosomal assessment after blastocyst biopsy: Prevalence, causative factors and outcomes after re-biopsy and re-vitrification Amulticenter experience. *Hum Reprod* 2018;**33**:1839–1846.

Cohen J, Wells D, Munné S. Removal of 2 cells from cleavage stage embryos is likely to reduce the efficacy of chromosomal tests that are used to enhance implantation rates. *Fertil Steril* 2007;

Feichtinger M, Vaccari E, Carli L, Wallner E, Mädler U, Figl K, Palini S, Feichtinger W. Non-invasive preimplantation genetic screening using array comparative genomic hybridization on spent culture media: a proof-of-concept pilot study. *Reprod Biomed Online* 2017;

Fiorentino F, Biricik A, Bono S, Spizzichino L, Cotroneo E, Cottone G, Kokocinski F, Michel CE. Development and validation of a next-generation sequencing-based protocol for 24-chromosome aneuploidy screening of embryos. *Fertil Steril* 2014;

Fragouli E, Alfarawati S, Spath K, Babariya D, Tarozzi N, Borini A, Wells D. Analysis of implantation and ongoing pregnancy rates following the transfer of mosaic diploid–aneuploid blastocysts. *Hum Genet* 2017;

Fragouli E, Alfarawati S, Spath K, Jaroudi S, Sarasa J, Enciso M, Wells D. The origin and impact of embryonic aneuploidy. *Hum Genet* 2013;**132**:1001–1013.

Fragouli E, Lenzi M, Ross R, Katz-Jaffe M, Schoolcraft WB, Wells D. Comprehensive

- molecular cytogenetic analysis of the human blastocyst stage. *Hum Reprod* 2008;
- Franasiak JM, Forman EJ, Hong KH, Werner MD, Upham KM, Treff NR, Scott RT. The nature of aneuploidy with increasing age of the female partner: A review of 15,169 consecutive trophoctoderm biopsies evaluated with comprehensive chromosomal screening. *Fertil Steril* 2014;
- Gianaroli L, Magli MC, Pomante A, Crivello AM, Cafueri G, Valerio M, Ferraretti AP. Blastocentesis: A source of DNA for preimplantation genetic testing. Results from a pilot study. *Fertil Steril* 2014;
- Giménez C, Sarasa J, Arjona C, Vilamajó E, Martínez-Pasarell O, Wheeler K, Valls G, Garcia-Guixé E, Wells D. Karyomapping allows preimplantation genetic diagnosis of a de-novo deletion undetectable using conventional PGD technology. *Reprod Biomed Online* 2015;
- Goodrich D, Xing T, Tao X, Lonczak A, Zhan Y, Landis J, Zimmerman R, Scott RT, Treff NR. Evaluation of comprehensive chromosome screening platforms for the detection of mosaic segmental aneuploidy. *J Assist Reprod Genet* 2017;**34**:975–981. *Journal of Assisted Reproduction and Genetics*.
- Gutiérrez-Mateo C, Colls P, Sánchez-García J, Escudero T, Prates R, Ketterson K, Wells D, Munné S. Validation of microarray comparative genomic hybridization for comprehensive chromosome analysis of embryos. *Fertil Steril* 2011;
- Hammond ER, McGillivray BC, Wicker SM, Peek JC, Shelling AN, Stone P, Chamley LW, Cree LM. Characterizing nuclear and mitochondrial DNA in spent embryo culture media: genetic contamination identified. *Fertil Steril* 2017;
- Hammond ER, Shelling AN, Cree LM. Nuclear and mitochondrial DNA in blastocoele fluid and embryo culture medium: Evidence and potential clinical use. *Hum Reprod* 2016;
- Handyside AH, Harton GL, Mariani B, Thornhill AR, Affara N, Shaw MA, Griffin DK. Karyomapping: A universal method for genome wide analysis of genetic disease based on mapping crossovers between parental haplotypes. *J Med Genet* 2010;**47**:651–658.
- Handyside AH, Kontogianni EH, Hardy K, Winston RML. Pregnancies from biopsied human preimplantation embryos sexed by Y-specific DNA amplification. *Nature* 1990;

- Handyside AH, Lesko JG, Tarín JJ, Winston RM I., Hughes MR. Birth of a Normal Girl after in Vitro Fertilization and Preimplantation Diagnostic Testing for Cystic Fibrosis. *N Engl J Med* 1992;
- Harton GL, Munné S, Surrey M, Grifo J, Kaplan B, McCulloh DH, Griffin DK, Wells D. Diminished effect of maternal age on implantation after preimplantation genetic diagnosis with array comparative genomic hybridization. *Fertil Steril* 2013;
- Hassold T, Hunt P. To err (meiotically) is human: The genesis of human aneuploidy. *Nat Rev Genet* 2001;
- Huang J, Yan L, Lu S, Zhao N, Xie XS, Qiao J. Validation of a next-generation sequencing–based protocol for 24-chromosome aneuploidy screening of blastocysts. *Fertil Steril* 2016;
- Kung A, Munné S, Bankowski B, Coates A, Wells D. Validation of next-generation sequencing for comprehensive chromosome screening of embryos. *Reprod Biomed Online* 2015;
- Lawrenz B, Khatib I El, Liñán A, Bayram A, Aranz A, Chopra R, Munck N De, Fatemi HM. The clinicians’ dilemma with mosaicism-an insight from inner cell mass biopsies. *Hum Reprod* 2019;
- Munné S, Spinella F, Grifo J, Zhang J, Beltran MP, Fragouli E, Fiorentino F. Clinical outcomes after the transfer of blastocysts characterized as mosaic by high resolution Next Generation Sequencing- further insights. *Eur J Med Genet* [Internet] 2019;103741. Elsevier Available from: <https://linkinghub.elsevier.com/retrieve/pii/S1769721219301545>.
- Munné S, Wells D. Detection of mosaicism at blastocyst stage with the use of high-resolution next-generation sequencing. *Fertil Steril* 2017;
- Natesan SA, Bladon AJ, Coskun S, Qubbaj W, Prates R, Munne S, Coonen E, Dreesen JCFM, Stevens SJC, Paulussen ADC, *et al.* Genome-wide karyomapping accurately identifies the inheritance of single-gene defects in human preimplantation embryos in vitro. *Genet Med* 2014a;**16**:838–845.
- Natesan SA, Handyside AH, Thornhill AR, Ottolini CS, Sage K, Summers MC,

- Konstantinidis M, Wells D, Griffin DK. Live birth after PGD with confirmation by a comprehensive approach (karyomapping) for simultaneous detection of monogenic and chromosomal disorders. *Reprod Biomed Online* 2014b;.
- Ottolini CS, Newnham LJ, Capalbo A, Natesan SA, Joshi HA, Cimadomo D, Griffin DK, Sage K, Summers MC, Thornhill AR, *et al.* Genome-wide maps of recombination and chromosome segregation in human oocytes and embryos show selection for maternal recombination rates. *Nat Genet* 2015;
- Poli M, Girardi L, Fabiani M, Moretto M, Romanelli V, Patassini C, Zuccarello D, Capalbo A. Past, present, and future strategies for enhanced assessment of embryo's genome and reproductive competence in women of advanced reproductive age. *Front Endocrinol (Lausanne)* 2019;**10**:1–12.
- Poli M, Jaroudi S, Sarasa J, Spath K, Child T, Wells D. The blastocoel fluid as a source of DNA for preimplantation genetic diagnosis and screening. *Fertil Steril* 2013;
- Poli M, Ori A, Turner K, Child T, Wells D. Defining the biochemical content of the human blastocoel using mass spectrometry: a novel tool for identifying biomarkers of embryo competence. *Fertil Steril* 2012;
- Popovic M, Dheedene A, Christodoulou C, Taelman J, Dhaenens L, Nieuwerburgh F Van, Deforce D, Abbeel E Van Den, Sutter P De, Menten B, *et al.* Chromosomal mosaicism in human blastocysts: The ultimate challenge of preimplantation genetic testing? *Hum Reprod* 2018;**33**:1–13.
- Rabinowitz M, Ryan A, Gemelos G, Hill M, Baner J, Cinnioglu C, Banjevic M, Potter D, Petrov DA, Demko Z. Origins and rates of aneuploidy in human blastomeres. *Fertil Steril* 2012;
- Rubio C, Bellver J, Rodrigo L, Castellón G, Guillén A, Vidal C, Giles J, Ferrando M, Cabanillas S, Remohí J, *et al.* In vitro fertilization with preimplantation genetic diagnosis for aneuploidies in advanced maternal age: a randomized, controlled study. *Fertil Steril* 2017;
- Rubio C, Rienzi L, Navarro-Sánchez L, Cimadomo D, García-Pascual CM, Albricci L, Soccia D, Valbuena D, Capalbo A, Ubaldi F, *et al.* Embryonic cell-free DNA versus

- trophectoderm biopsy for aneuploidy testing: concordance rate and clinical implications. *Fertil Steril* 2019a;
- Rubio C, Rodrigo L, Garcia-Pascual C, Peinado V, Campos-Galindo I, Garcia-Herrero S, Simón C. Clinical application of embryo aneuploidy testing by next-generation sequencing. *Biol Reprod* 2019b;0:1–8.
- Rycke M De, Belva F, Goossens V, Moutou C, SenGupta SB, Traeger-Synodinos J, Coonen E. ESHRE PGD Consortium data collection XIII: Cycles from January to December 2010 with pregnancy follow-up to October 2011. *Hum Reprod* 2015;
- SA N, JM F, EJ F, MD W, SJ M, Tao X, NR T, RT S. High relative deoxyribonucleic acid content of trophectoderm biopsy adversely affects pregnancy outcomes. *Fertil Steril* 2016;
- Schmittgen TD, Livak KJ. Analyzing real-time PCR data by the comparative C(T) methodSchmittgen, T.D., Livak, K.J., 2008. Analyzing real-time PCR data by the comparative C(T) method. *Nat. Protoc.* 3, 1101–1108.. *Nat Protoc* 2008;
- Scott RT, Upham KM, Forman EJ, Zhao T, Treff NR. Cleavage-stage biopsy significantly impairs human embryonic implantation potential while blastocyst biopsy does not: A randomized and paired clinical trial. *Fertil Steril* 2013;
- Shamonki MI, Jin H, Haimowitz Z, Liu L. Proof of concept: preimplantation genetic screening without embryo biopsy through analysis of cell-free DNA in spent embryo culture media. *Fertil Steril* 2016;
- Thornhill AR, Handyside AH, Ottolini C, Natesan SA, Taylor J, Sage K, Harton G, Cliffe K, Affara N, Konstantinidis M, *et al.* Karyomapping—a comprehensive means of simultaneous monogenic and cytogenetic PGD: comparison with standard approaches in real time for Marfan syndrome. *J Assist Reprod Genet* 2015;
- Treff NR, Fedick A, Tao X, Devkota B, Taylor D, Scott RT. Evaluation of targeted next-generation sequencing-based preimplantation genetic diagnosis of monogenic disease. *Fertil Steril* 2013;
- Treff NR, Levy B, Su J, Northrop LE, Tao X, Scott RT. SNP microarray-based 24 chromosome aneuploidy screening is significantly more consistent than FISH. *Mol Hum*



*Reprod* 2010;

Treff NR, Tao X, Ferry KM, Su J, Taylor D, Scott RT. Development and validation of an accurate quantitative real-time polymerase chain reaction-based assay for human blastocyst comprehensive chromosomal aneuploidy screening. *Fertil Steril* [Internet] 2012;**97**:819-824.e2. Elsevier Inc.

Vera-Rodriguez M, Diez-Juan A, Jimenez-Almazan J, Martinez S, Navarro R, Peinado V, Mercader A, Meseguer M, Blesa D, Moreno I, *et al.* Origin and composition of cell-free DNA in spent medium from human embryo culture during preimplantation development. *Obstet Gynecol Surv* 2018;

Vera-Rodríguez M, Michel CE, Mercader A, Bladon AJ, Rodrigo L, Kokocinski F, Mateu E, Al-Asmar N, Blesa D, Simón C, *et al.* Distribution patterns of segmental aneuploidies in human blastocysts identified by next-generation sequencing. *Fertil Steril* 2016;**105**:1047-1055.e2.

Victor AR, Griffin DK, Brake AJ, Tyndall JC, Murphy AE, Lepkowsky LT, Lal A, Zouves CG, Barnes FL, McCoy RC, *et al.* Assessment of aneuploidy concordance between clinical trophectoderm biopsy and blastocyst. *Hum Reprod* 2019;**34**:181–192.

Wu H, Ding C, Shen X, Wang J, Li R, Cai B, Xu Y, Zhong Y, Zhou C. Medium-based noninvasive preimplantation genetic diagnosis for human  $\alpha$ -thalassemias-SEA. *Med (United States)* 2015;

Zhou S, Cheng D, Ouyang Q, Xie P, Lu C, Gong F, Hu L, Tan Y, Lu G, Lin G. Prevalence and authenticity of de-novo segmental aneuploidy (>16 Mb) in human blastocysts as detected by next-generation sequencing. *Reprod Biomed Online* [Internet] 2018;**37**:511–520. Elsevier Ltd.

Zimmerman RS, J alas C, Tao X, Fedick AM, Kim JG, Pepe RJ, Northrop LE, Scott RT, Treff NR. Development and validation of concurrent preimplantation genetic diagnosis for single gene disorders and comprehensive chromosomal aneuploidy screening without whole genome amplification. *Fertil Steril* 2016;



## Appendix 1

Barcode Name	Sample	Bases	$\geq Q20$	Reads	Mean Read Length	Read Length Histogram
No barcode	none	22,448,391	16,700,716	216,716	103 bp	
SingleSeq_001	NA10315_1	21,968,541	18,600,393	191,690	114 bp	
SingleSeq_002	NA10315_2	21,764,442	17,878,817	193,168	112 bp	
SingleSeq_003	NA07408_1	16,728,956	14,274,007	145,459	115 bp	
SingleSeq_004	NA07408_2	18,544,718	15,696,924	161,303	114 bp	
SingleSeq_005	NA03576_1	23,425,228	19,670,600	206,235	113 bp	
SingleSeq_006	NA03576_2	16,784,201	14,199,067	146,702	114 bp	
SingleSeq_007	GM04606_SINGLE	17,720,616	18,094,082	191,553	113 bp	
SingleSeq_008	GM04606_POOL	17,992,643	15,059,991	158,018	113 bp	
SingleSeq_009	GM03102_SINGLE	20,142,300	16,943,673	176,303	114 bp	
SingleSeq_010	GM03102_POOL	19,729,582	16,528,425	173,232	113 bp	
SingleSeq_011	GM09326_SINGLE	24,280,696	22,315,820	229,748	114 bp	
SingleSeq_012	GM09326_POOL	10,260,747	8,122,421	92,464	110 bp	
SingleSeq_013	GM03330_SINGLE	17,014,030	15,314,685	154,963	115 bp	
SingleSeq_014	GM03330_POOL	10,548,801	8,808,541	92,623	113 bp	
SingleSeq_015	GM01359_SINGLE	16,592,813	16,733,196	171,875	114 bp	
SingleSeq_016	GM01359_POOL	16,241,839	13,617,464	142,992	113 bp	
SingleSeq_017	GM04592_SINGLE	15,223,371	15,219,556	160,188	113 bp	
SingleSeq_018	GM04592_POOL	15,396,681	12,807,322	135,325	113 bp	
SingleSeq_019	NORMAL_XX_SINGLE	13,900,637	13,954,918	145,428	114 bp	
SingleSeq_020	NORMAL_XX_POOL	13,299,299	20,494,609	212,568	114 bp	
SingleSeq_021	NORMAL_XY_SINGLE	13,800,615	16,806,116	173,466	114 bp	
SingleSeq_022	NORMAL_XY_POOL	20,351,351	20,526,386	211,861	114 bp	
SingleSeq_023	NA03576_3	19,674,334	16,627,519	172,647	113 bp	
SingleSeq_024	NA03576_4	17,377,339	14,432,219	153,313	113 bp	

## Appendix 2

Barcode Name	Sample	Bases	$\geq Q20$	Reads	Mean Read Length	Read Length Histogram
No barcode	none	22,261,387	16,886,983	210,721	105 bp	
SingleSeq_025	NA10315.1	23,342,445	20,016,787	205,168	113 bp	
SingleSeq_026	NA10315.2	24,031,154	20,456,083	211,714	113 bp	
SingleSeq_027	NA07408.1	25,189,796	21,433,577	222,030	113 bp	
SingleSeq_028	NA07408.2	22,805,520	19,470,072	200,551	113 bp	
SingleSeq_029	NA03576.1	25,396,751	21,614,950	224,145	113 bp	
SingleSeq_030	NA03576.2	26,668,436	22,433,940	237,787	112 bp	
SingleSeq_031	GM04626_SINGLE	19,908,527	10,784,004	129,491	107 bp	
SingleSeq_032	GM04626_POOL	17,288,546	14,645,034	152,358	113 bp	
SingleSeq_033	GM03102_SINGLE	15,526,382	15,783,932	163,214	113 bp	
SingleSeq_034	GM03102_POOL	16,036,961	13,669,546	140,940	113 bp	
SingleSeq_035	GM09326_SINGLE	16,649,544	17,420,677	183,140	112 bp	
SingleSeq_036	GM09326_POOL	15,994,856	13,483,945	141,553	112 bp	
SingleSeq_037	GM03330_SINGLE	15,389,830	13,017,856	135,030	113 bp	
SingleSeq_038	GM03330_POOL	15,767,848	13,045,951	141,076	111 bp	
SingleSeq_039	GM01359_SINGLE	16,305,727	17,164,874	179,381	113 bp	
SingleSeq_040	GM01359_POOL	14,190,033	11,713,861	125,481	113 bp	
SingleSeq_041	GM04592_SINGLE	15,557,069	13,327,566	135,749	114 bp	
SingleSeq_042	GM04592_POOL	12,570,352	10,595,882	111,040	113 bp	
SingleSeq_043	NORMALXX_SINGLE	18,801,800	18,766,718	193,936	113 bp	
SingleSeq_044	NORMALXX_POOL	16,877,824	22,249,224	234,345	112 bp	
SingleSeq_045	NORMALXY_SINGLE	18,841,830	20,409,721	208,501	114 bp	
SingleSeq_046	NORMALXY_POOL	16,847,847	15,203,869	155,989	114 bp	
SingleSeq_047	NA10315.3	19,723,207	16,809,407	173,663	113 bp	
SingleSeq_048	NA10315.4	19,221,401	16,388,603	168,681	113 bp	